

The use of the satellite imagery of Meteosat for the diagnosis of severe weather events and the issue of warnings

Manfred Kurz

Neustadt/Weinstraße

Germany

Outline

- Introduction
- Deficits of NWP models – Advantages of the forecaster
- The importance of satellite data
- Diagnosis of cyclogenetic effects
- Examples
- Conclusions

Introduction (1)

- Weather forecasting is nowadays based on the extensive use of numerical models. The model output covers nearly all scales and ranges – from the local forecast for a few hours up to forecasts world-wide for weeks or even seasons. It also contains important information on the occurrence of hazardous weather.
- The accuracy of the model output is rather high. Verification results show, that – on an average – forecasters are not more able to add much value to the model output. Therefore many forecast products are not only produced fully automatically, but also transmitted to the customer without stronger control by forecasters.

Introduction (2)

- The most important forecasting task, however, **the issue of warnings of hazardous weather like gale force winds, heavy thunderstorms or flash floods**, cannot be automated. Since the models still show deficits in simulating these events, the weather has to be carefully monitored and the wrong model forecasts have to be corrected, if significant deviations from the real development become visible.
- **This has to be done by forecasters being able to do their work also without guidance or any other assistance by NWP products. The information from meteorological satellites like METEOSAT can be very useful for this task !**

Deficits of NWP models

- According to the findings of COST 78, there are three areas for which deficits exist in the numerical simulation:
- Fronts and cyclogenesis, esp. with regard to the weather activity of fronts and the rapid intensification some cyclones undergo
- Strong convection, esp. with regard to the origin of meso-scale convective systems
- Fog and low stratus

Advantages of the forecaster

- He/she can analyse more exactly with regard to some key observations
- He/she is always quicker than the model runs, i.e. he/she already knows the real weather development when the new model output becomes available
- He/she is able to recognise typical signatures and patterns in the data, and
- He/she has the ability to imagine alternative scenarios of the development

Importance of satellite data

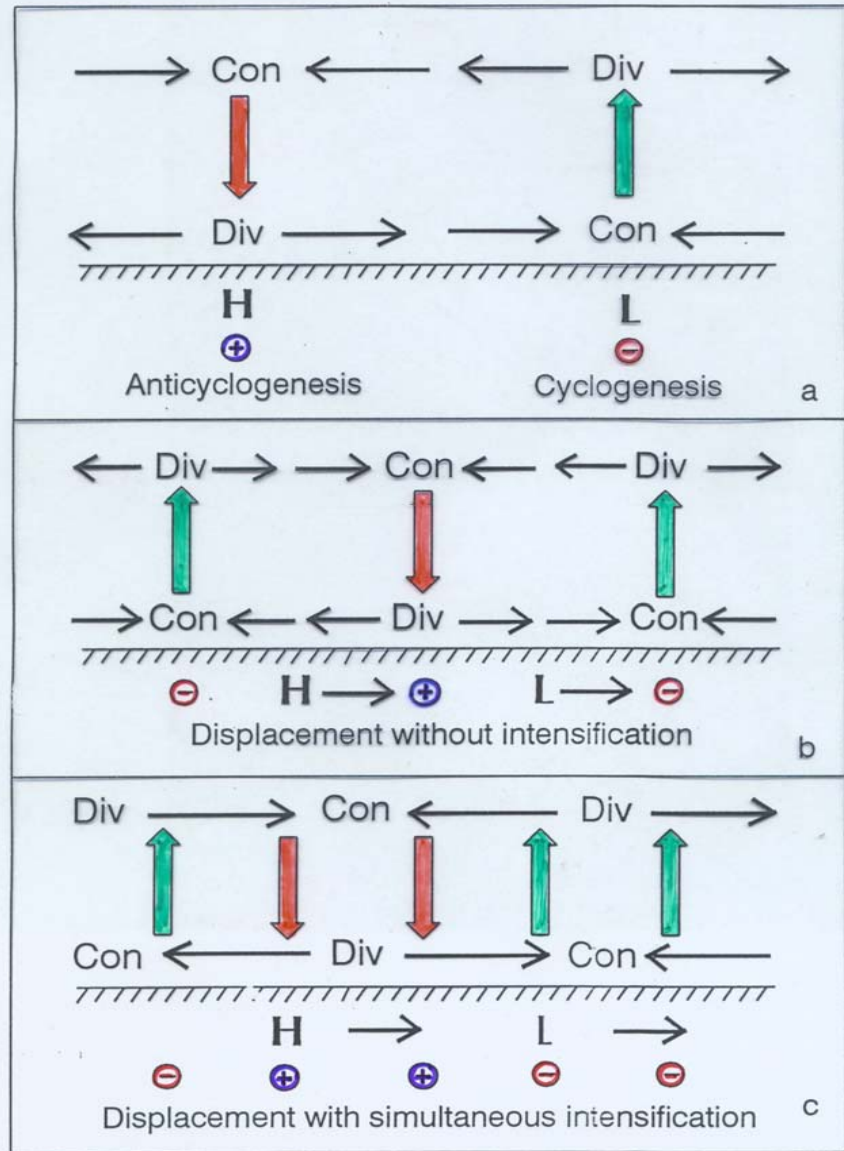
- In order to detect model failures as early as possible, the model forecasts have to be continuously compared with the real weather. **In addition to the conventional observations remote sensing data like satellite data are very important – esp. in data sparse areas.**
- If there are significant deviations of the actual weather development from the model output, an alternative forecast or a warning has to be formulated and issued. Decisive for this is an own **Synoptic Diagnosis**, i.e. an assessment of the three-dimensional state of the atmosphere with regard to the existing synoptic systems and their potential for further development.

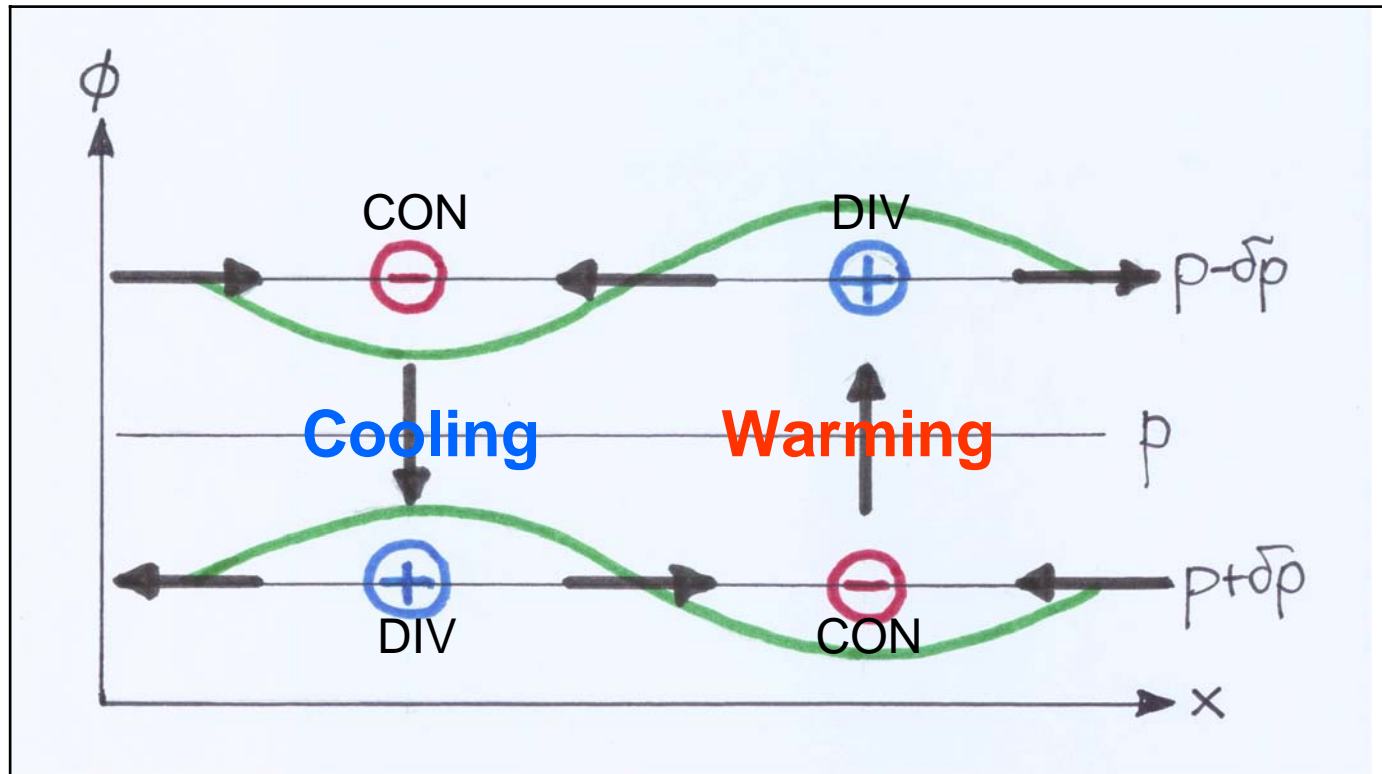
Importance of satellite data

- Since the normally used diagnostic parameters are derived from numerical analyses or forecasts, their use might appear questionable in cases with significant errors in the model output. **Then diagnostic means have to be used which are mainly based on observations. Very important in this respect are „Conceptual models“ combining the imagery of meteorological satellites with conventional observations and manual analyses.**

Diagnosis of cyclogenetic effects

For cyclogenesis near surface there must be at first divergence effective at upper levels in order to produce pressure fall, followed by convergence in lower levels in order to produce cyclonic vorticity. Due to continuity there must be an ascending motion in mid levels. That applies also to the movement of a cyclone.



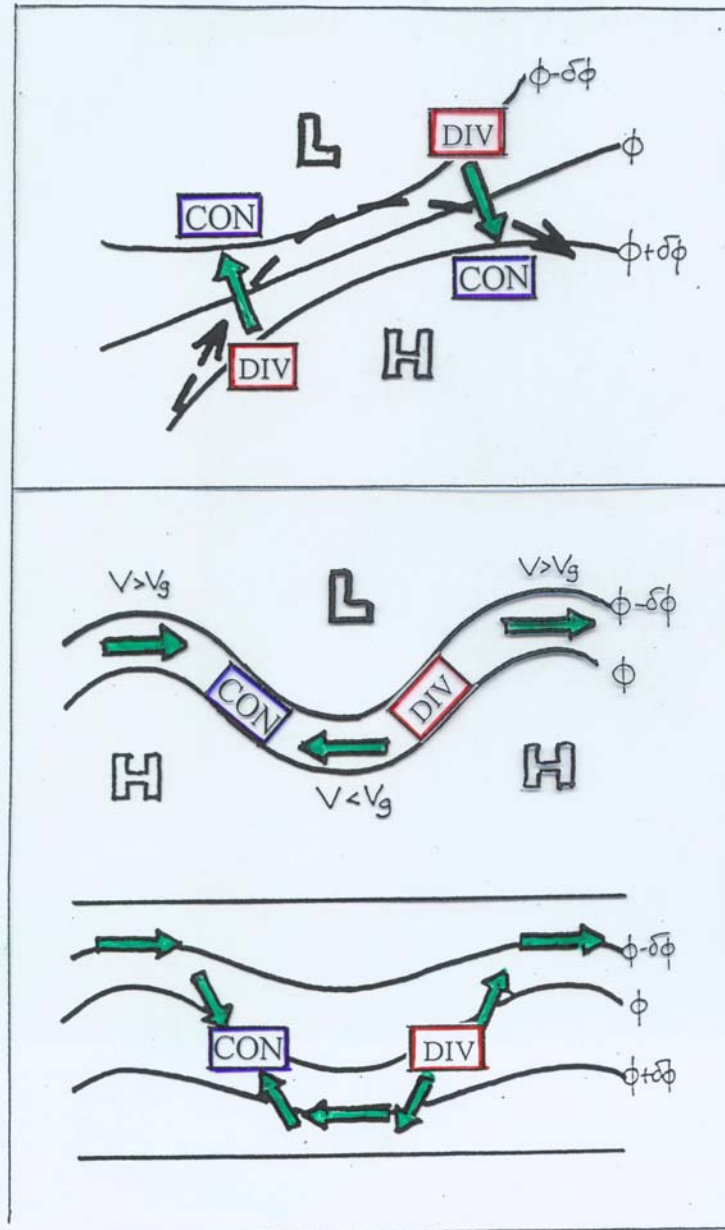


Geopotential changes of pressure surfaces due to advective or diabatic temperature changes

Divergence/convergence due to transverse ageostrophic motions in the entrance and exit region of a jet streak

Divergence/convergence due to ageostrophic components along the flow in short and progressively moving baroclinic waves

Combination of both effects

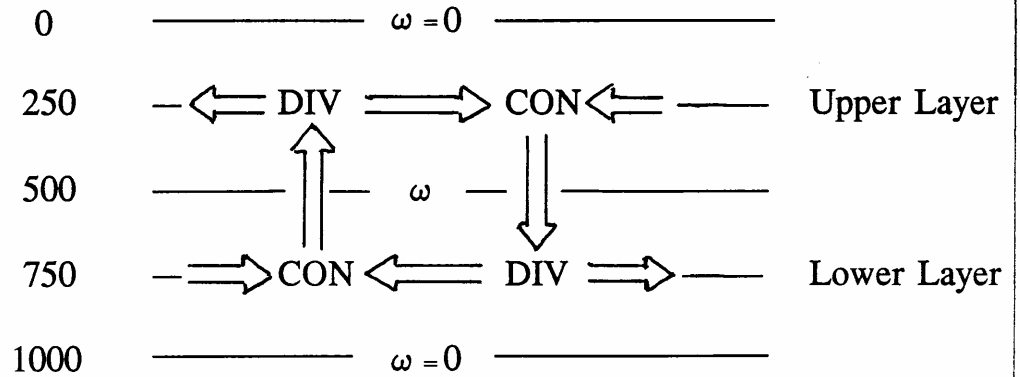


SCHERHAG 1934

BJERKNES / HOLMBOE

1944

Scheme of a two-layer model and cyclogenetic and anticyclonic effects for the lower and the upper layer, respectively.



Lower layer (lower troposphere, surface)

C	in regions with	A	in regions with
-	PVA aloft	-	NVA aloft
-	maximized WA	-	maximized CA
-	(maximized diabatic heating)	-	(maximized diabatic cooling)

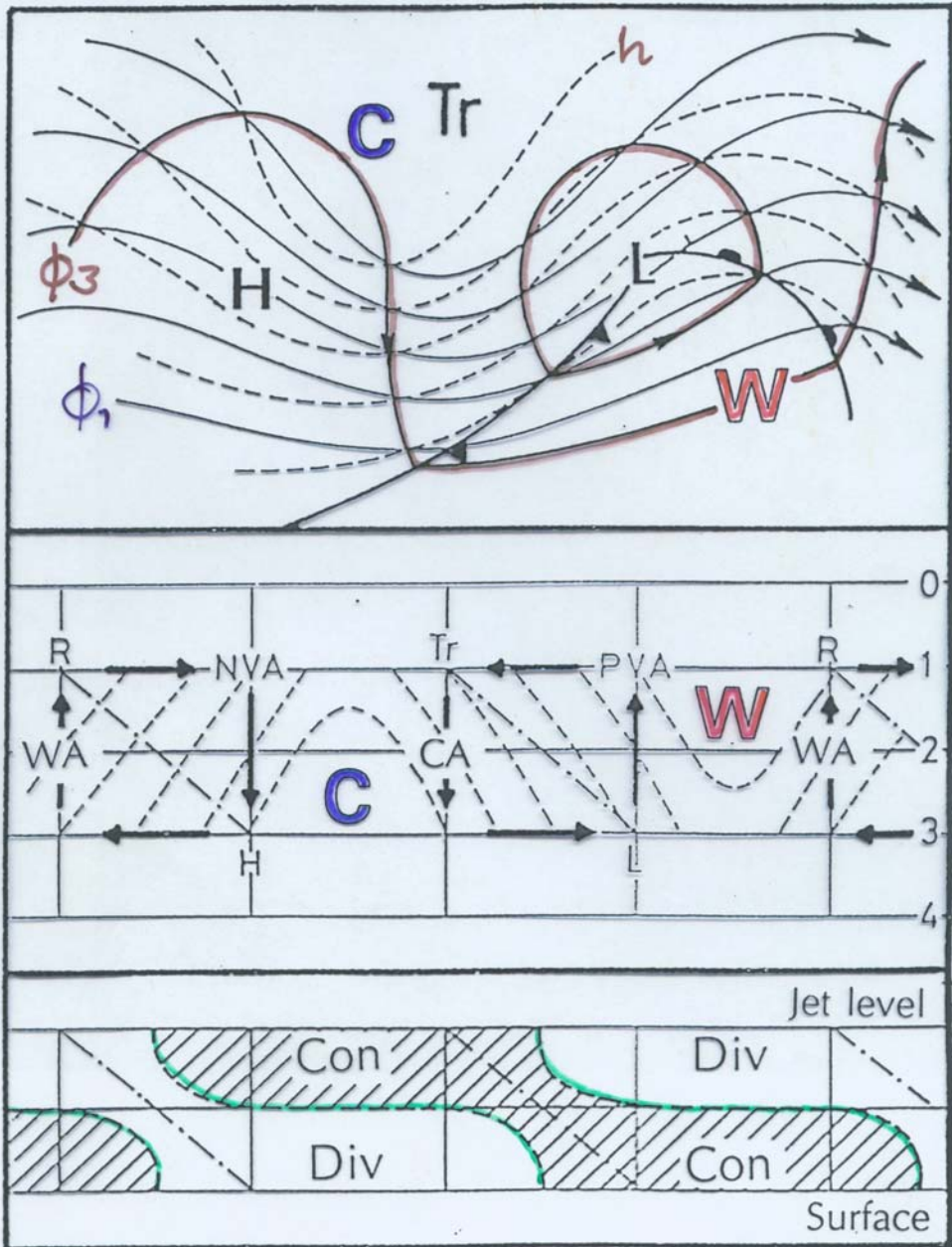
Upper layer (upper troposphere, jetstream level)

C	in regions with	A	in regions with
-	PVA	-	NVA
-	maximized CA	-	maximized WA
-	(maximized diabatic cooling)	-	(maximized diabatic heating)

C local vorticity increase connected with (at least relative) geopotential fall

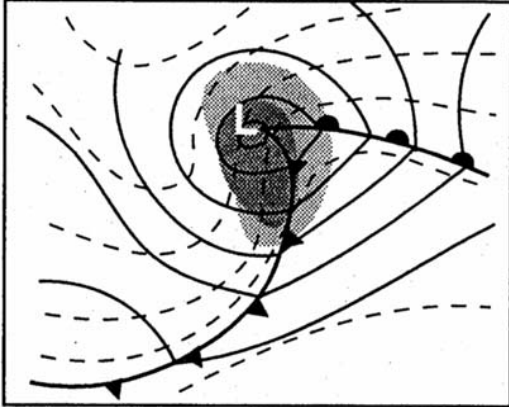
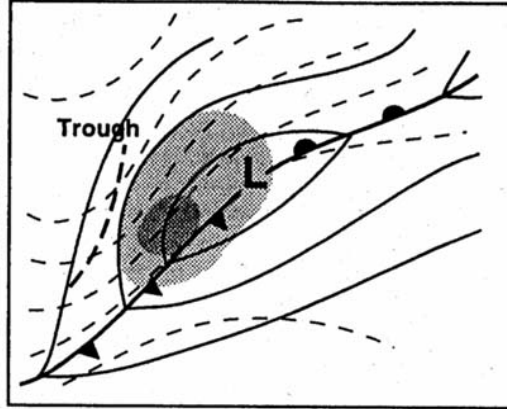
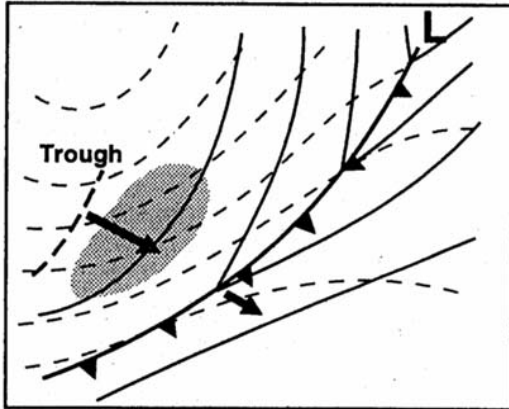
A local vorticity decrease connected with (at least relative) geopotential rise

Scheme of an
unstable baroclinic
wave



Cyclogenesis due to superposition of an upper vorticity maximum (Petterssen scheme)

Cyclone
development



Shading shows the region of appreciable positive vorticity advection (PVA) aloft

Petterssen S 1956

Features

Cyclogenesis can be expected where and when an upper vorticity maximum (e.g. within a cold upper trough or at the cyclonic flank of a jet-streak) approaches and engages a slower moving frontal trough or frontal wave in the lower troposphere.

A coupled system with a backward tilted trough axis can develop.

The movement of the upper vorticity maximum can often be seen in satellite imagery - either from cloud associated with the vorticity maximum itself or from dark (dry) regions in water vapour imagery.

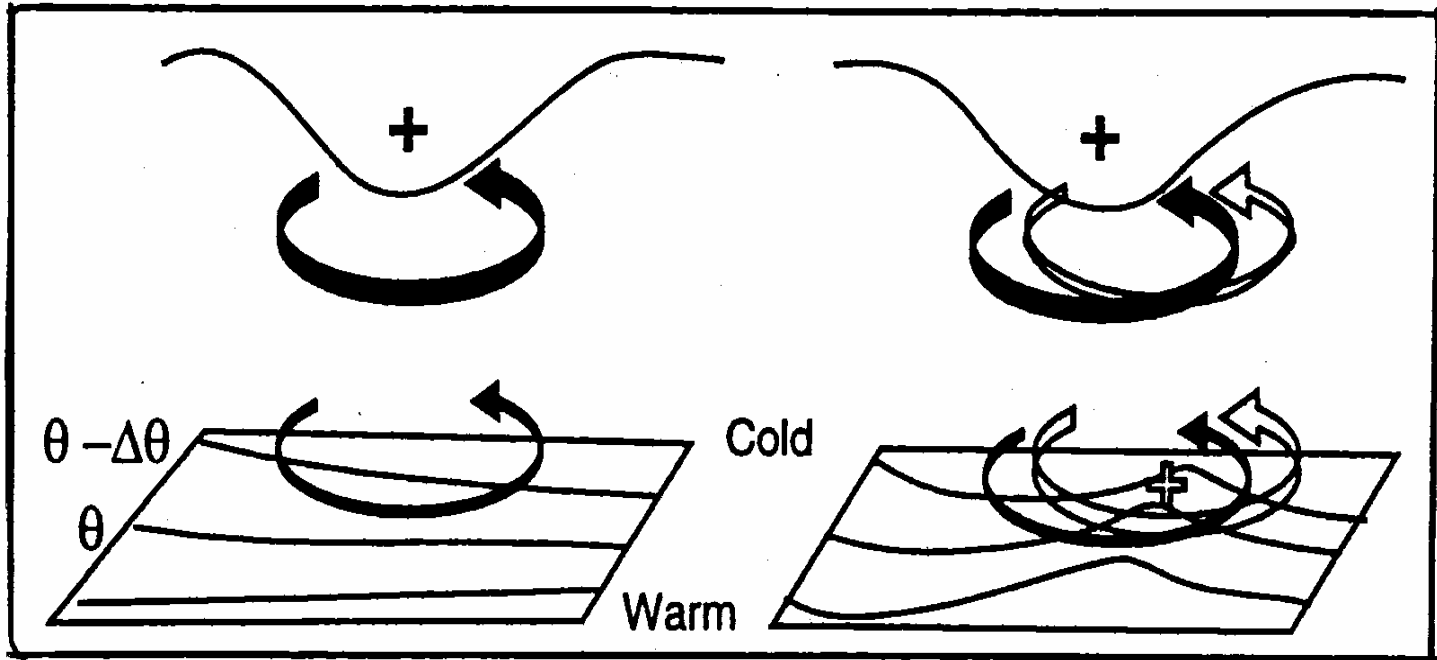
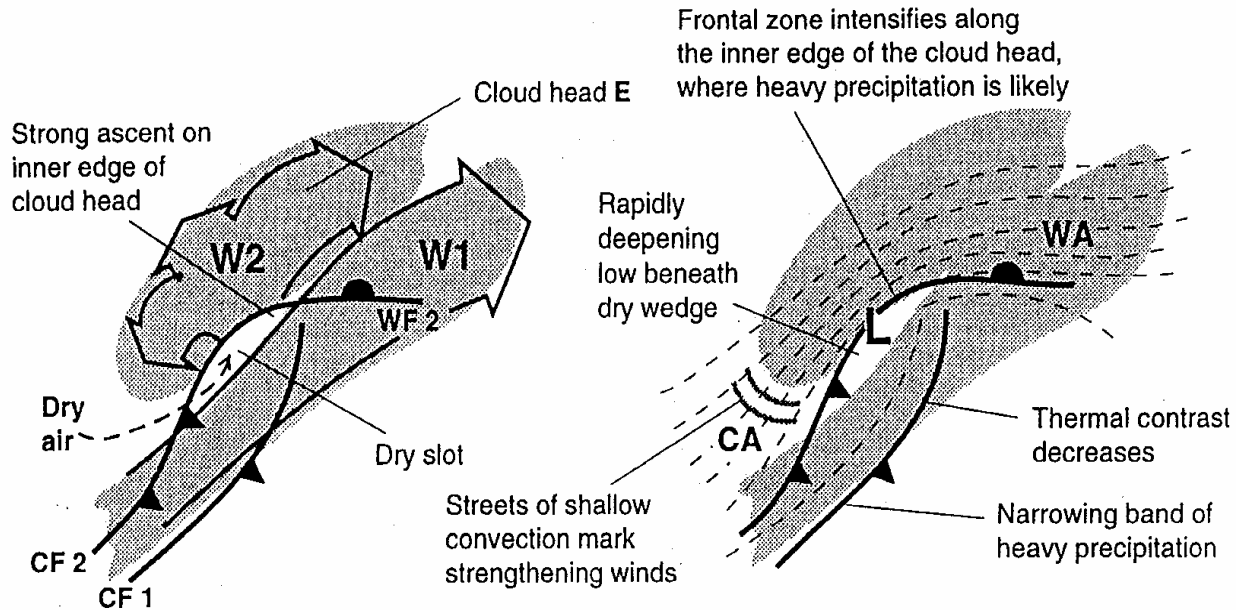


Fig. 2: Schematic picture of cyclogenesis associated with the arrival of an upper-level positive PV anomaly over a low-level baroclinic zone. The circulation induced by the upper-level PV anomaly is indicated by the solid arrows. The advection by the circulation leads to a warm temperature anomaly ahead of the PV anomaly. This warm anomaly induces the cyclonic circulation indicated by the open arrows. From Hoskins et al. (1985).



From Bader et al 1995

Features

This cloud signature is usually followed by explosive cyclogenesis .

Cloud head (leaf) E composed of rapidly ascending warm conveyor belt W2 is seen in imagery to be particularly broad and 'leaf shaped' with a sharp convex poleward boundary.

A pronounced and narrow 'dark zone' or 'dry slot' or 'dry intrusion' separates the cloud head from the polar front cloud band associated with W1. This dry slot is usually associated with a tongue of stratospheric air, recently descended into the troposphere which has high values of potential vorticity

Examples (I)

**The storm „Anatol“
(02/04-12-1999)**

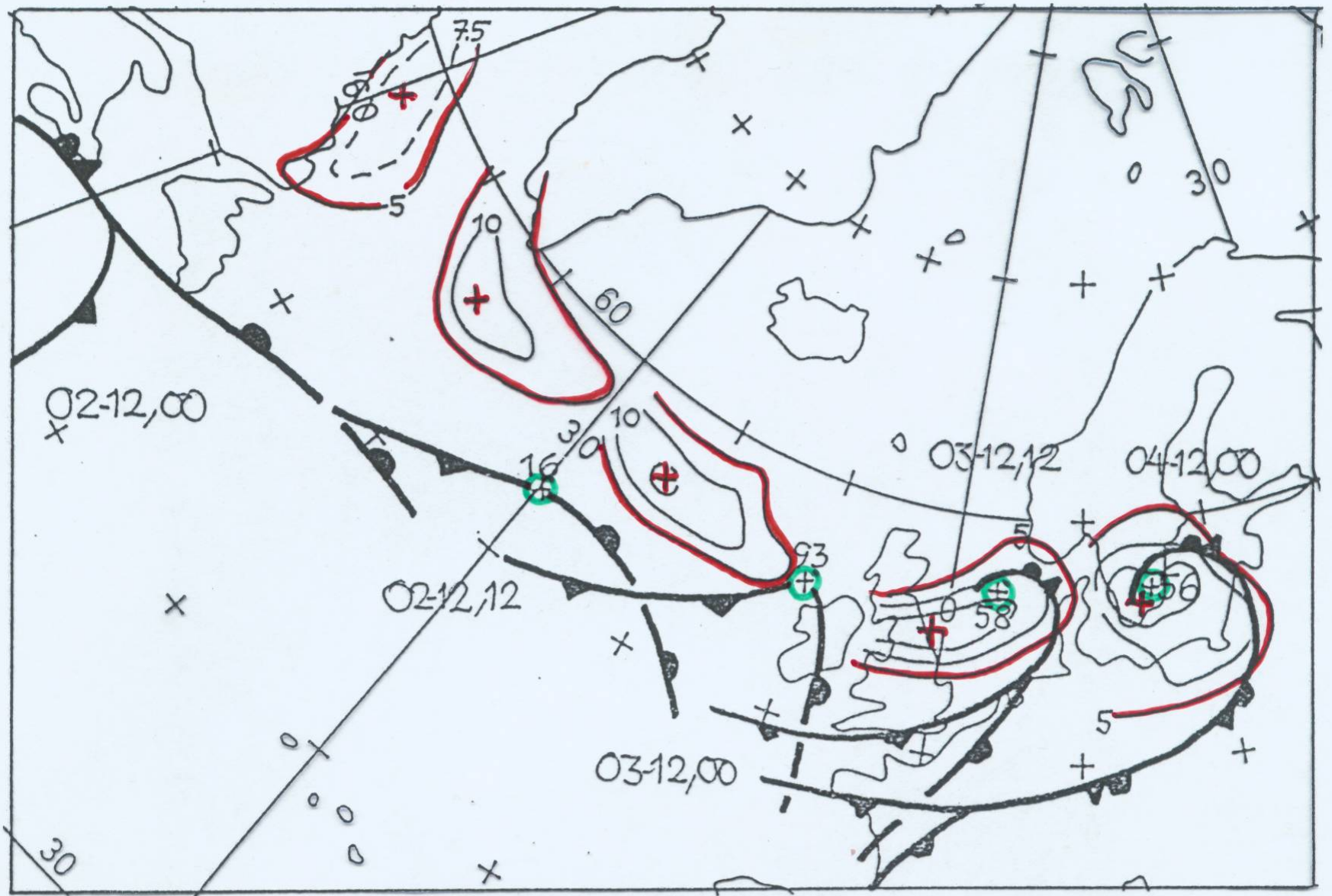
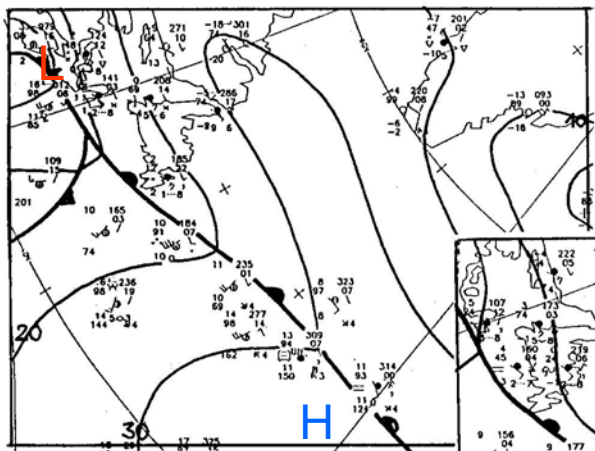
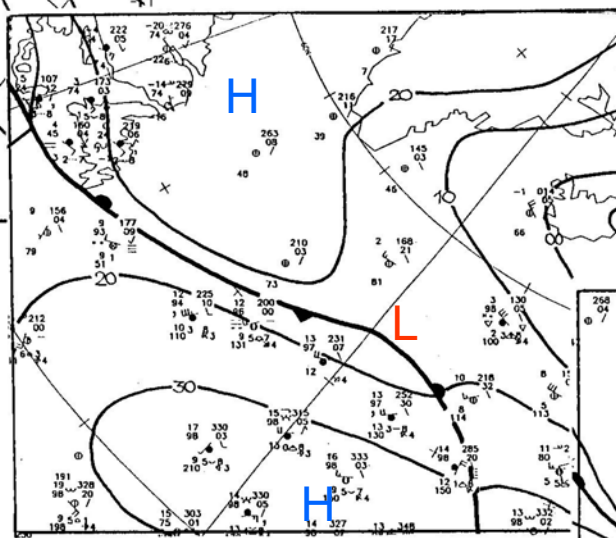


Fig.1: Movement of surface low „Anatol“ as well as the vorticity maximum at 500 hPa between 02-12-99, 00 UTC, and 04-12-99, 00 UTC in 12-hourly intervals.

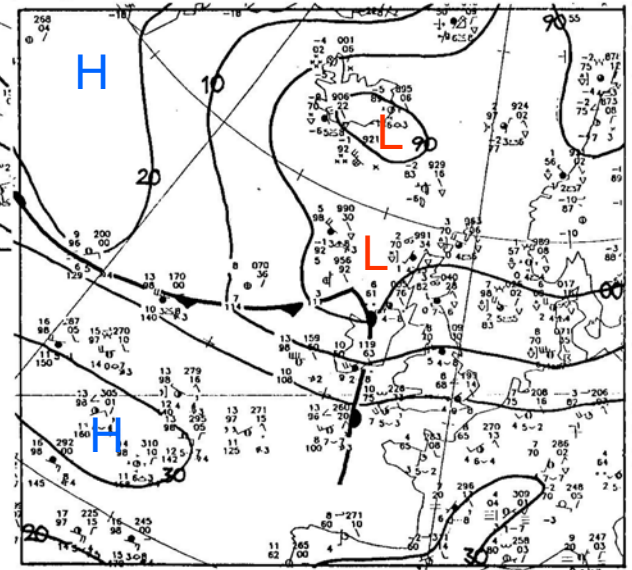
„ANATOL“



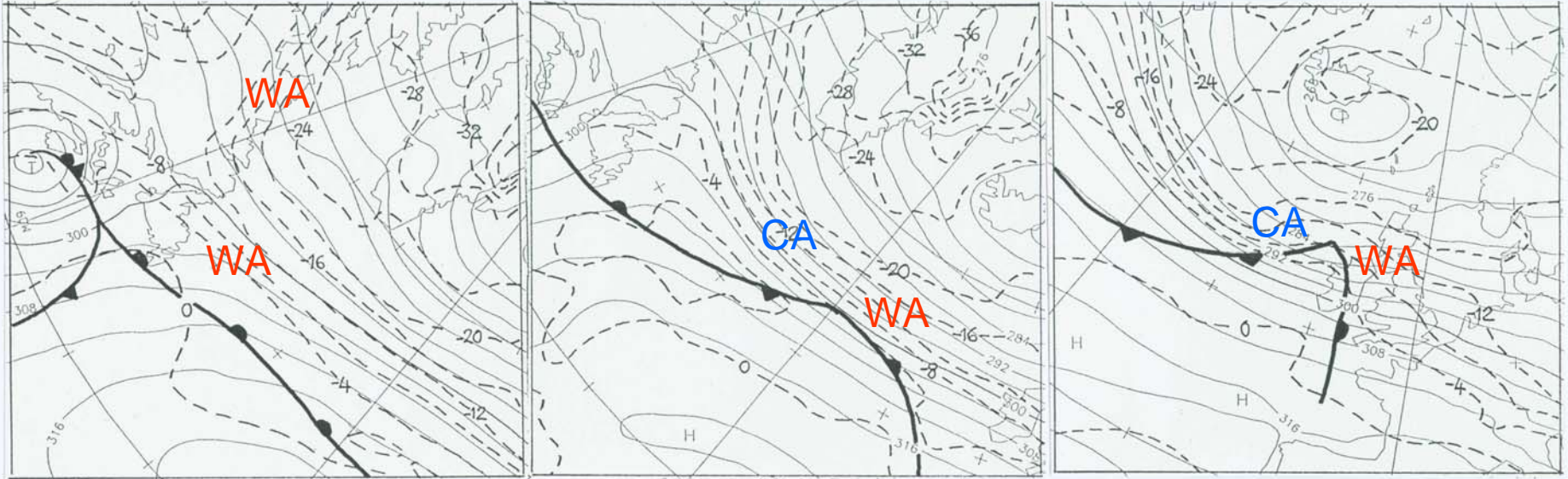
02-12-99, 00



02-12-99, 12



03-12-99, 00

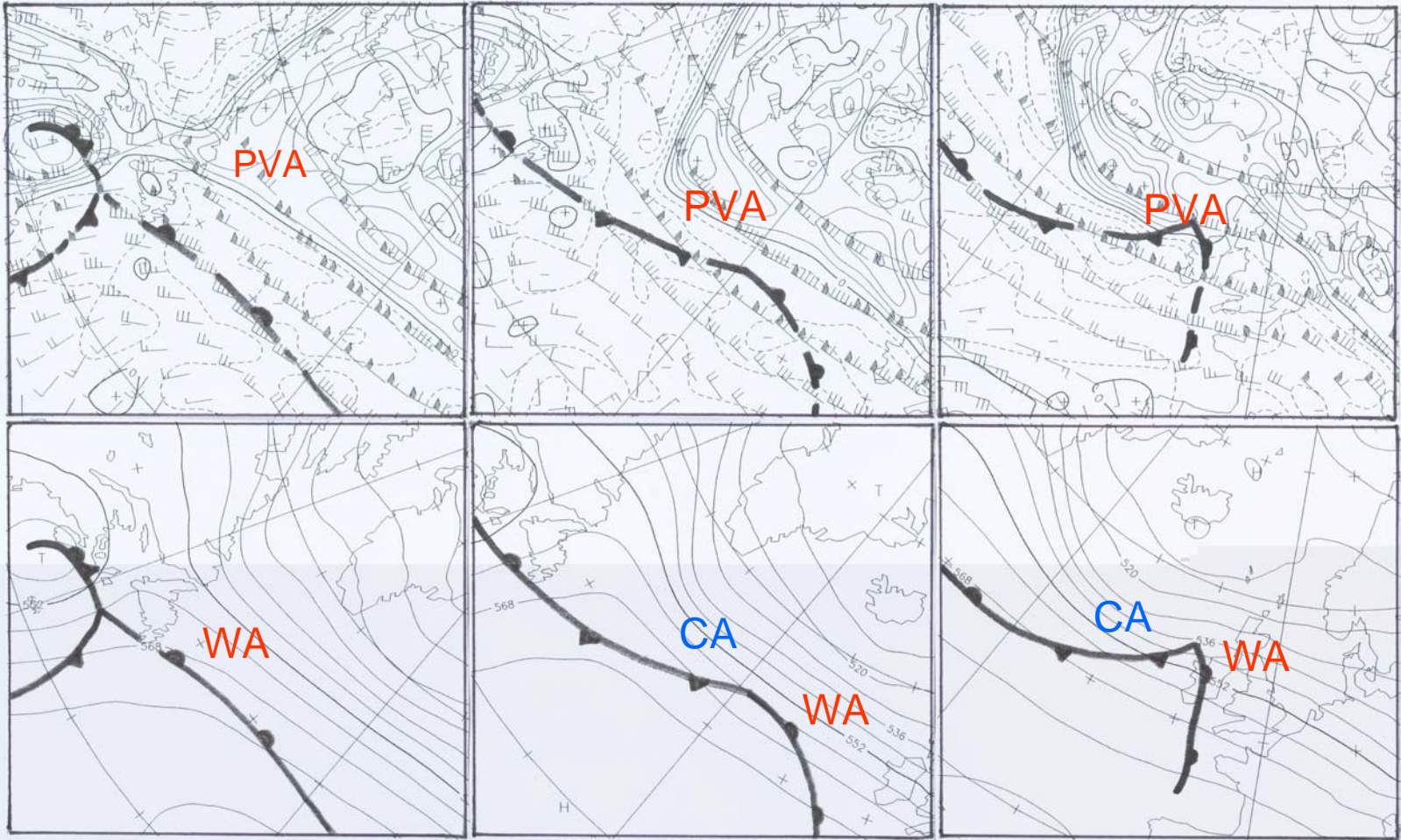


02-12-99, 00

02-12-99, 12

03-12-99, 00

700hPa : Isohypes and isotherms



02-12-99, 00

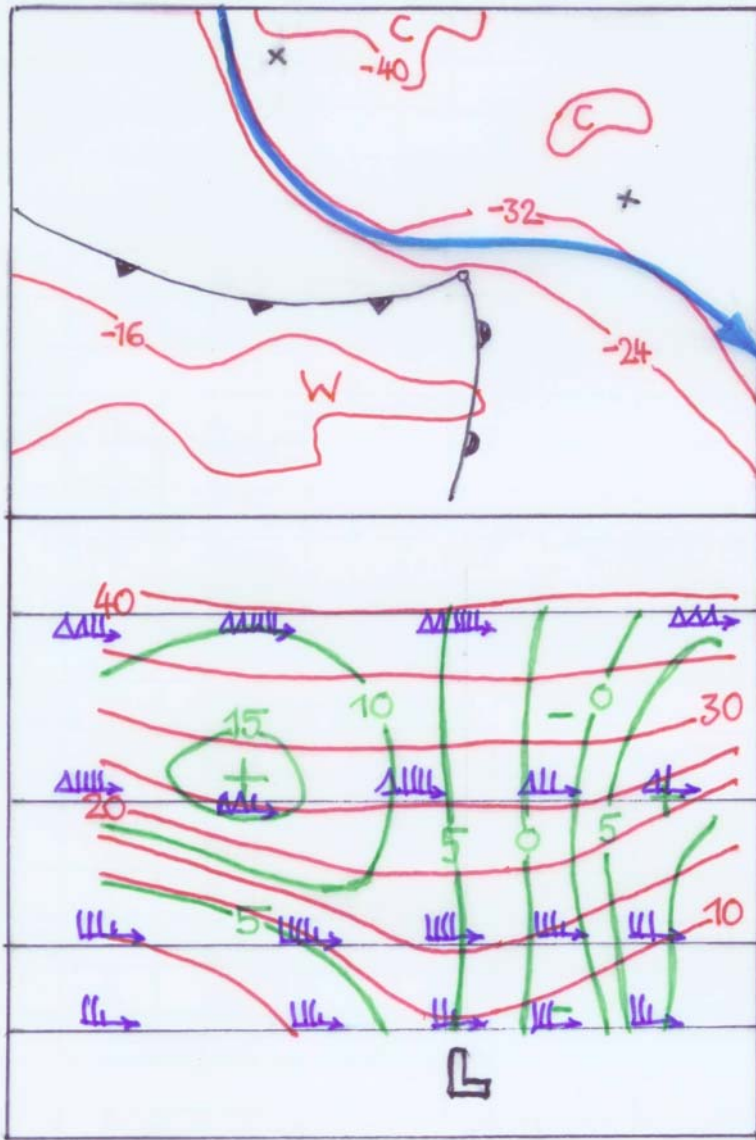
02-12-99, 12

03-12-99, 00

500 hPa: Geopotential, winds and relative vorticity

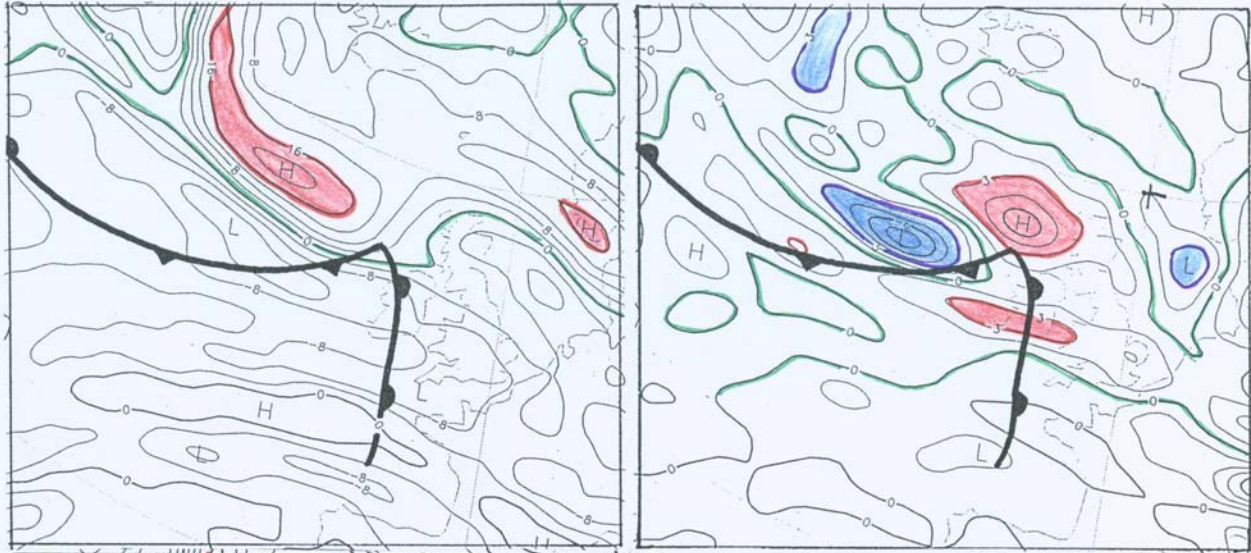
03-12-99, 00 UTC::

**Jet axis 300 hPa, isotherms
500 hPa and surface fronts**

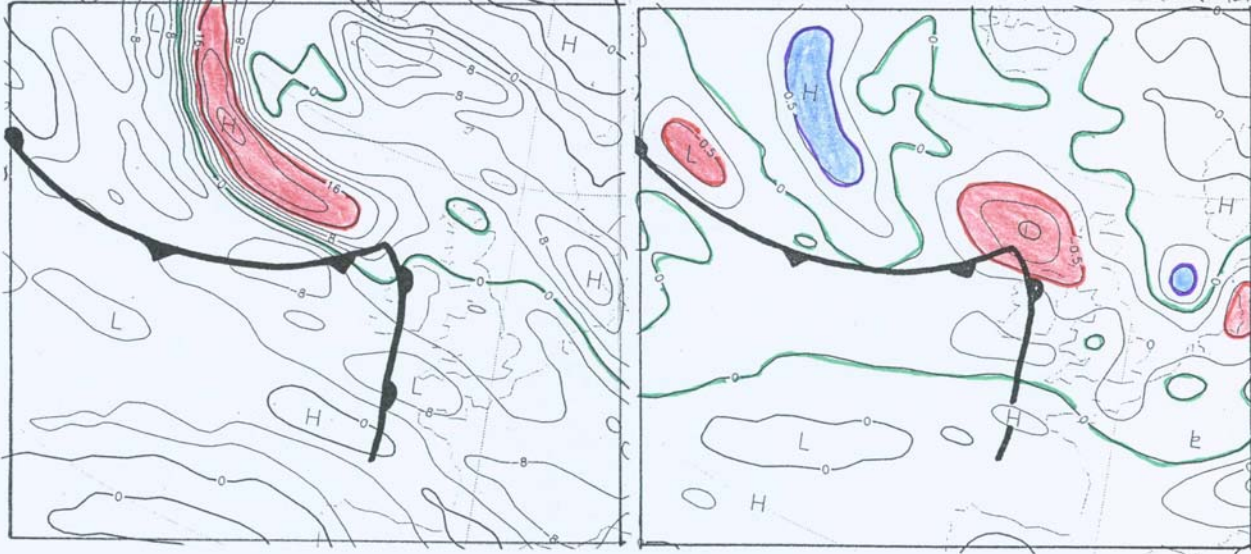


**Cross-section along the jet axis
with potential temperature (red),
relative vorticity (green)
and winds**

300 hPa



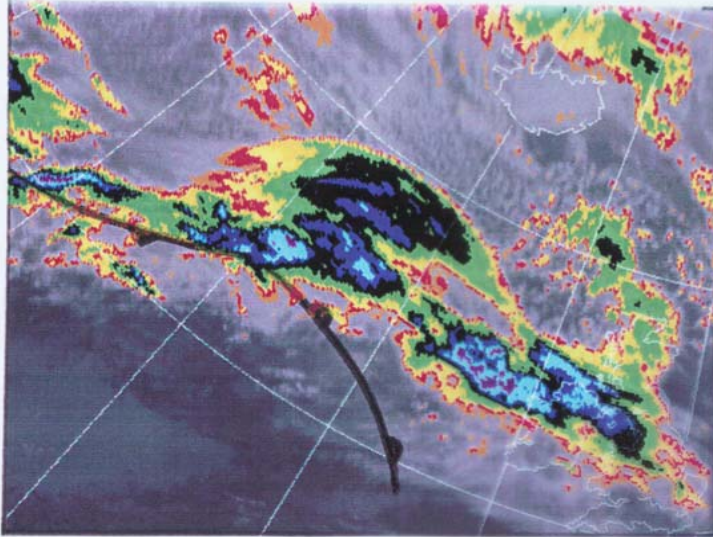
500hPa



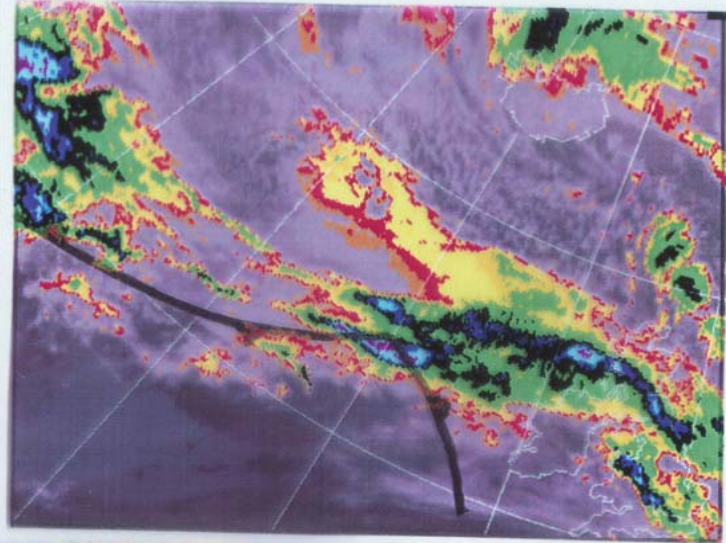
Relative vorticity

Divergence/omega

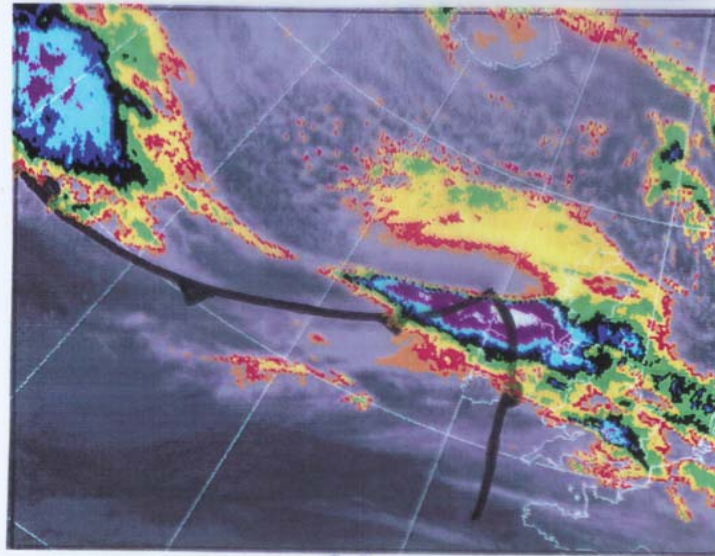
IR-images of Meteosat



12

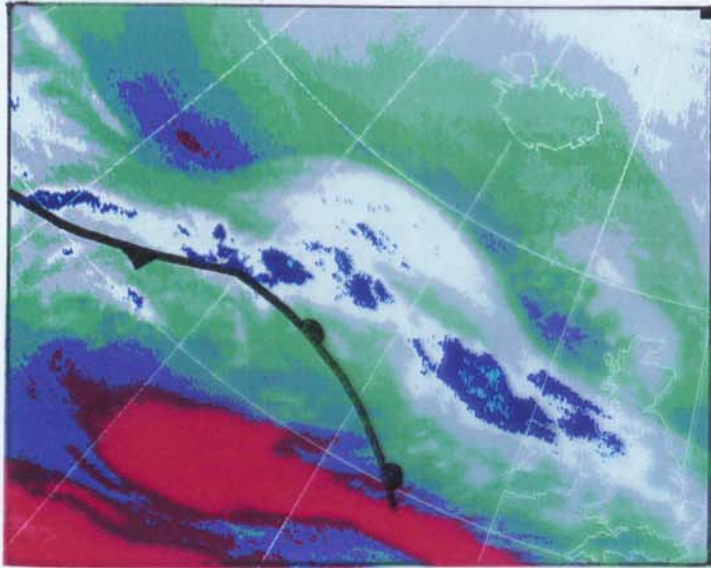


18

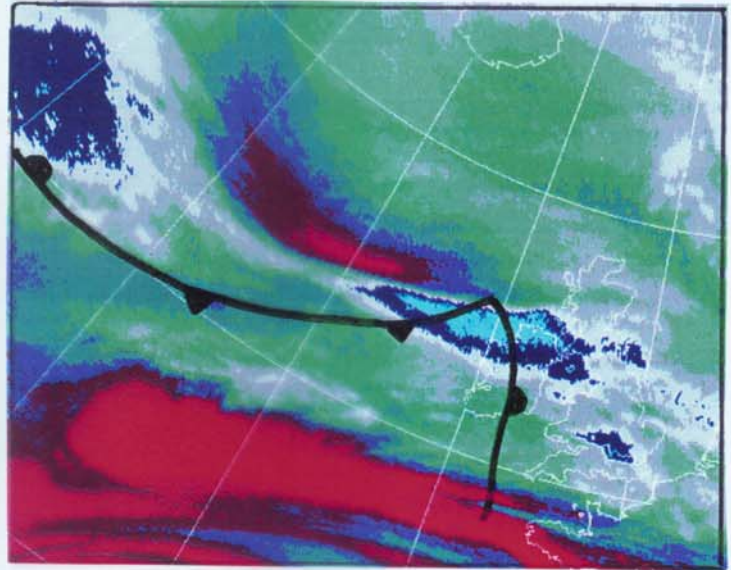


00

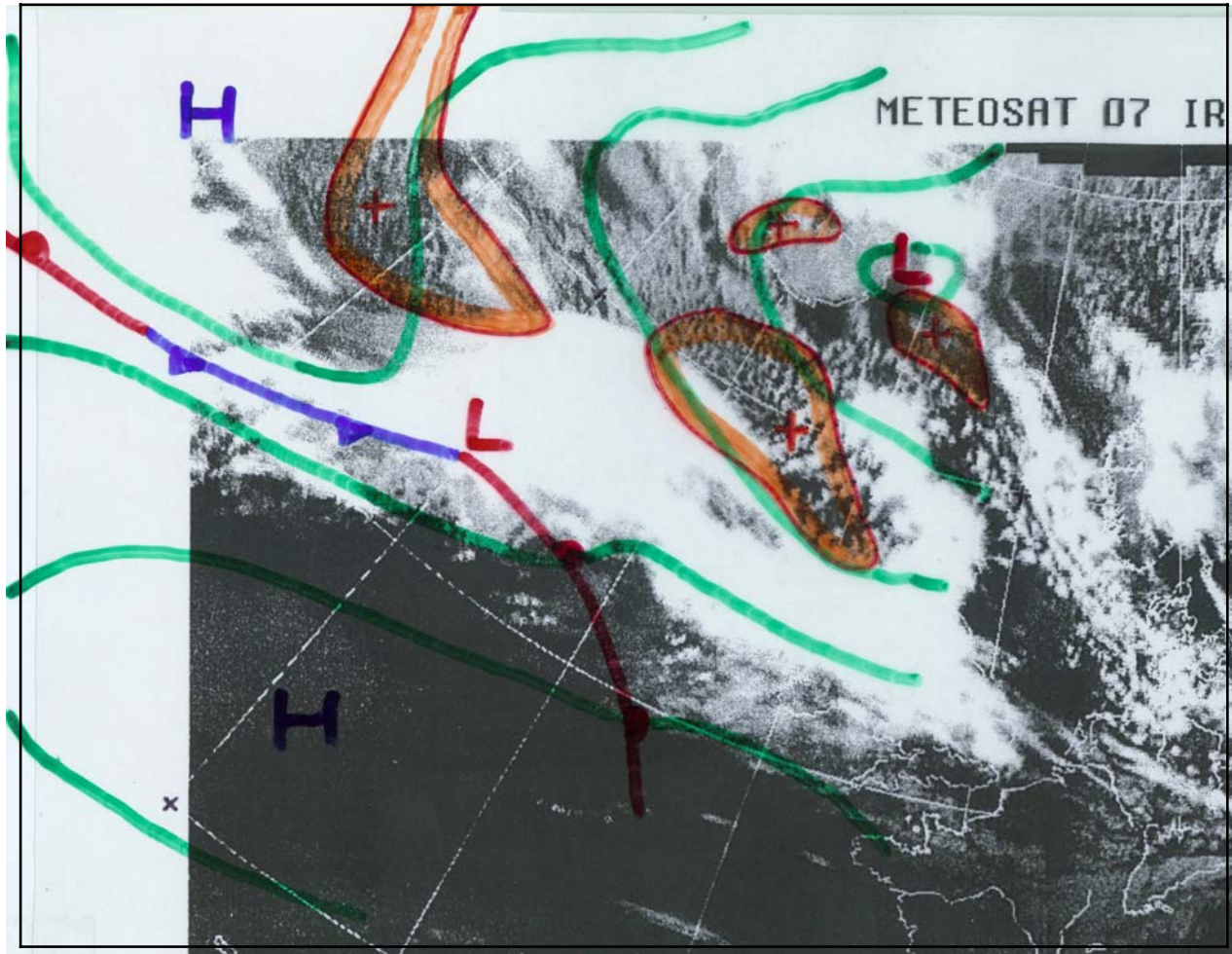
WV-images of Meteosat



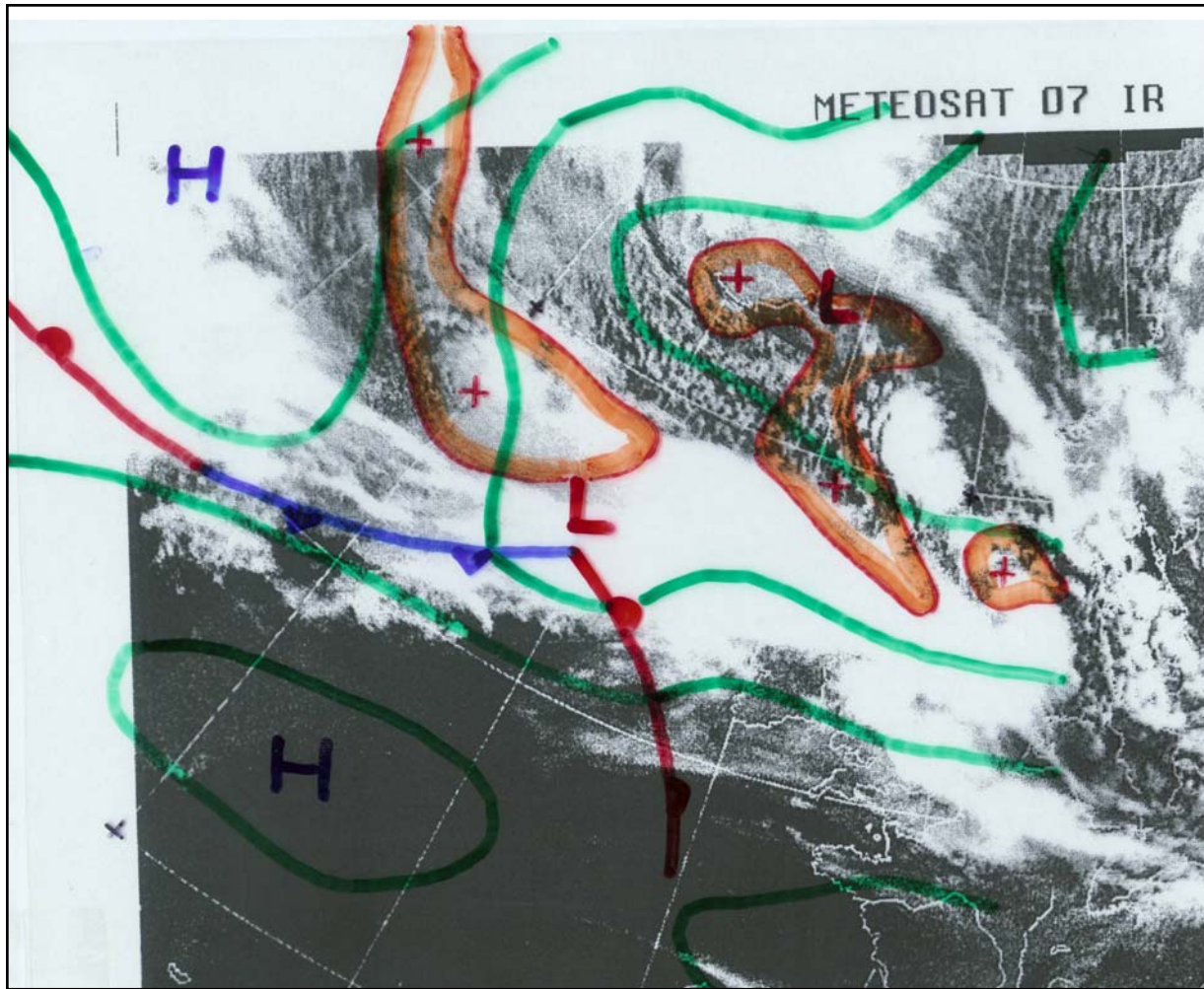
12



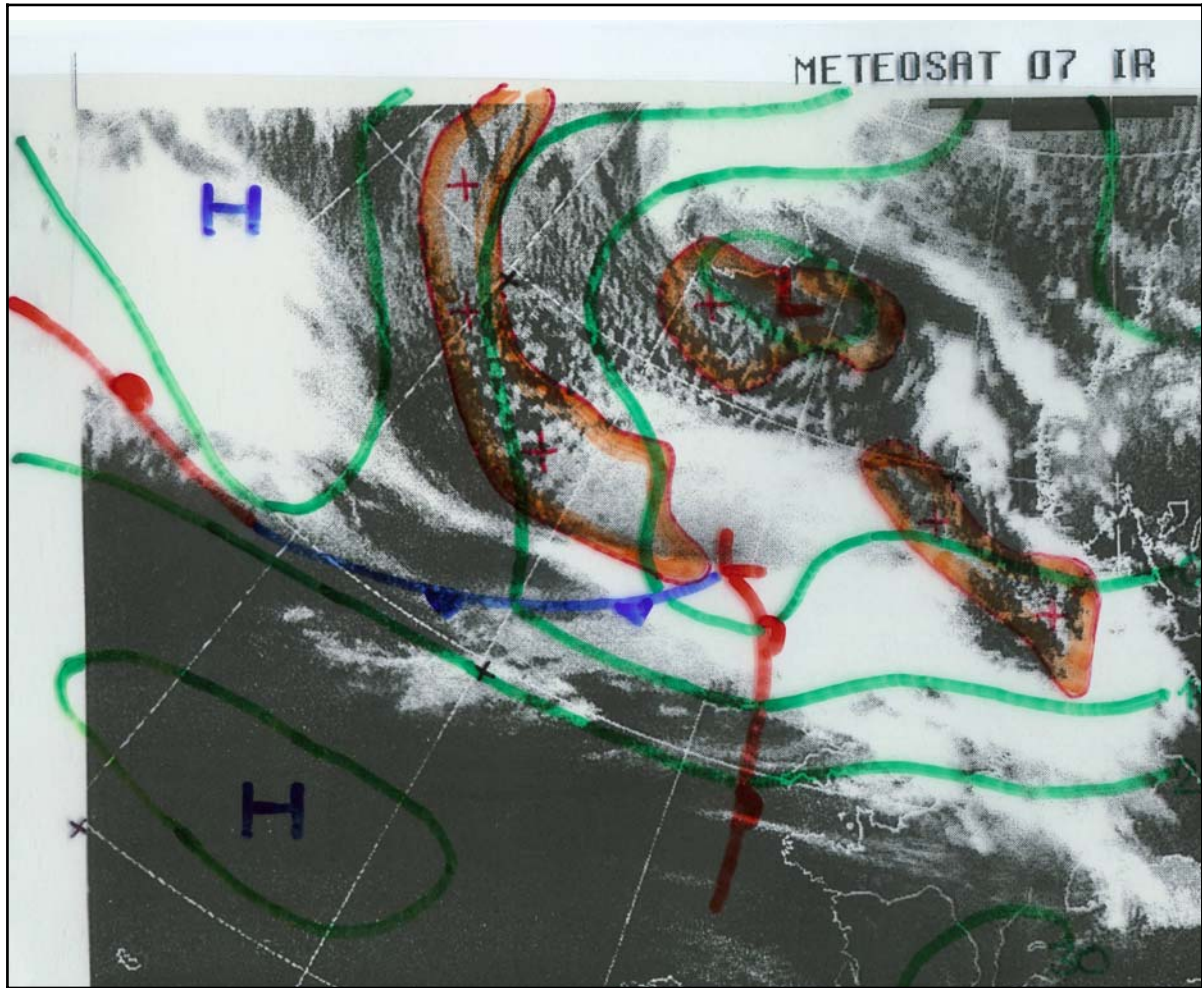
00



02-12-99, 12 UTC: IR-image, surface isobars and fronts, and relative vorticity 500 hPa



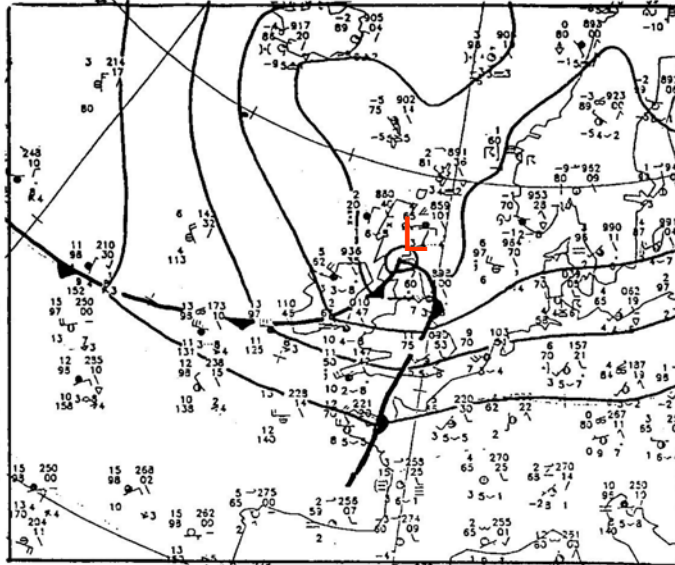
02-12-99, 18 UTC



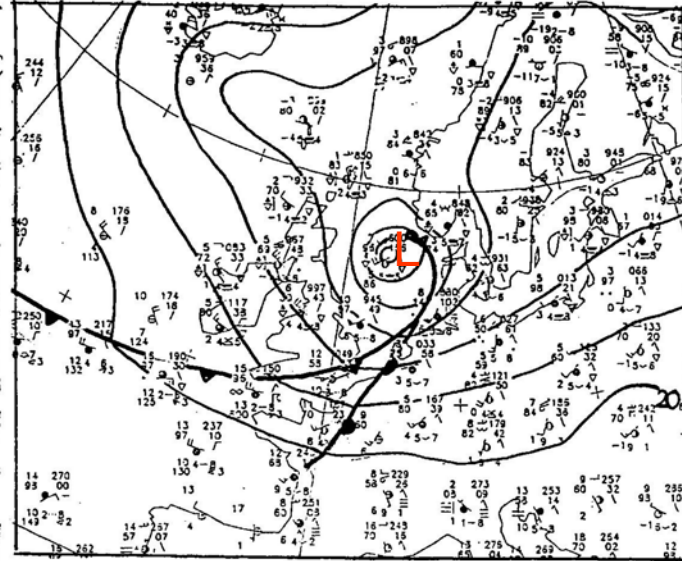
03-12-99, 00 UTC

03/04-12-99

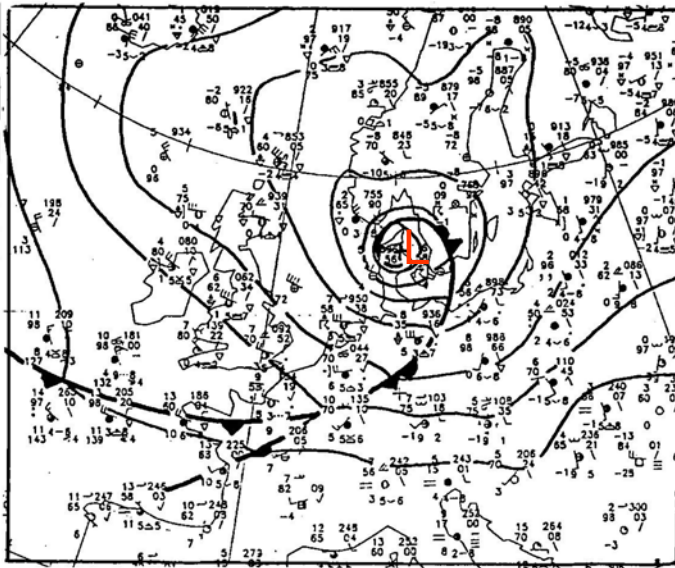
06



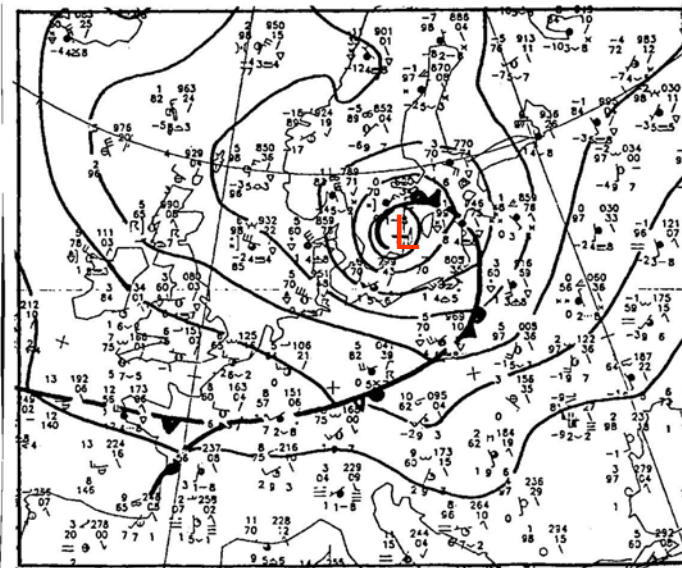
12

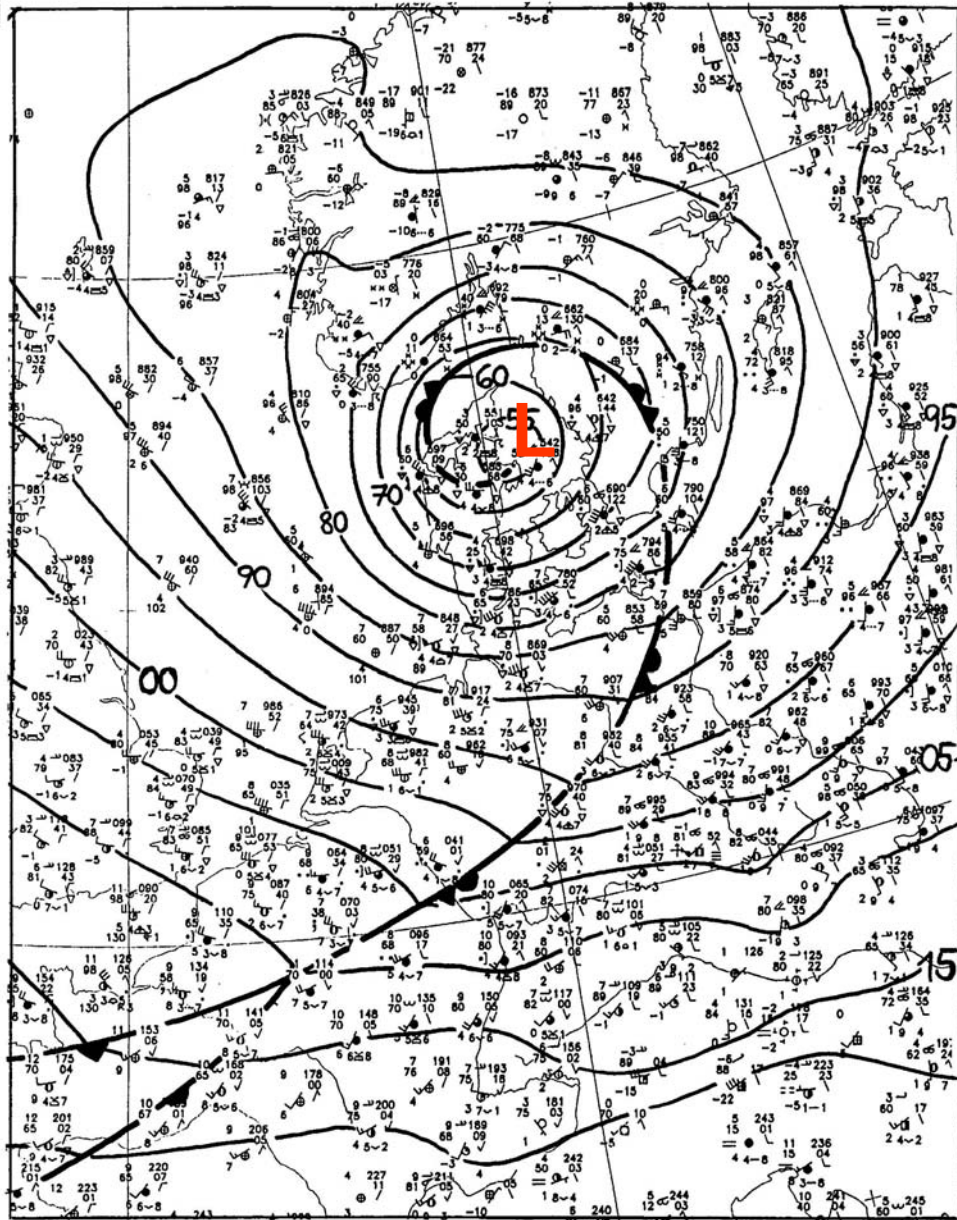


18



00





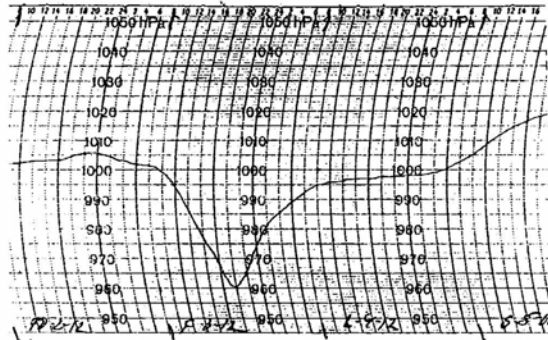
03-12-99, 18 UTC

Abb. 10 b Detailanalyse vom 03.12.99, 18 UTC

HURRICANE ADAM HITS DENMARK

Denmark was hit by the strongest hurricane *since the start of records in 1874*. Seven people were killed and many injured. The centre of the depression went through Denmark in a line from Thyboron in North Jutland and eastward between Laeso and Anholt in Kattegat. The lowest pressure recorded was 952.4 hPa in Anholt at 2000 local time. South of the hurricane (later named Adam) hurricane-strength winds ruled where wind gusts of 40 m/s (144 km/h) or more were recorded. The strongest gusts were in southern Jutland at 51.7 m/s or 186 km/h. Mean 10-minute wind was highest at Rosnaes with 39 m/s or 140 km/h. In spite of the ebb tide there was a notable storm surge in southern Jutland where the water level rose to 5.6 metres above normal with much flooding. Some dikes, as at Romo, were broken and sheep drowned. There was considerable damage to buildings and farms with roofs blown off and even a church smashed. The power supply was cut in many areas, and in places took up to 8 days to restore. The woods are badly affected, and in the south many trees were snapped off one to two metres above the ground. The total cost of the damage is unknown, but current indications suggest more than 4 million d. kr. This is five times as costly as the nation's last hurricane which was on 24 November 1981.

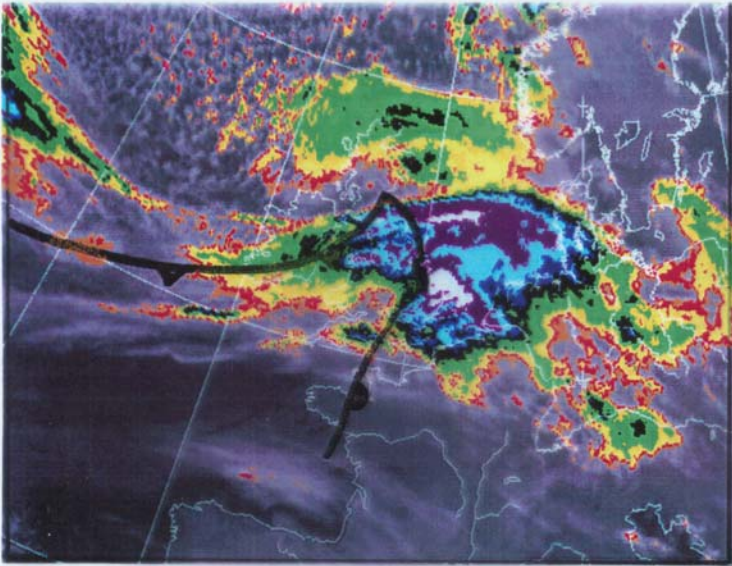
At my place in Frederikssund, the house survived without hurt but five trees were damaged. One tree crashed into my garage. I recorded a gust of 40.3 m/s, or 145 km/h, and a mean 10-minute wind of 29.2 m/s, 105 km/h (Beaufort force 11). Both are by far the highest that I have measured. My lowest pressure was 961.2 hPa at 2000 hrs.



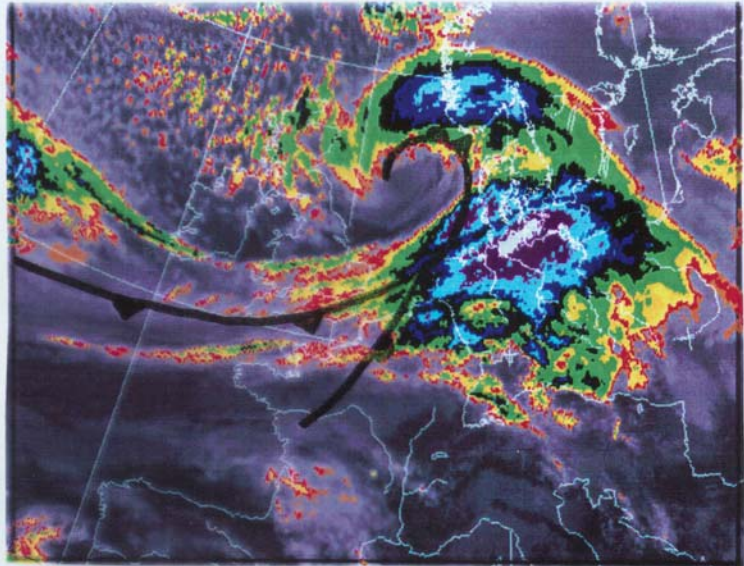
DK-3600 Frederikssund, Denmark

EBBE SKJODT

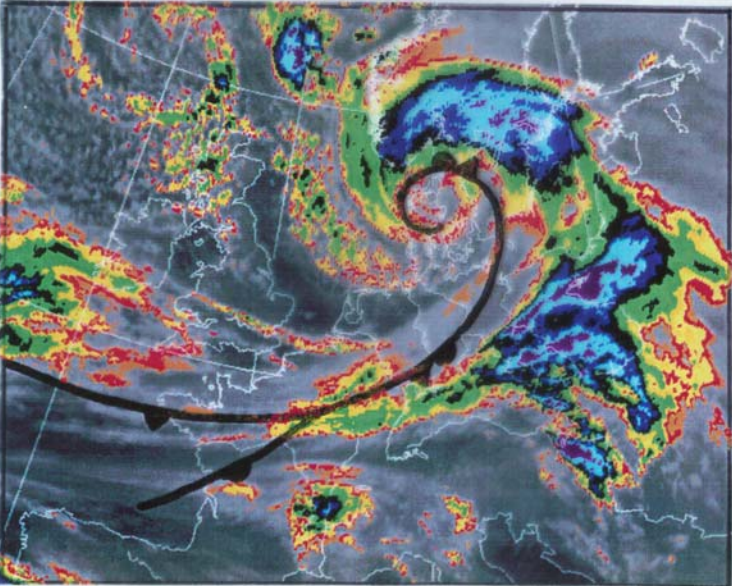
06



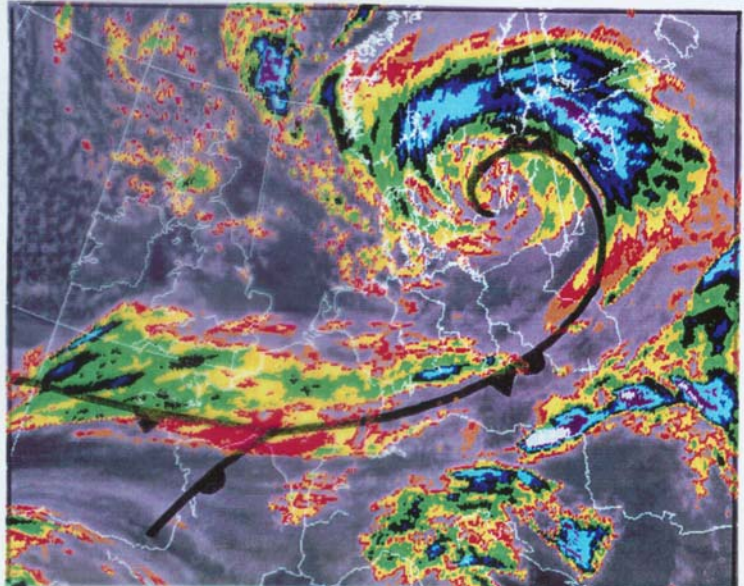
12

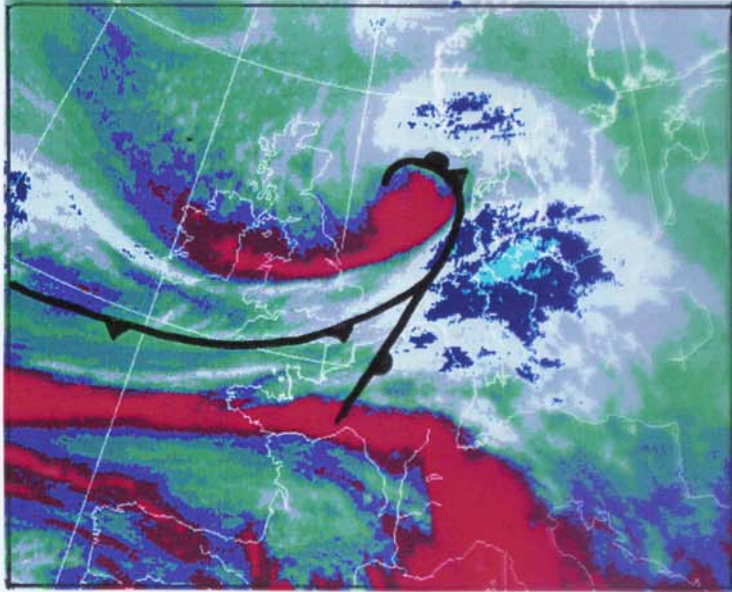


18

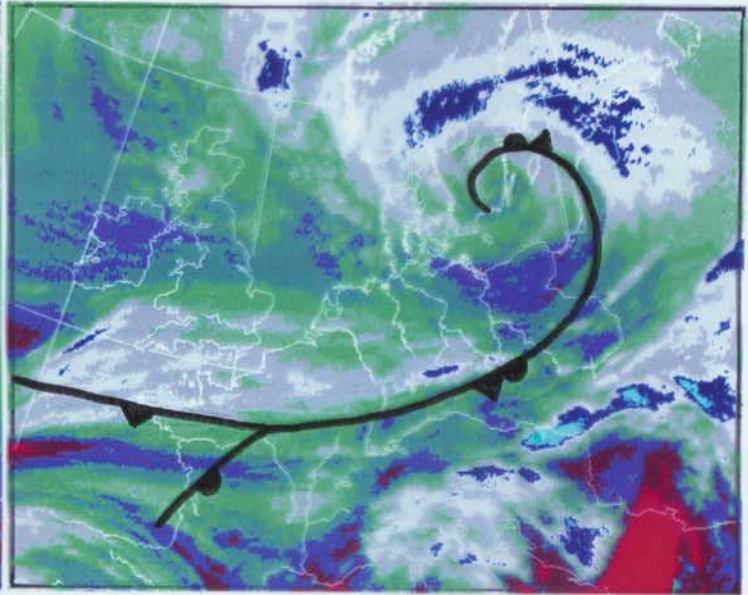


00



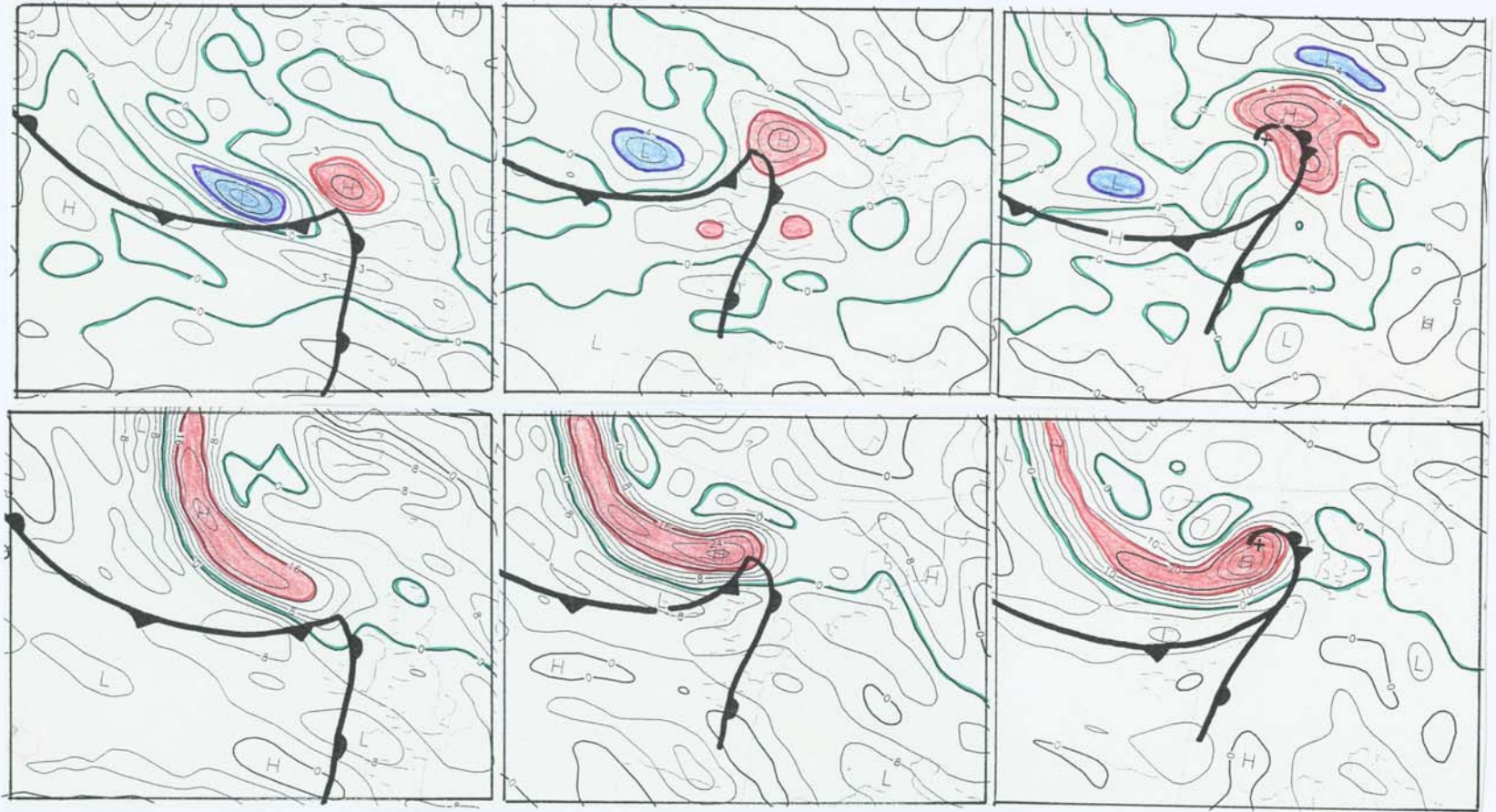


12



00

03-12-1999



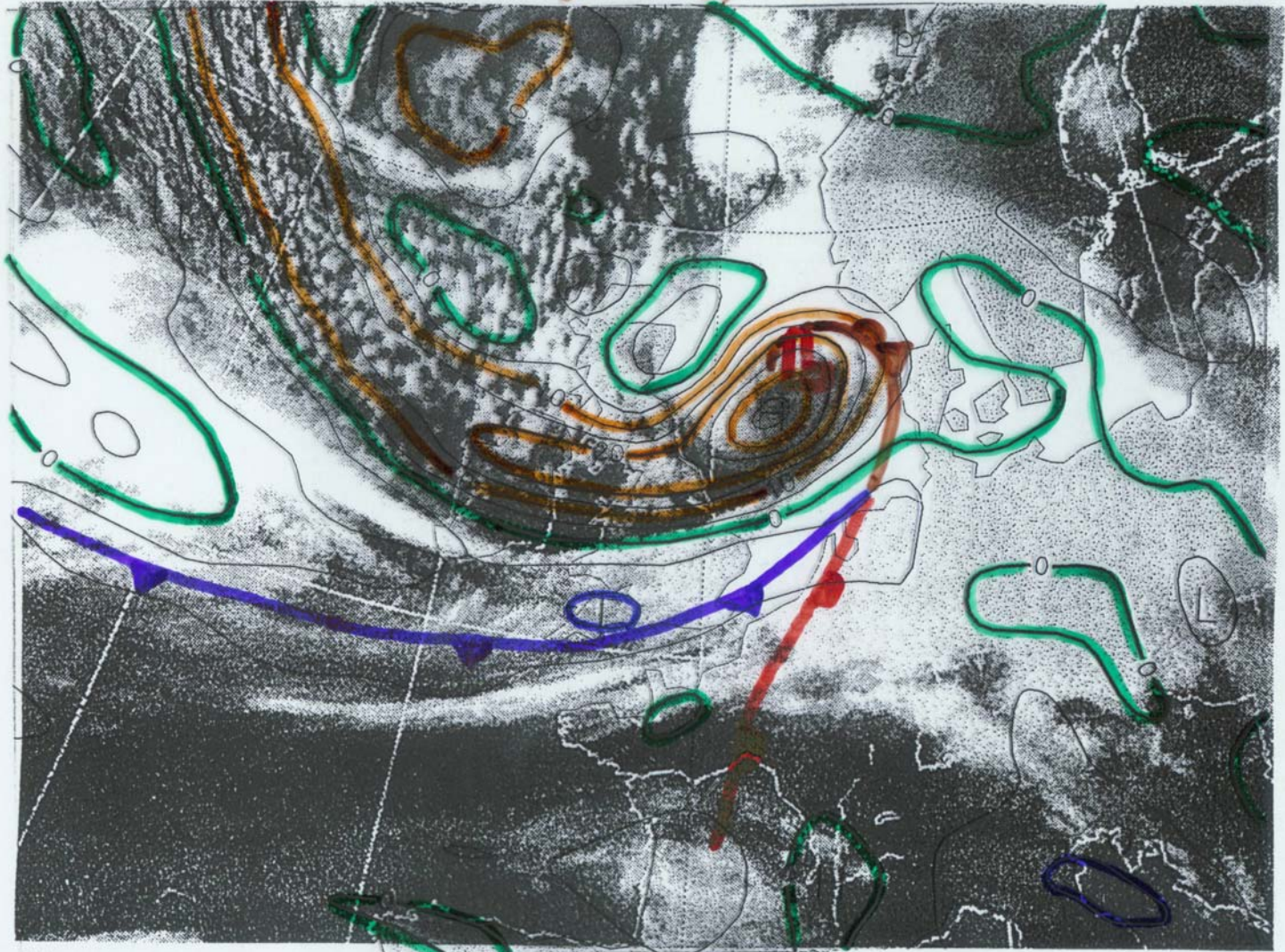
00

06

12

Top: Divergence 300 hPa; bottom: Relative vorticity 500 hPa

ECMWF analysis: ζ 500hPa

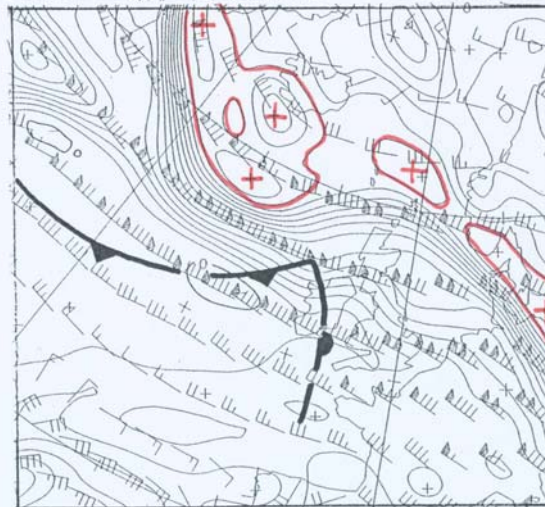
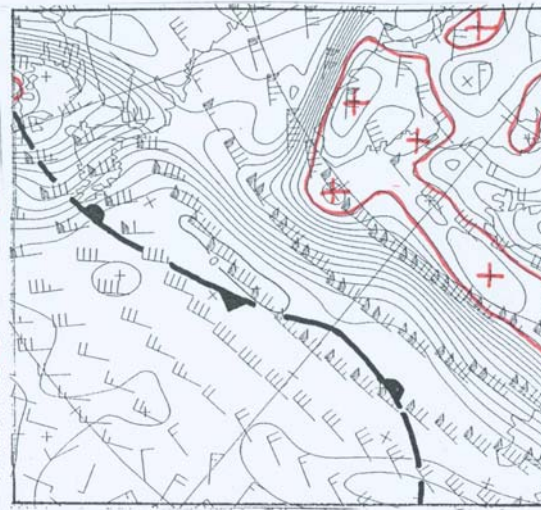


03-12-99,12

02-12-99,
00

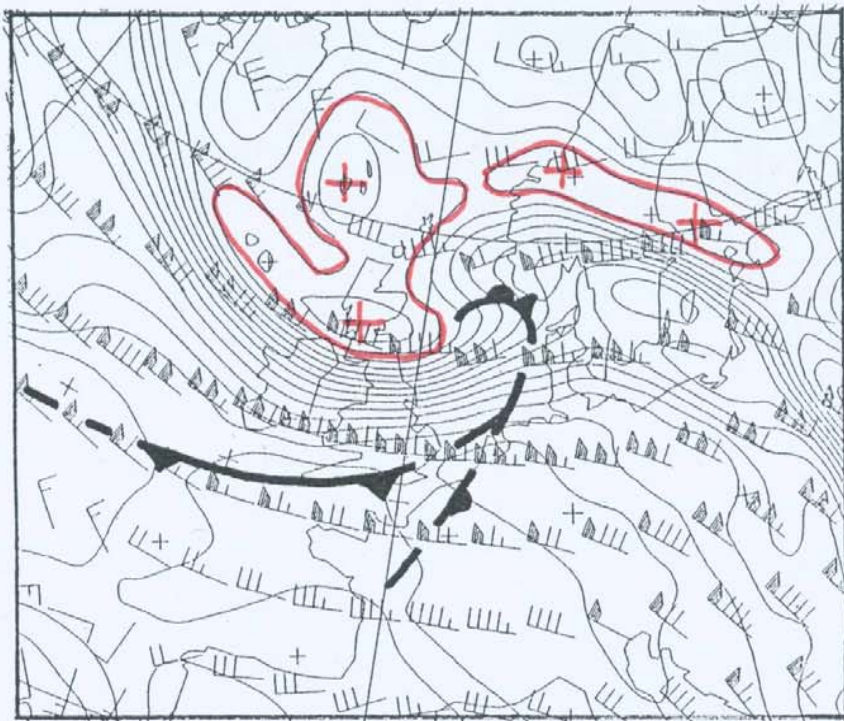


02-12-99,
12

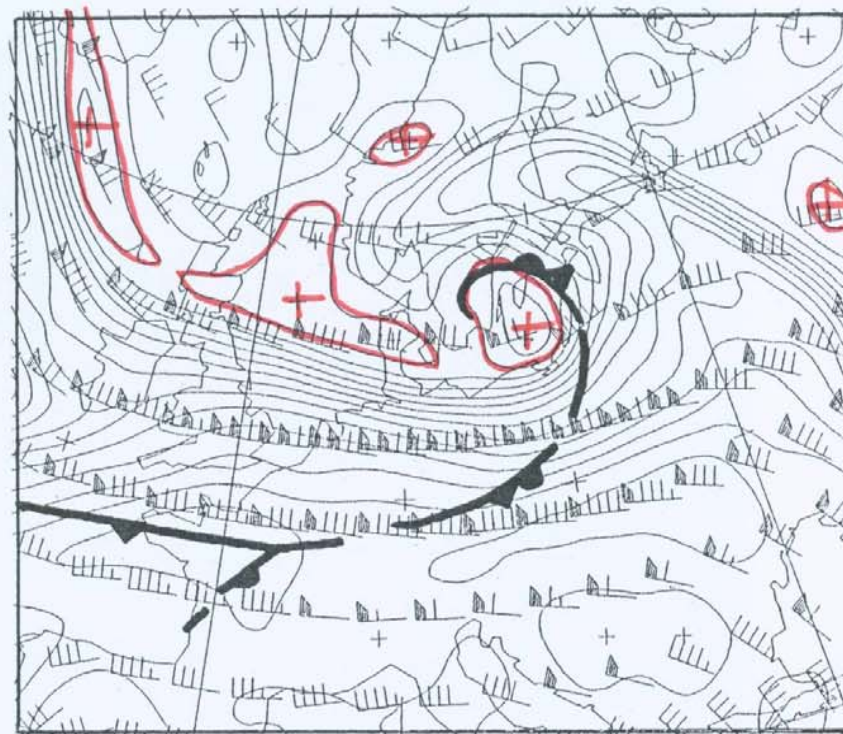


03-12-99, 00

Isentropic potential vorticity (IPV) and winds on 320 K

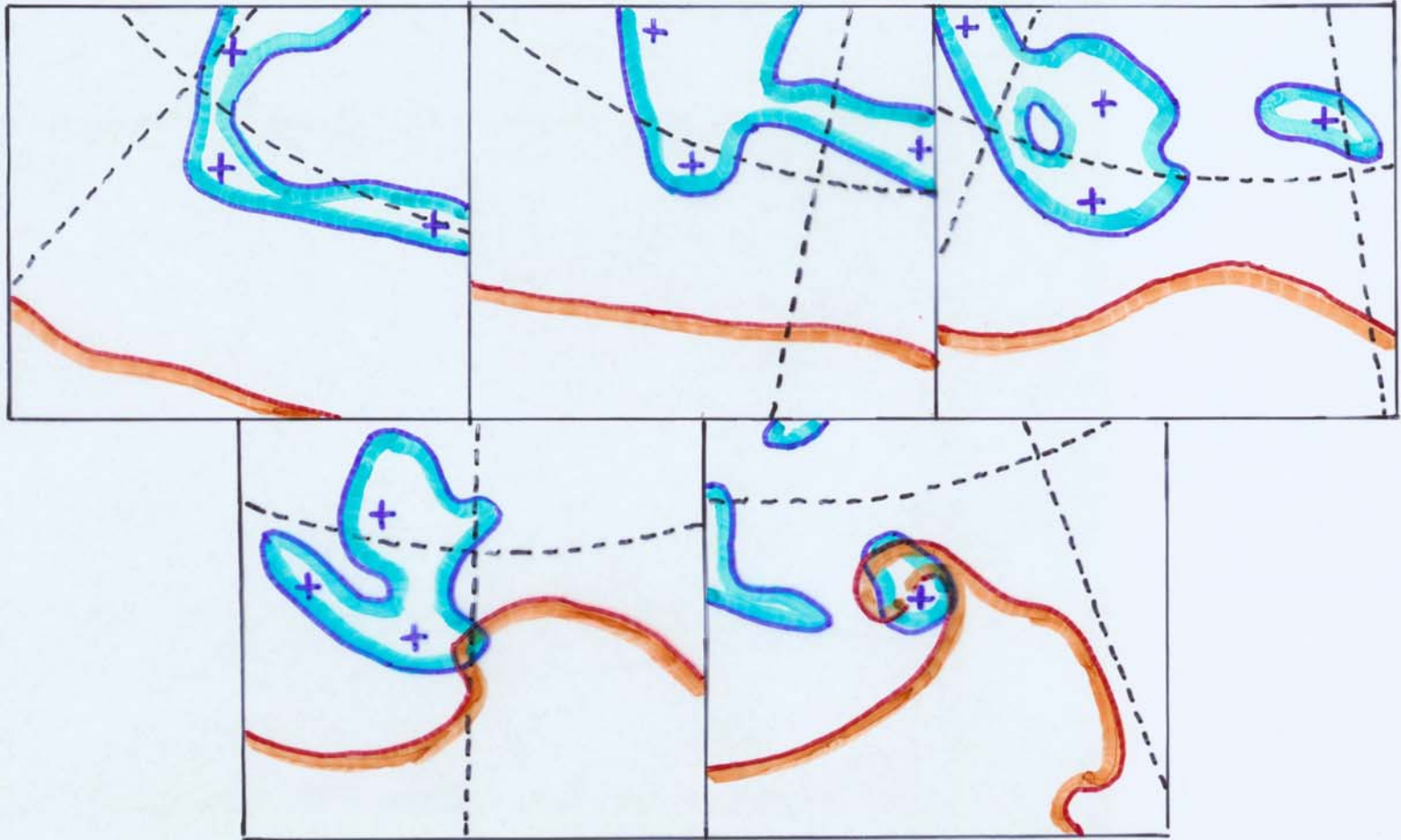


03-12-99, 12



04-12-99, 00

IPV and winds on 320 K



IPV on 320 K (blue) ; EPT 850 hPa (red)

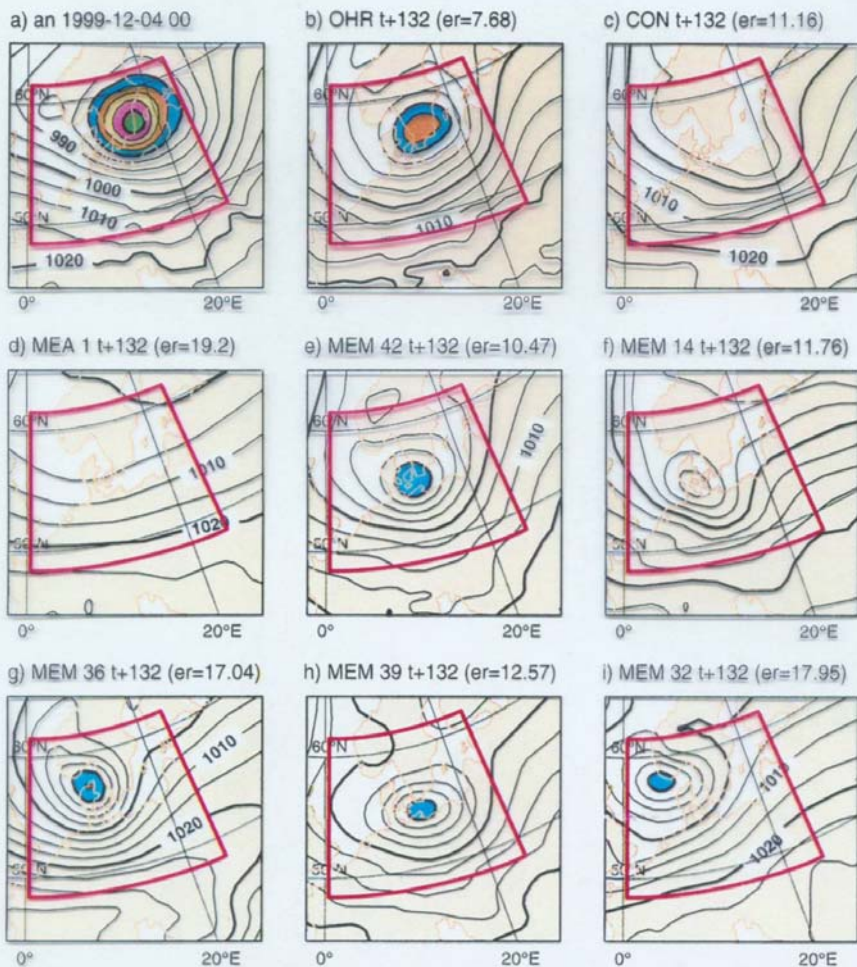
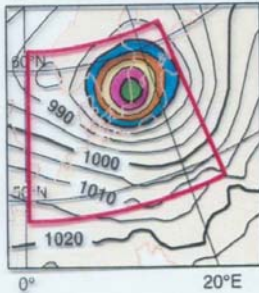
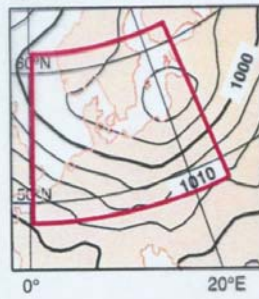


Figure 1 The Danish storm. (a) The MSLP analysis at the verification time 00 UTC 4 December 1999. The other panels show t+132h forecasts started at 12 UTC 28 November (er is the root-mean-square error (hPa), IE is the intensity error (hPa) and PE is the position error (km)). (b) The T_L319L60 forecast (IE=13hPa, PE=149km), (c) the EPS control forecast (IE=33hPa, PE=348km), (d) the EPS ensemble-mean forecast, (e) EPS member 42 (the lowest RMSE, IE=18hPa (the second lowest), PE=341km), (f) EPS member 14 (the second lowest RMSE, IE=25hPa, PE=452km), (g) EPS member 36 (IE=17hPa (the lowest), PE=637km), (h) EPS member 39 (IE=21hPa, PE=333km), and (i) EPS member 32 (IE=20hPa, PE=637km). No EPS member had an RMSE smaller than the T_L319L60 forecast and one member had an RMSE smaller than the EPS control. The contour interval is 5hPa, with shading for values below 980hPa.

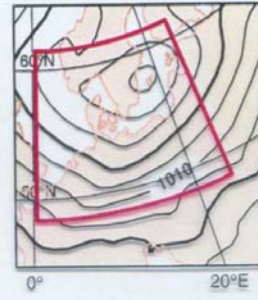
a) an 1999-12-04 00



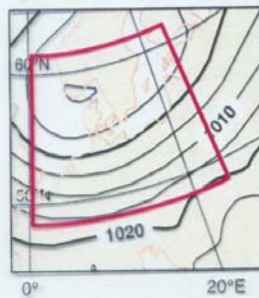
b) OHR t+84 (er=10.58)



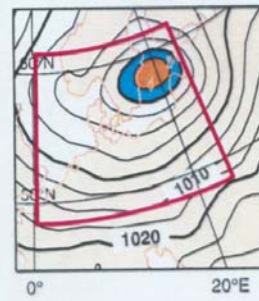
c) CON t+84 (er=9.42)



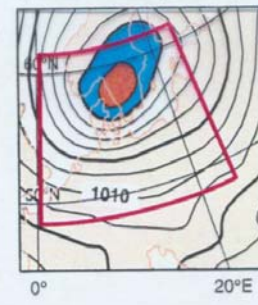
d) MEA 1 t+84 (er=12.12)



e) MEM 6 t+84 (er=6.11)



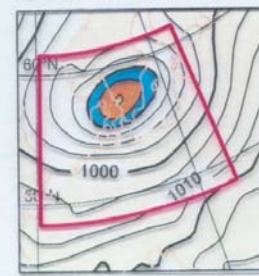
f) MEM 14 t+84 (er=6.62)



g) MEM 29 t+84 (er=9.32)



h) MEM 48 t+84 (er=7.7)



i) MEM 40 t+84 (er=11.08)



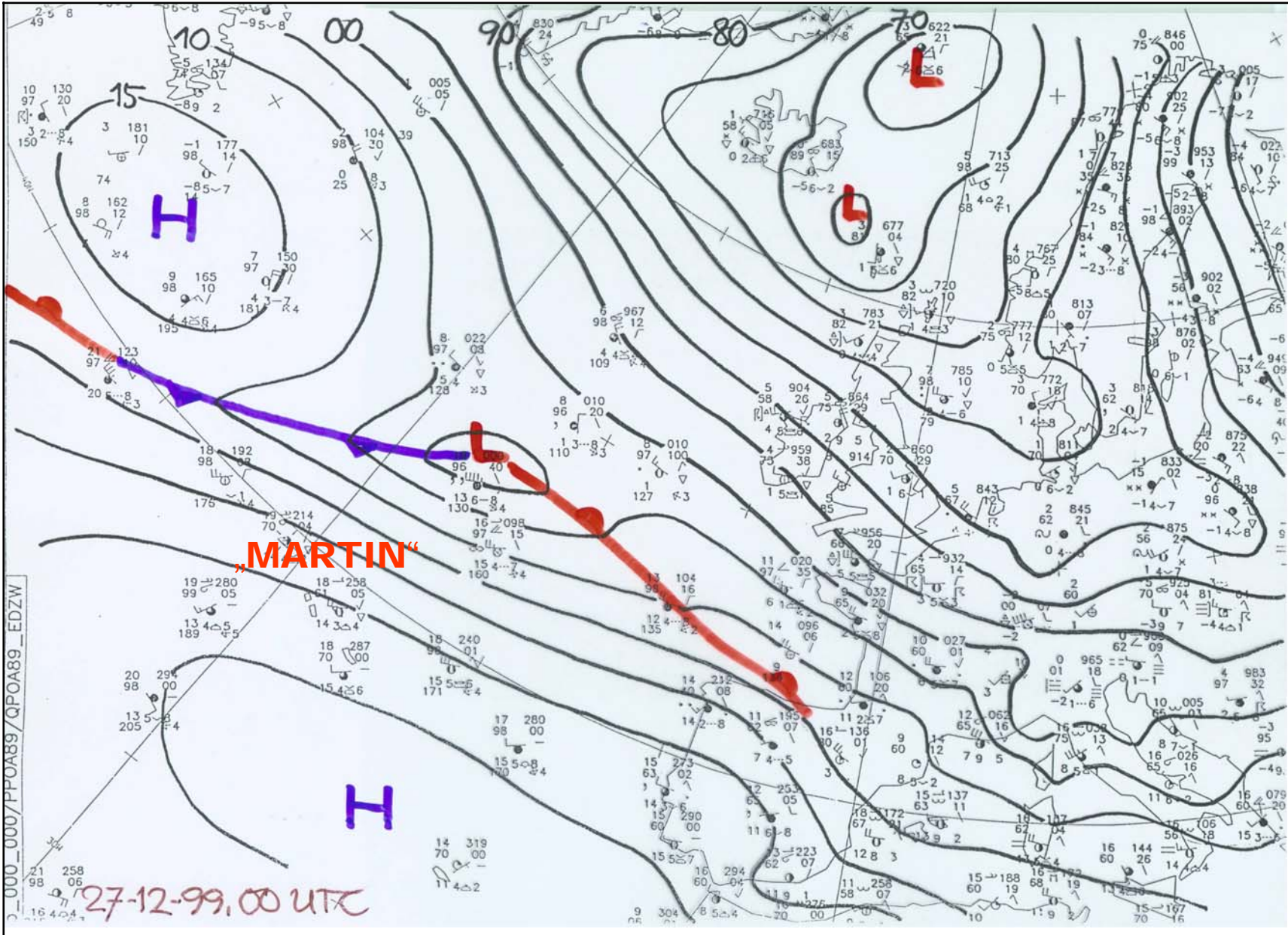
Figure 2 The Danish storm. (a) The MSLP analysis at the verification time 00 UTC 4 December 1999. The other panels show t+84h forecasts started at 12 UTC 30 November (er is the root-mean-square error (hPa), IE is the intensity error (hPa) and PE is the position error (km)). (b) The T_L319L60 forecast (IE=28hPa, PE=292km), (c) the EPS control forecast (IE=25hPa, PE=107km), (d) the EPS ensemble-mean forecast, (e) EPS member 6 (the lowest RMSE, IE=14hPa, PE=202km), (f) EPS member 14 (the second lowest RMSE, IE=14hPa, PE=228km), (g) EPS member 29 (IE=7hPa (the lowest), PE=115km), (h) EPS member 48 (IE=13hPa (the second lowest), PE=226km), and (i) EPS member 40 (IE=20hPa, PE=329km). Ten EPS members had RMSEs smaller than the T_L319L60 forecast and seven member had RMSEs smaller than the EPS control. The contour interval is 5hPa, with shading for values below 980hPa.

Conclusions

- The development of the storm „Anatol“ was a typical example for the PETTERSEN scheme of cyclogenesis.
- The approach of the upper vorticity maximum to the frontal wave in the lower troposphere was made visible by the satellite imagery of METEOSAT and could be monitored with the aid of it.
- Most of the operationally available NWP models performed well in simulating this development already some days ago. Therefore the issue of warnings well in advance was possible.

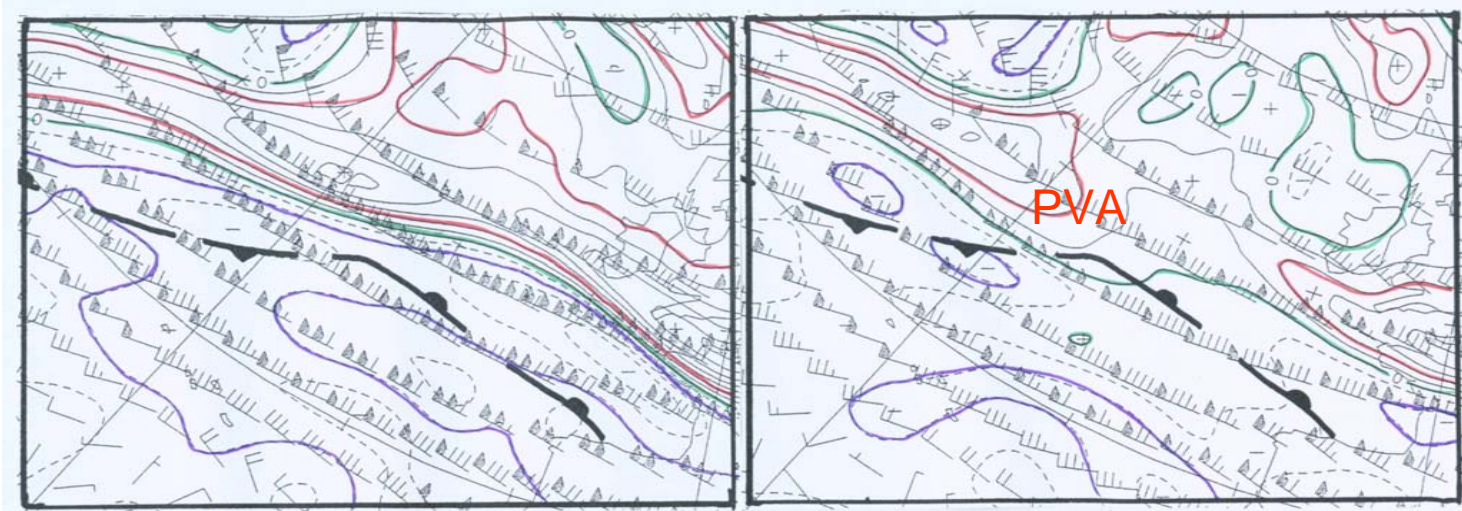
Examples (II)

- **The storm „Martin“
(27/28-12-1999)**

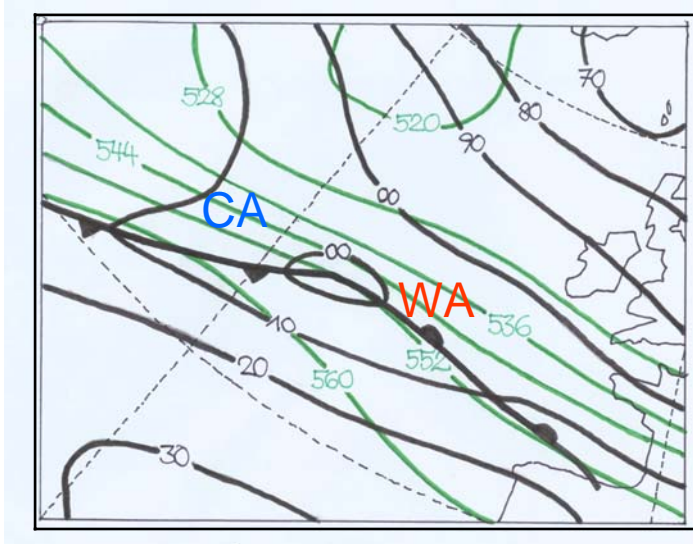


Relative vorticity and winds

300 hPa

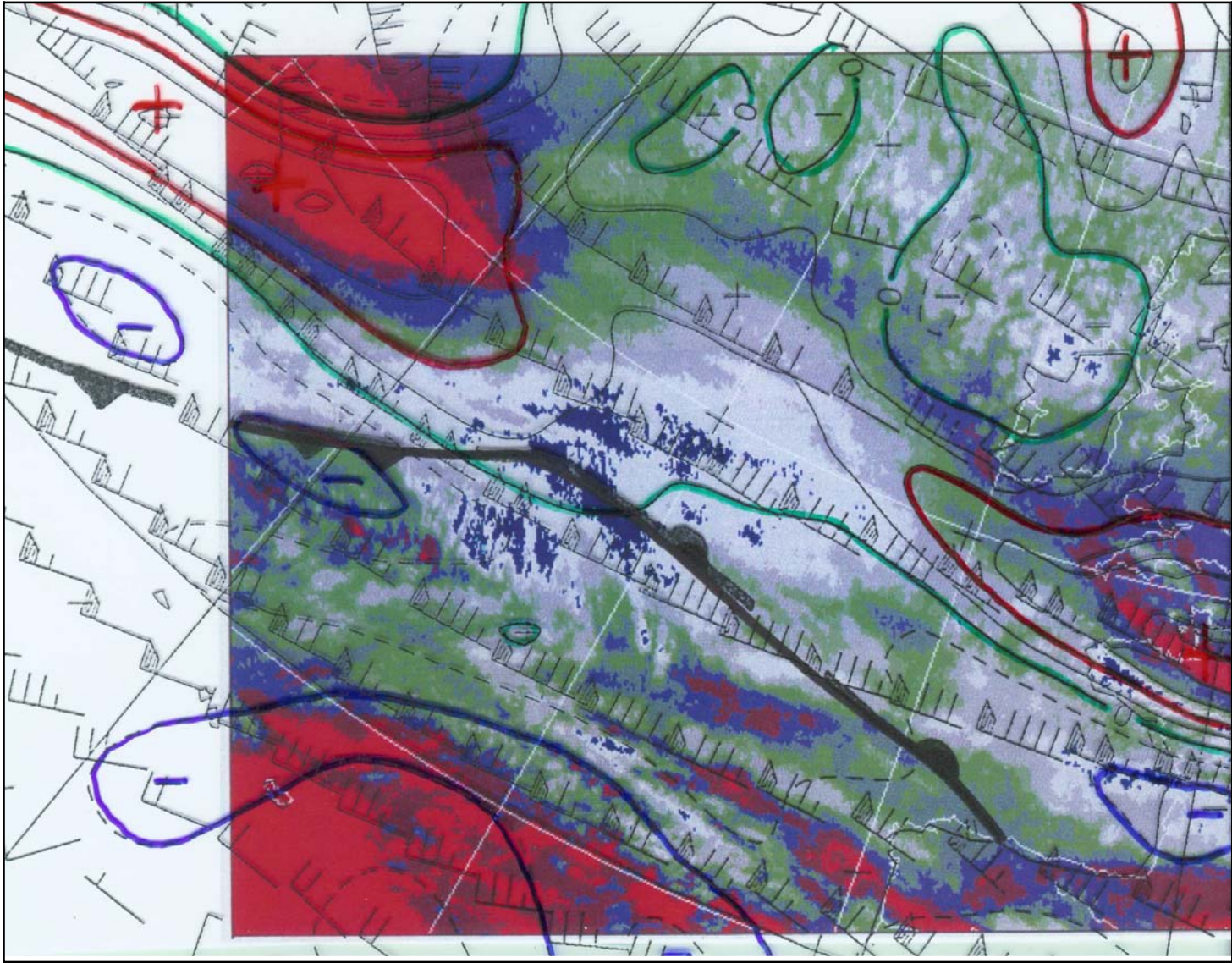


500 hPa



Surface pressure and
relative topographic
500/1000 hPa (green)

27-12-99, 00 UTC



27-12-99, 00 UTC:: WV image and vorticity and winds 500 hPa

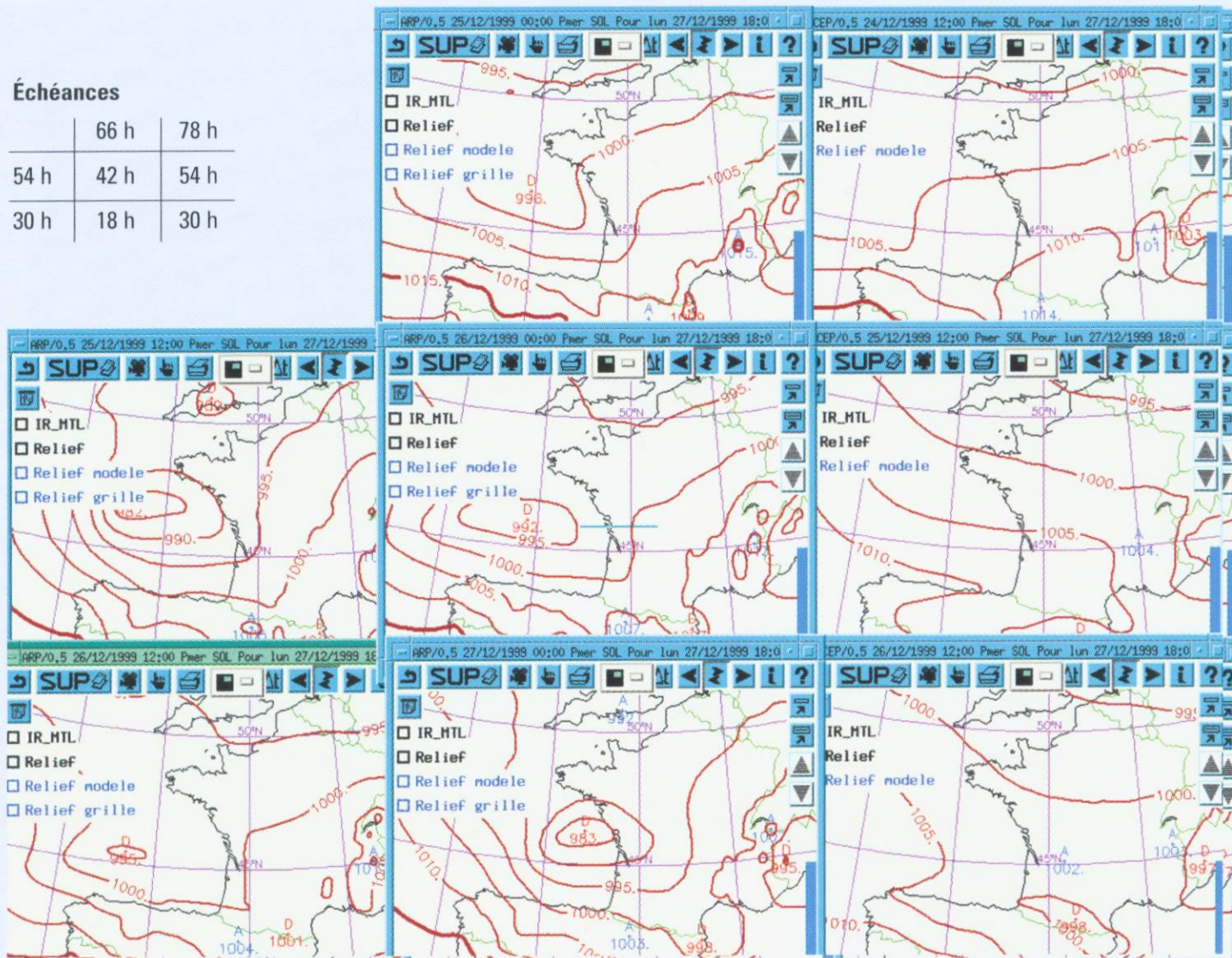
ARPEGE base 12 UTC

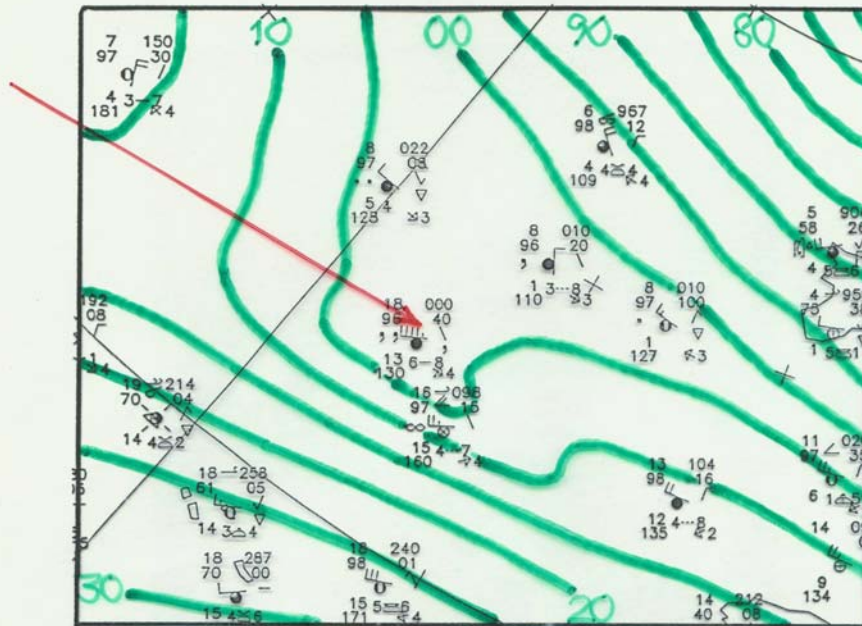
ARPEGE base 00 UTC

CEP base 12 UTC

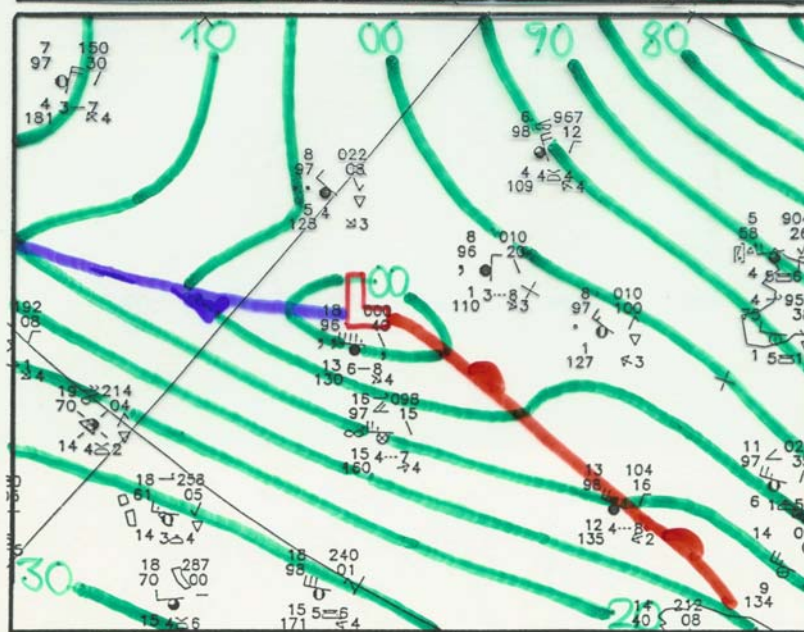
Échéances

	66 h	78 h
54 h	42 h	54 h
30 h	18 h	30 h





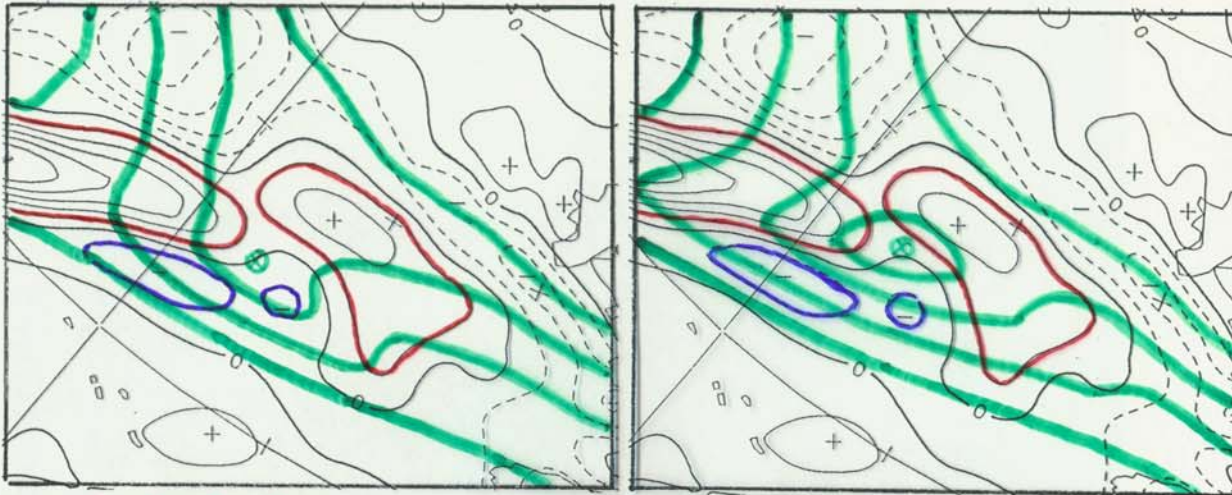
num.
Analyse



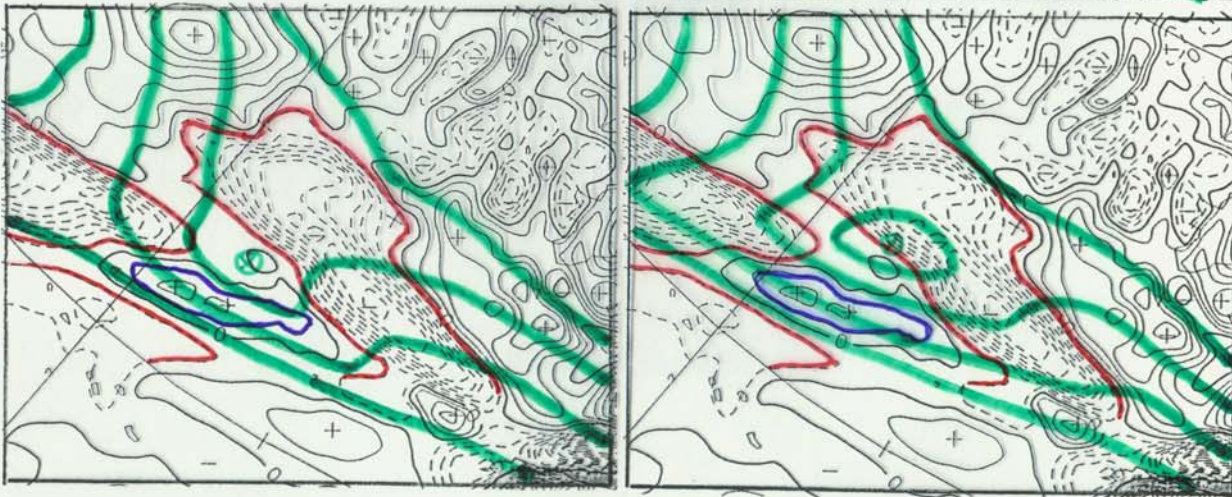
man.
Analyse

27-12-99,00

27-12-99,00



$\nabla \cdot \mathbf{v}$ 300 hPa

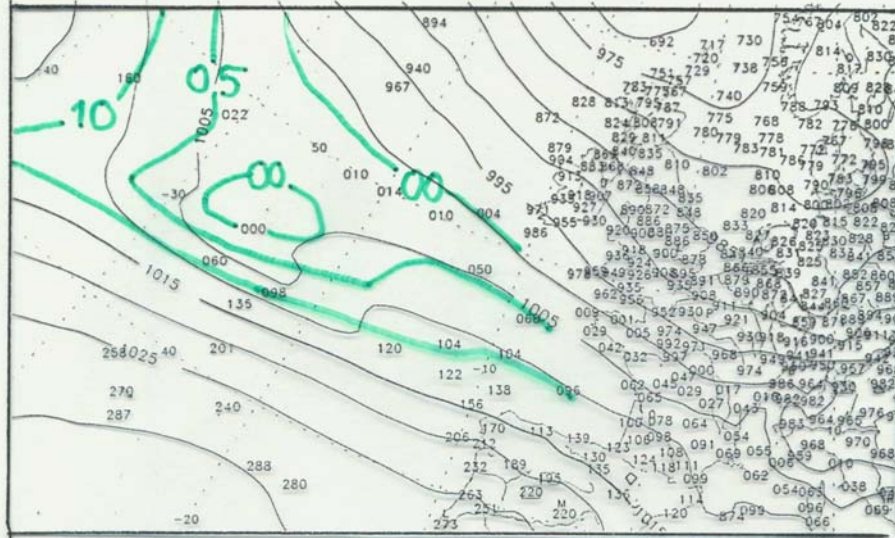


ω 500 hPa

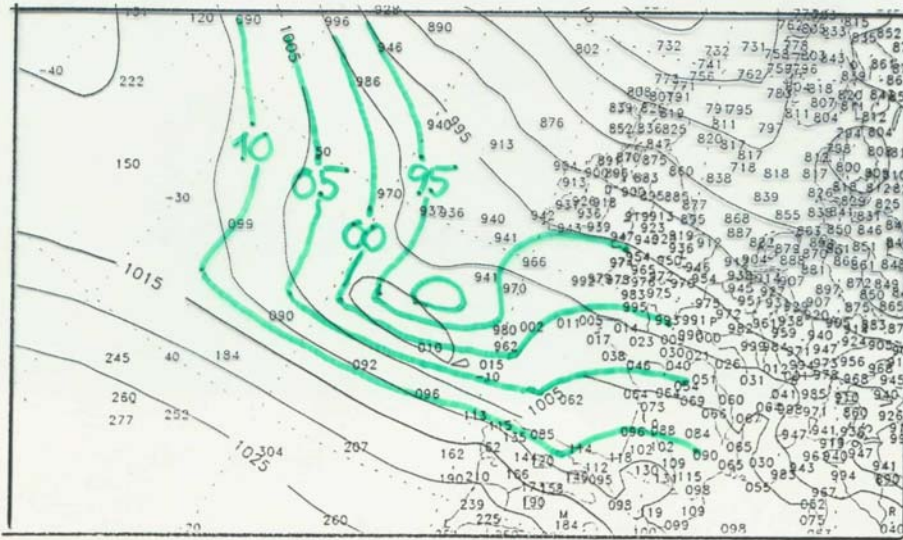
num. Analyse

man. Analyse

27-12-99, 00 UTC

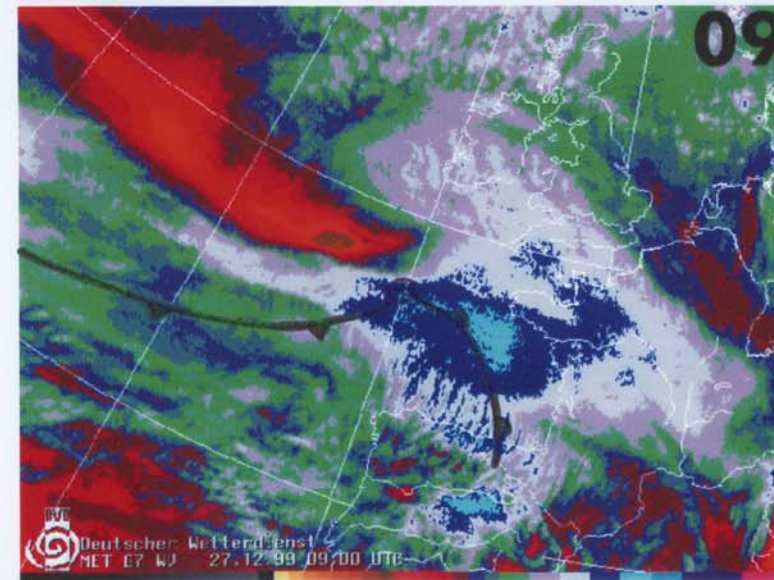
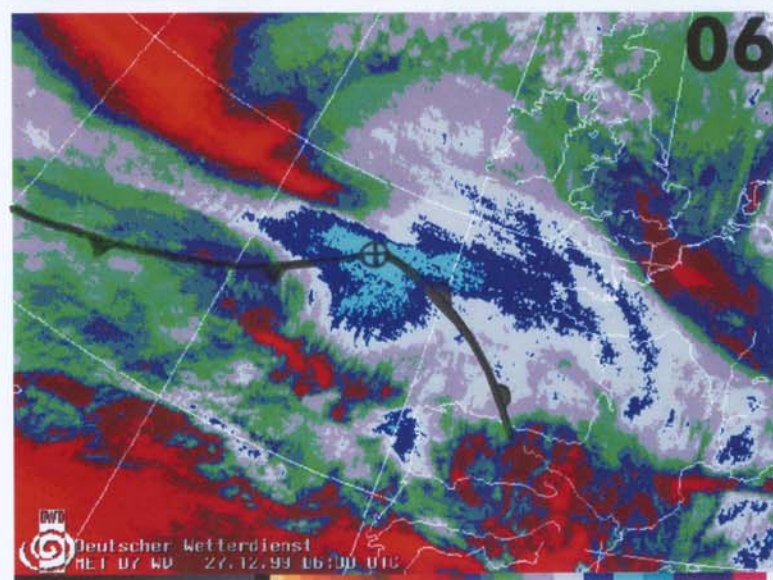
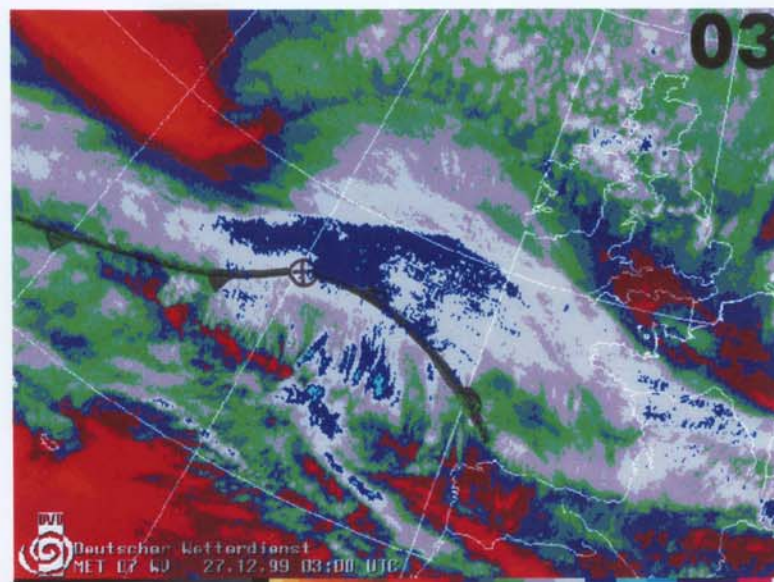
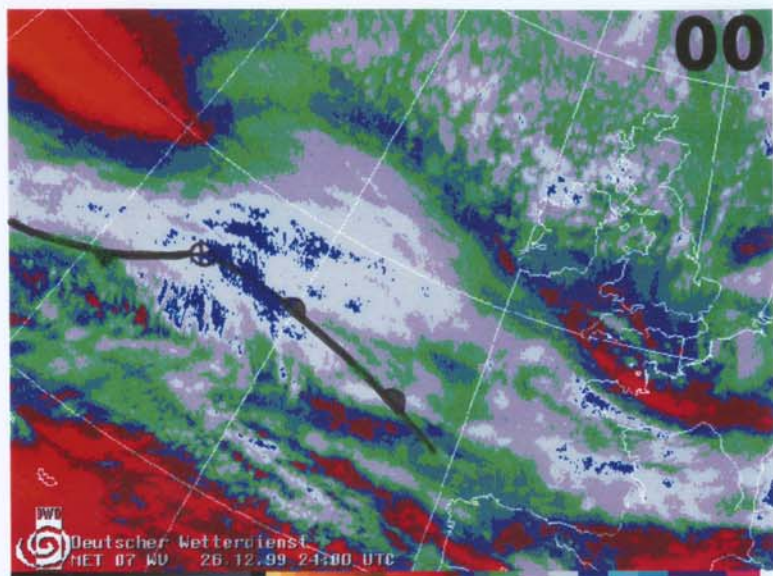


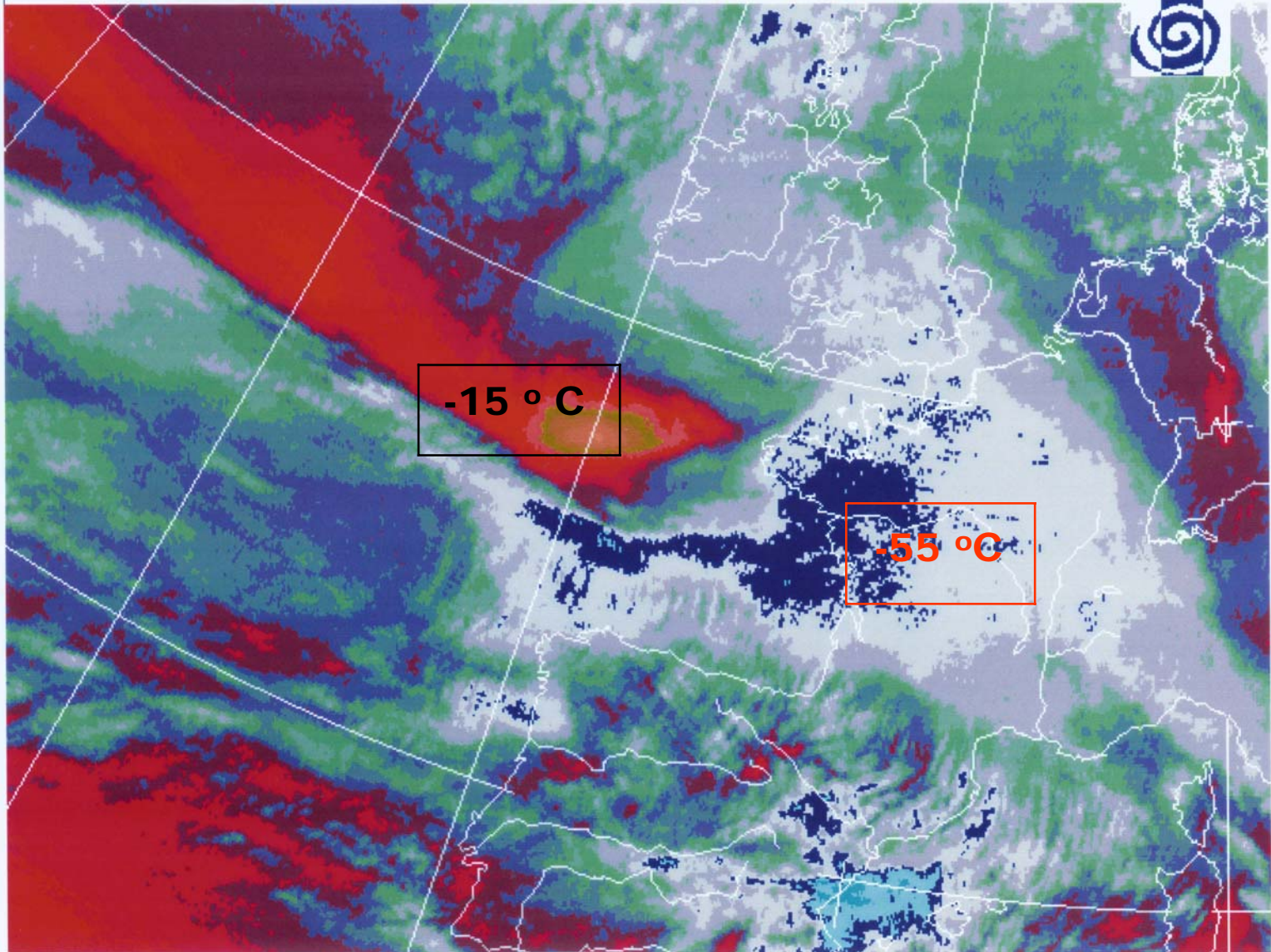
ANA



+06

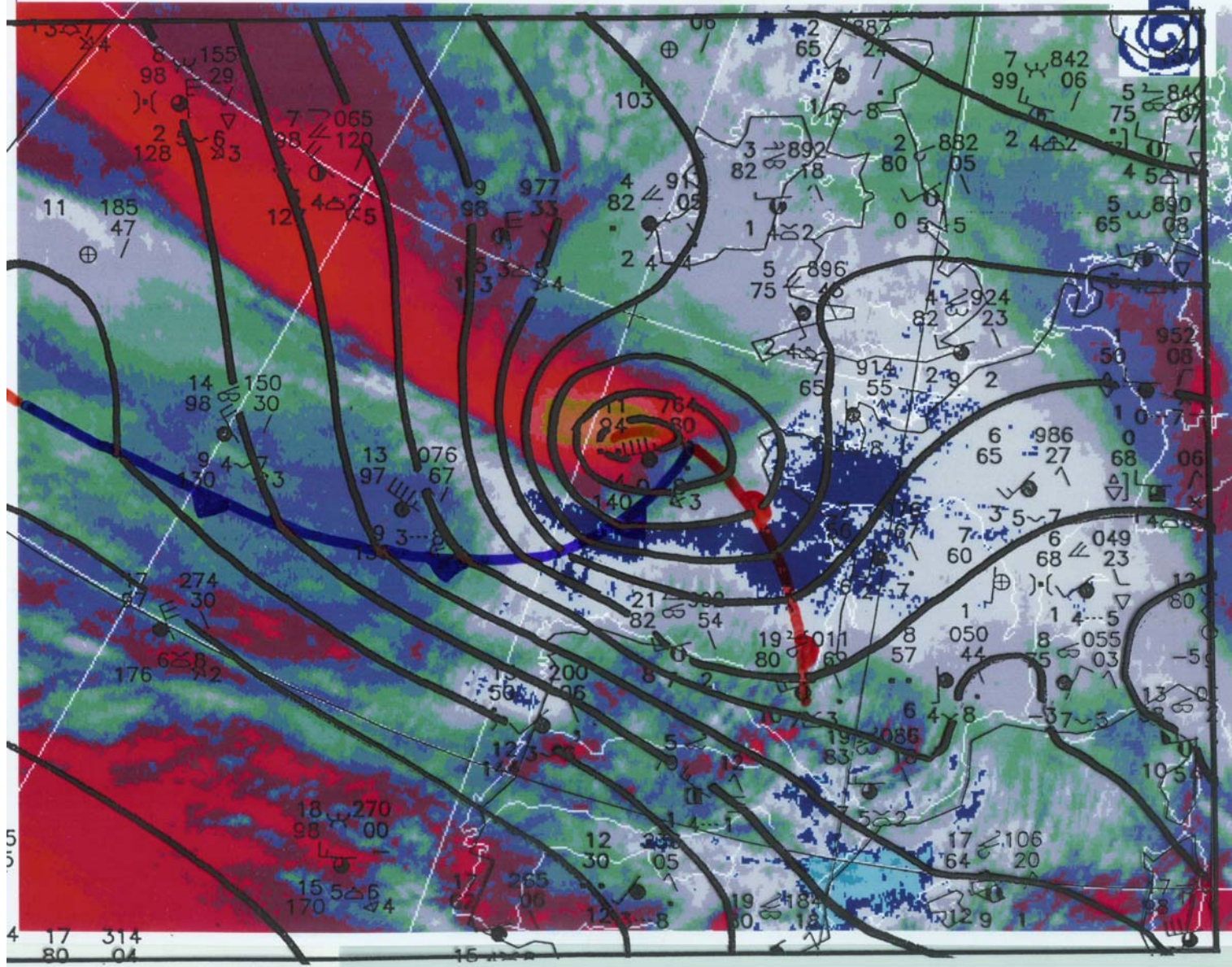
forecasted: 998 hPa observed: 989 hPa

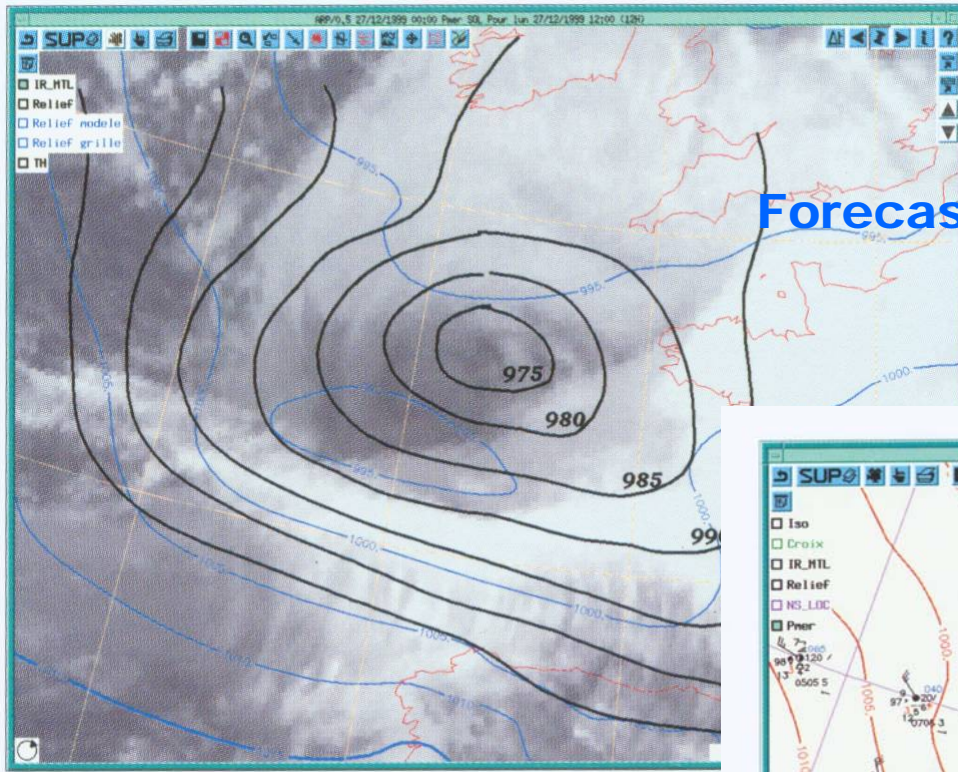




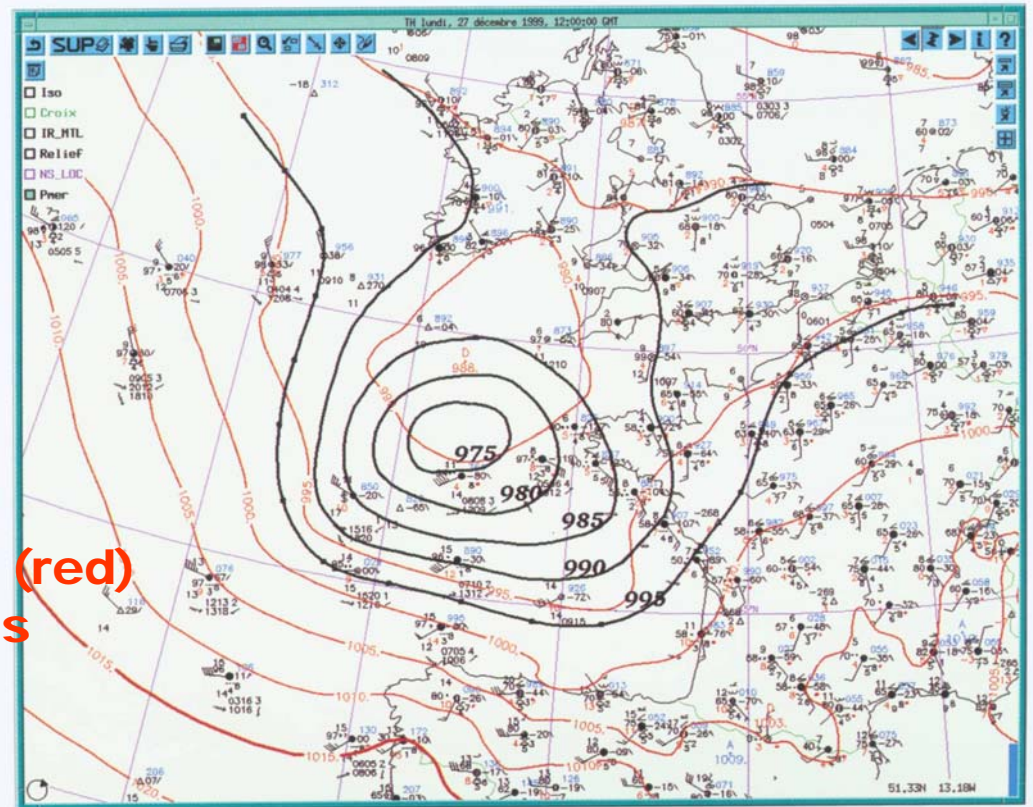
METEOSAT 07 WU 27-Dez-1999 12:00

DWD

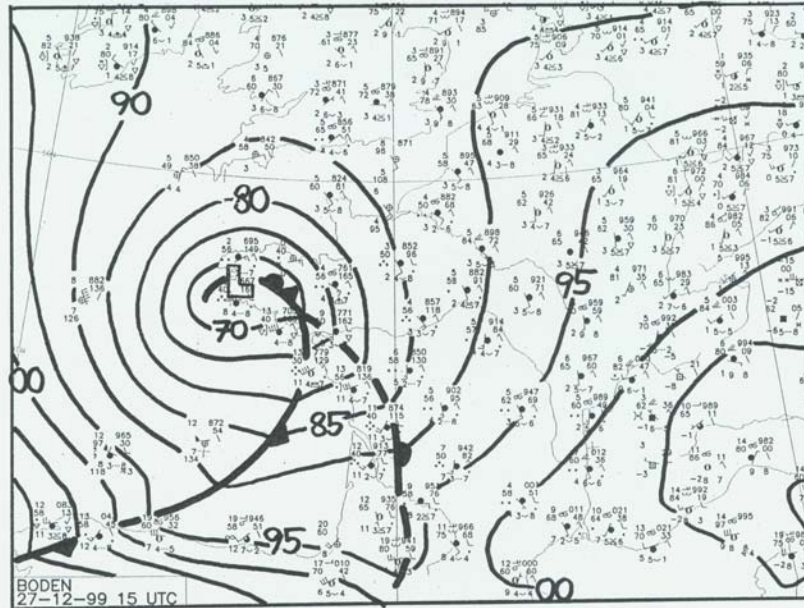




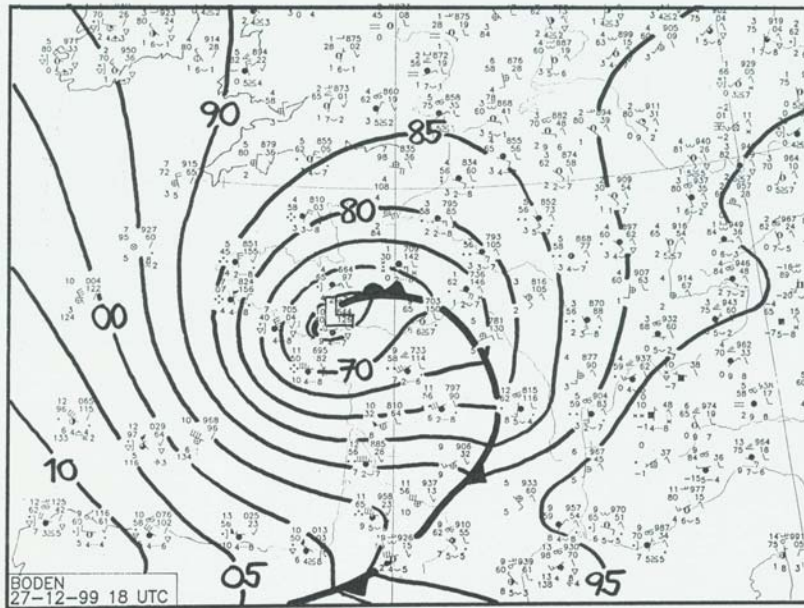
Forecast (blue) and manual analysis



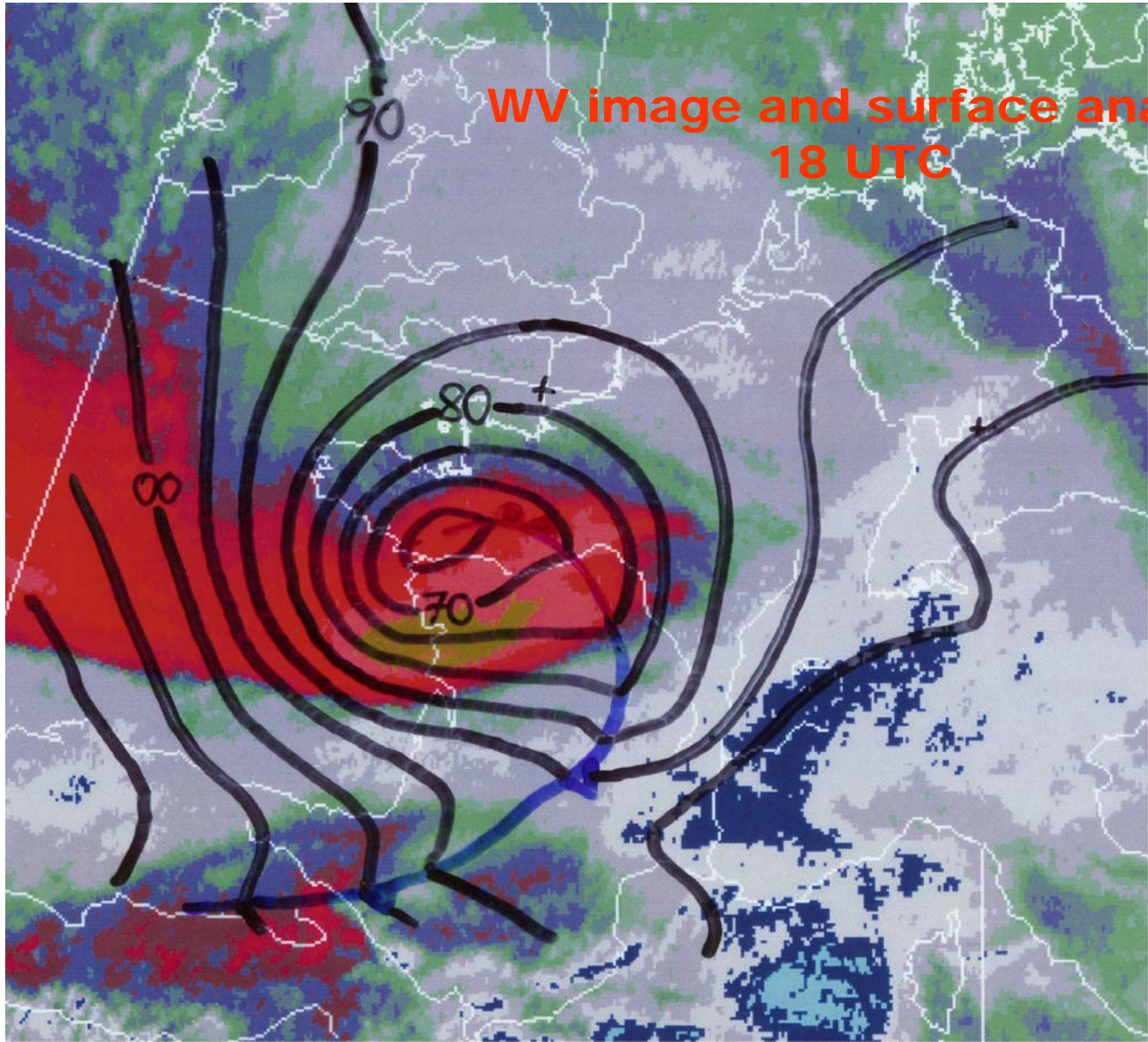
Numerical analysis (red) and manual analysis



15 UTC

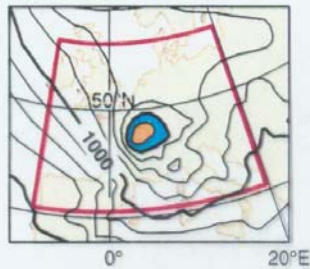


18 UTC

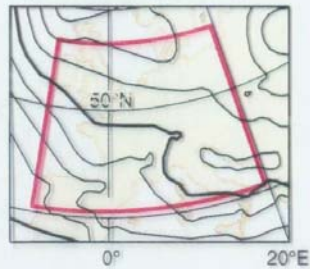


WV image and surface analysis
18 UTC

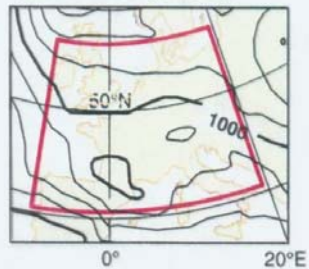
a) an 1999-12-28 00



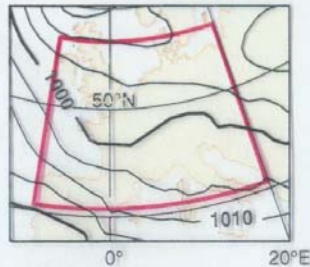
b) OHR t+60 (er=7.71)



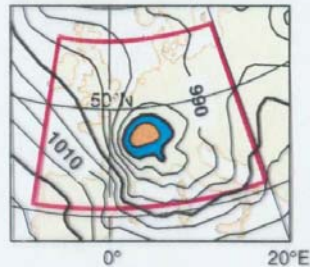
c) CON t+60 (er=9.5)



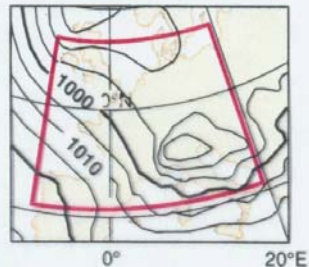
d) MEA e1uk t+60 (er=8.2)



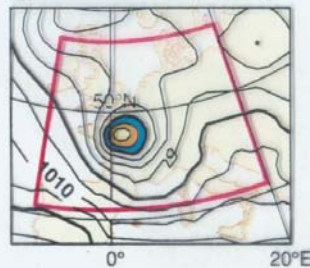
e) MEM 45 t+60 (er=2.23)



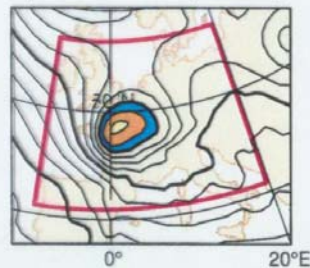
f) MEM 43 t+60 (er=6.06)



g) MEM 25 t+60 (er=6.2)



h) MEM 31 t+60 (er=6.24)



i) MEM 48 t+60 (er=7.4)

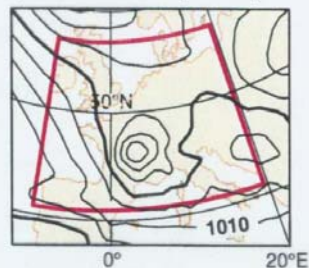


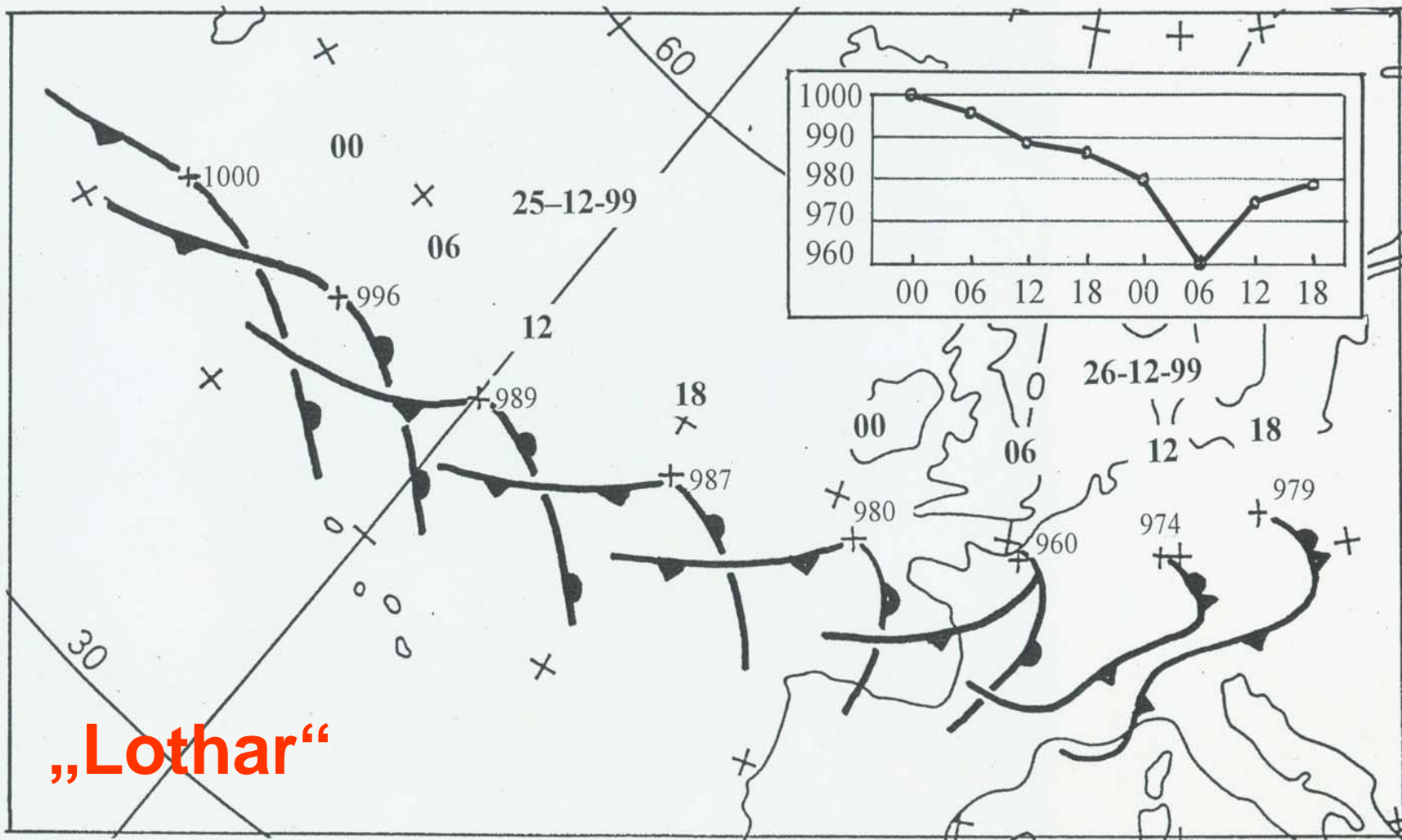
Figure 9 The second French storm. (a) The MSLP analysis at the verification time 00 UTC 28 December 1999. The other panels show t+60h forecasts started at 12 UTC 25 December (er is the root-mean-square error (hPa), IE is the intensity error (hPa) and PE is the position error (km)). (b) The $T_L319L60$ forecast (IE=23hPa, PE=904km) (c) the high-resolution ensemble (HEPS) control forecast (IE=30hPa, PE=481km), (d) the HEPS ensemble-mean forecast, (e) EPS member 45 (the lowest RMSE, IE=1hPa (the lowest), PE=38km), (f) EPS member 43 (the second lowest RMSE, IE=10hPa, PE=475km), (g) EPS member 25 (IE=4hPa, PE=222km), (h) EPS member 31 (IE=2hPa (the second lowest), PE=276km), and (i) EPS member 48 (IE=10hPa, PE=185km). Nine HEPS members had RMSEs smaller than the $T_L319L60$ forecast and 19 members had RMSEs smaller than the HEPS control. The contour interval is 5hPa, with shading for values below 980hPa.

Conclusions

- Also the rapid deepening of the storm „Martin“ was released by the approach of an upper trough to a frontal wave in the lower troposphere. This process could be clearly recognized by the comparison of the manual surface analysis with the upper air charts and the satellite imagery.
- In spite of that, the NWP models nearly totally failed to simulate this development – possibly due to great errors of the surface analysis.
- The forecasters of Meteo France, however, could overcome this deficit and issue detailed warnings by monitoring the real weather development and applying the CM for rapid cyclogenesis based on the satellite imagery.

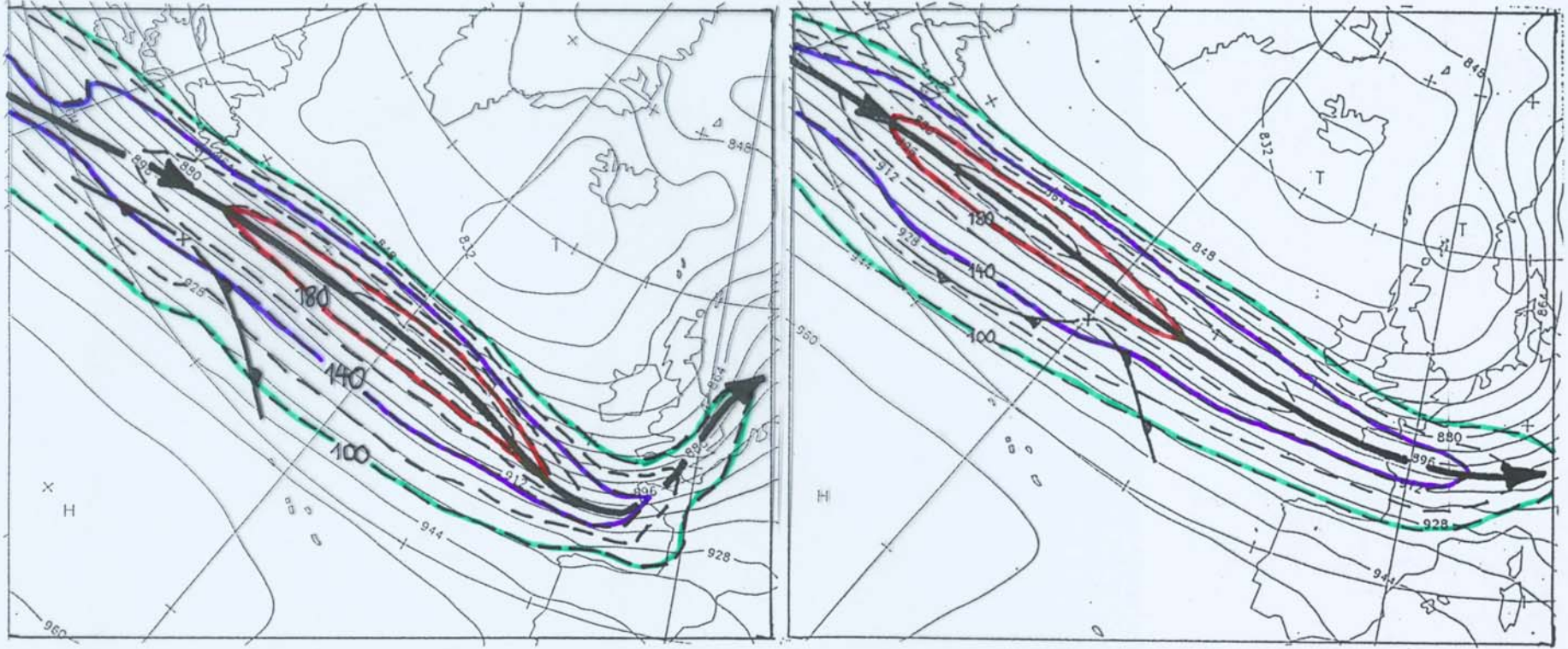
Examples (III)

- **Storm „Lothar“**
(25/26 -12- 1999)



„Lothar“

Geopotential and isotachs 300 hPa

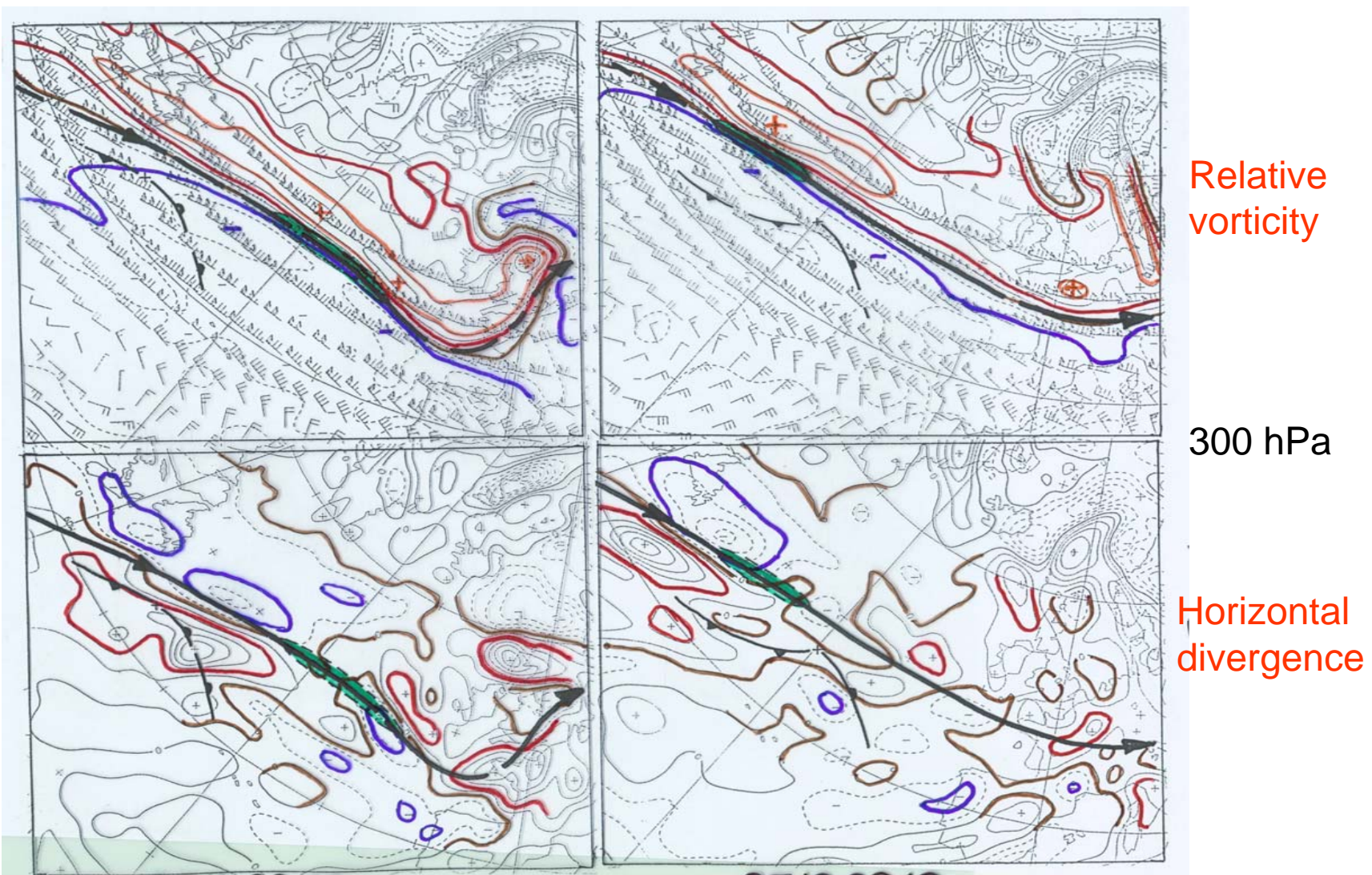


25-12-99, 00

25-12-99, 12

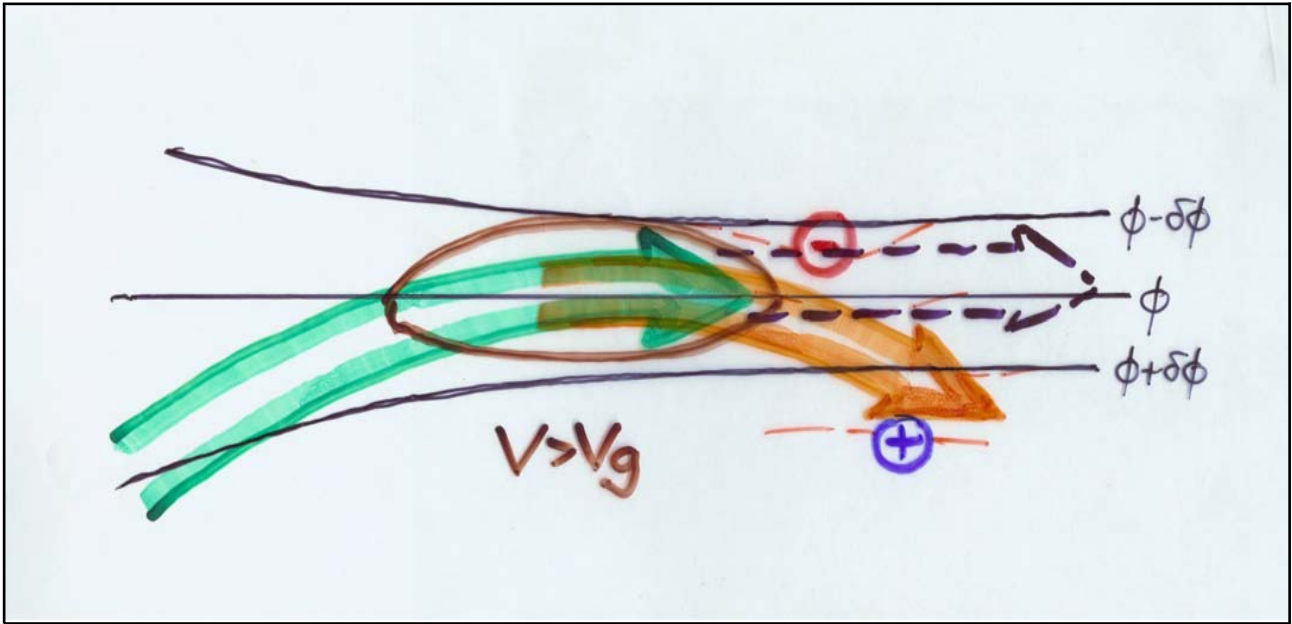
At the beginning some deepening under the entrance region of a first jet streak

A new jet streak developed upstream so that „Lothar“ had for some time an unfavourable position regarding further deepening

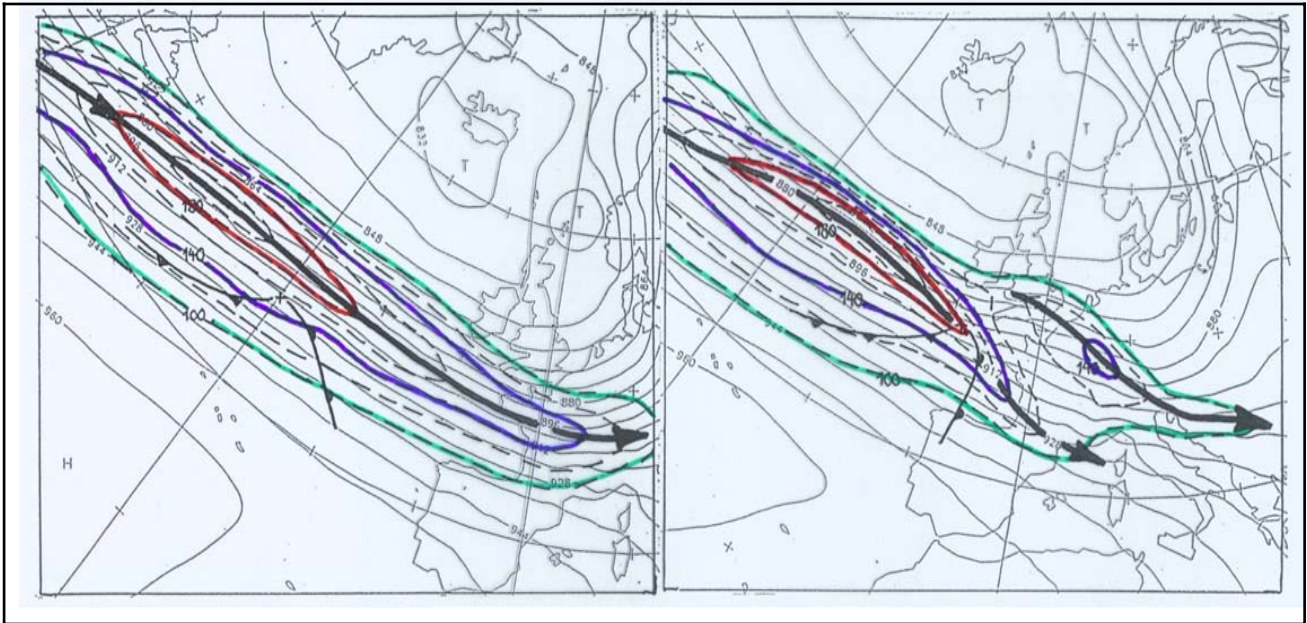


25-12-99, 00

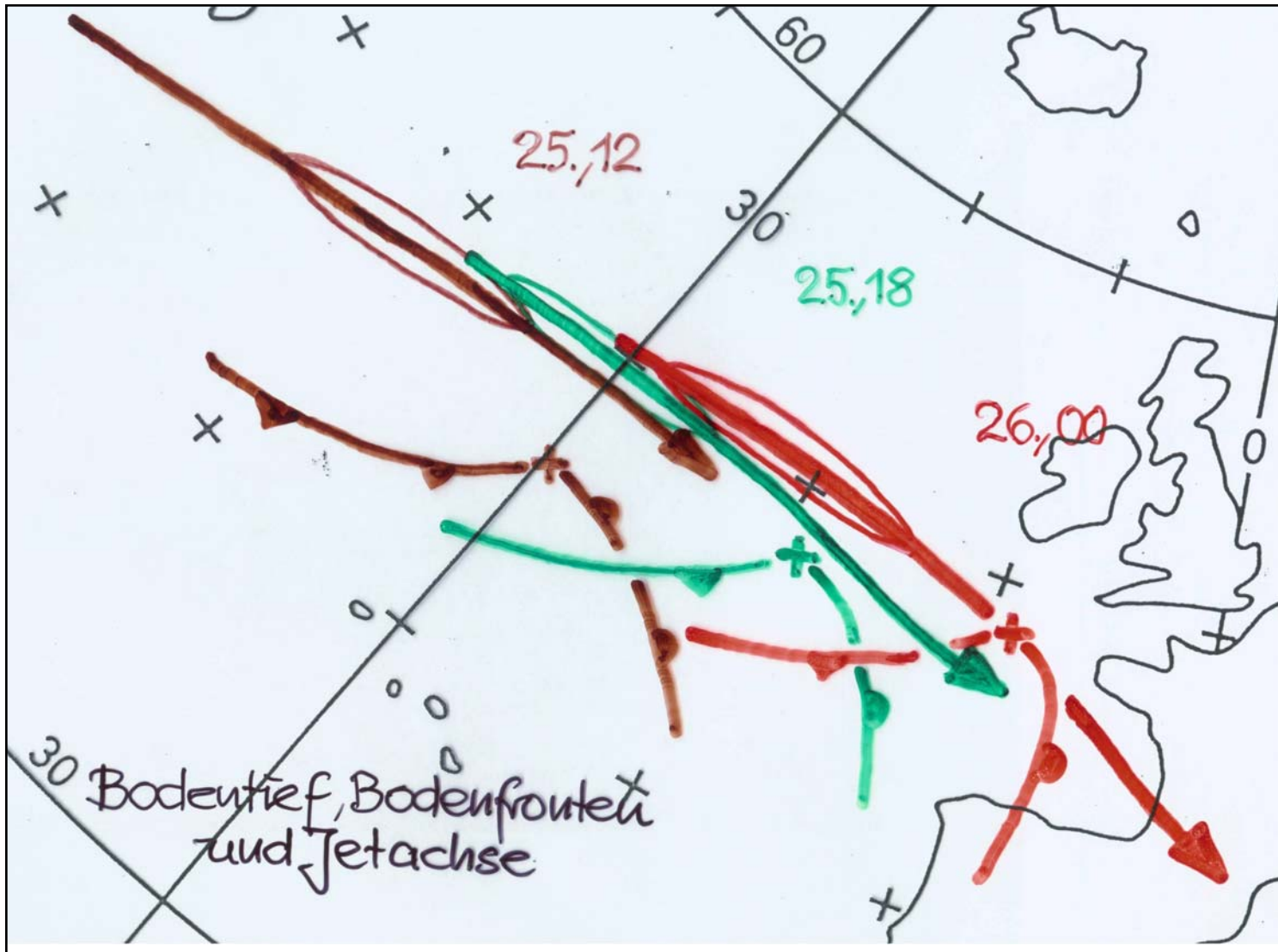
25-12-99, 12



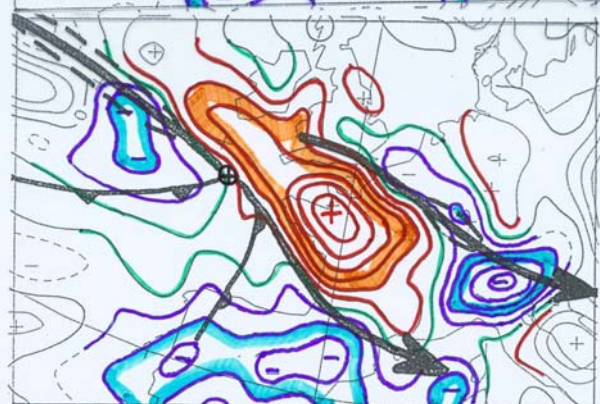
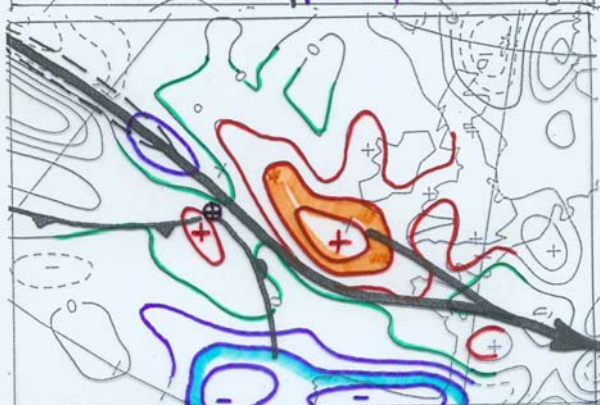
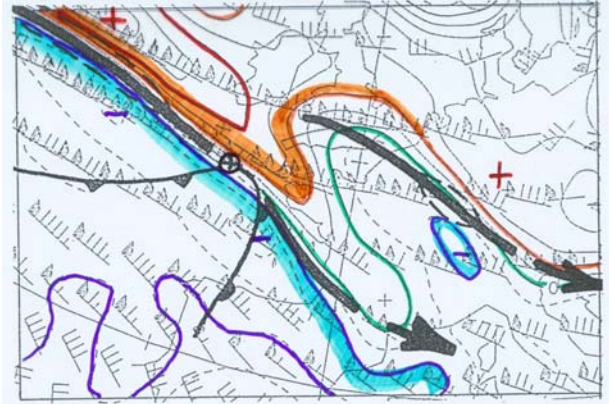
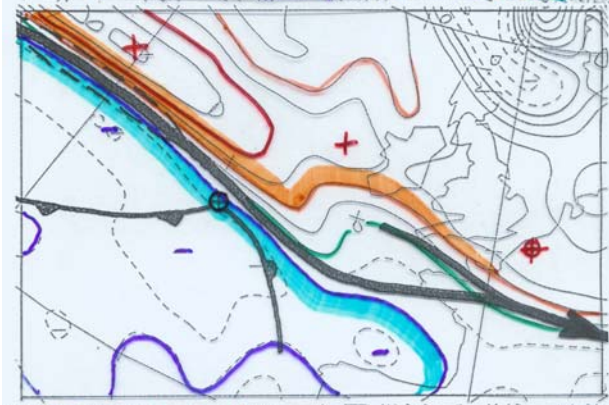
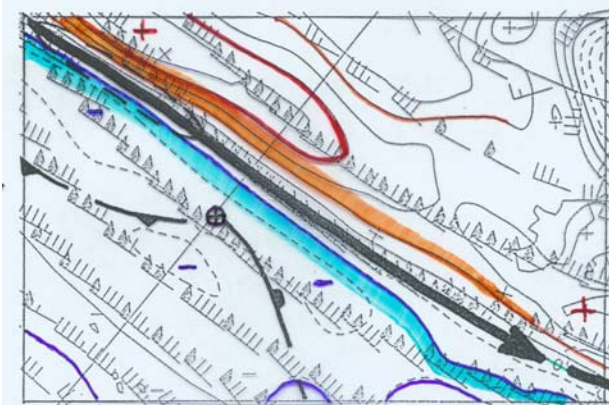
25-12-99
12



26-12-99
00



Position of surface low, surface fronts and jet axis



25-12-99, 12

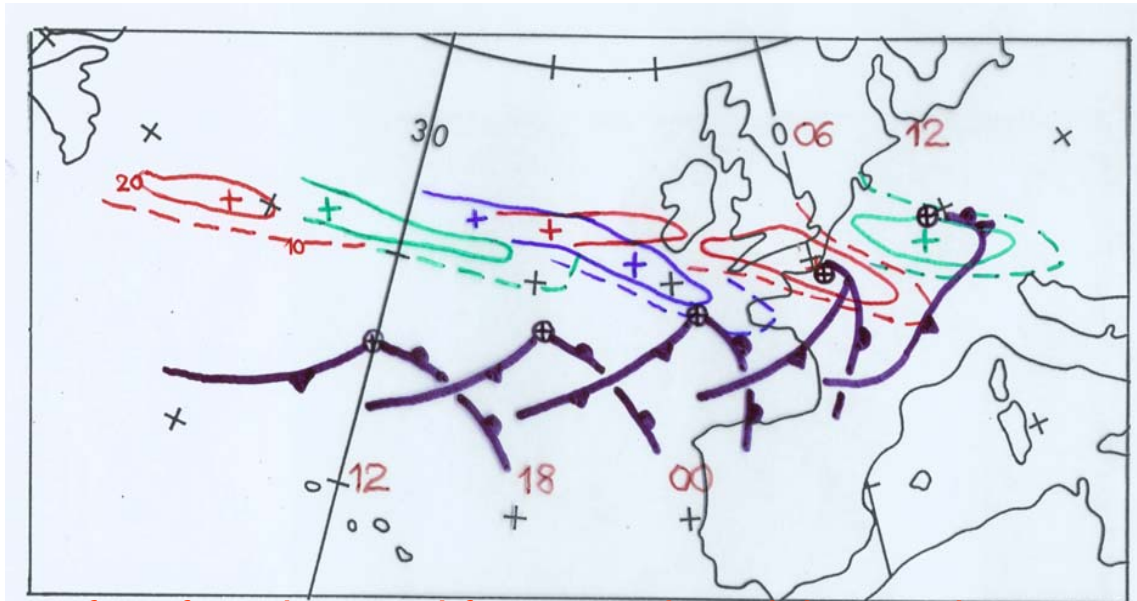
25-12-99, 18

26-12-99, 00

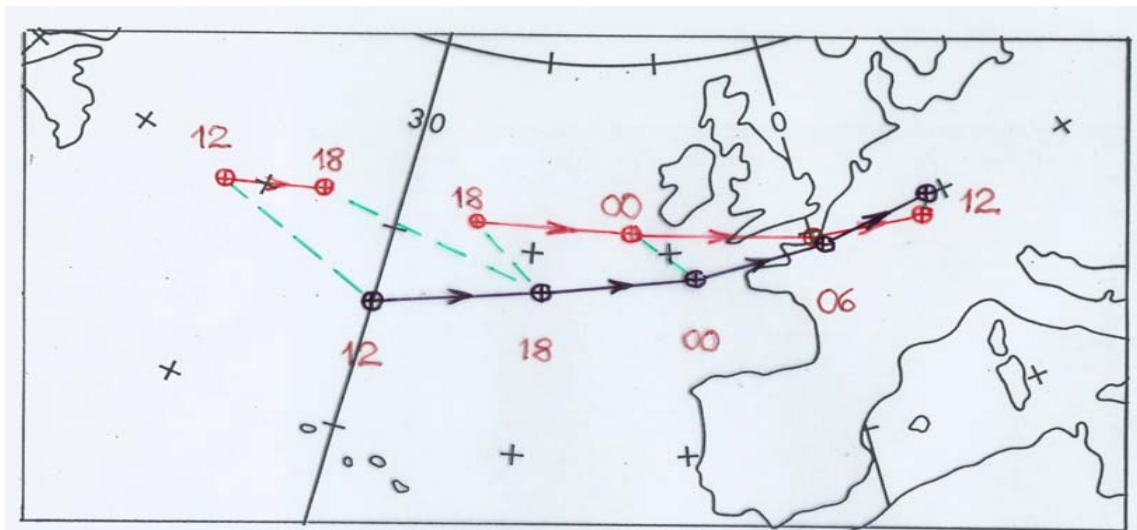
300 hPa

Relative vorticity, winds

Horizontal divergence

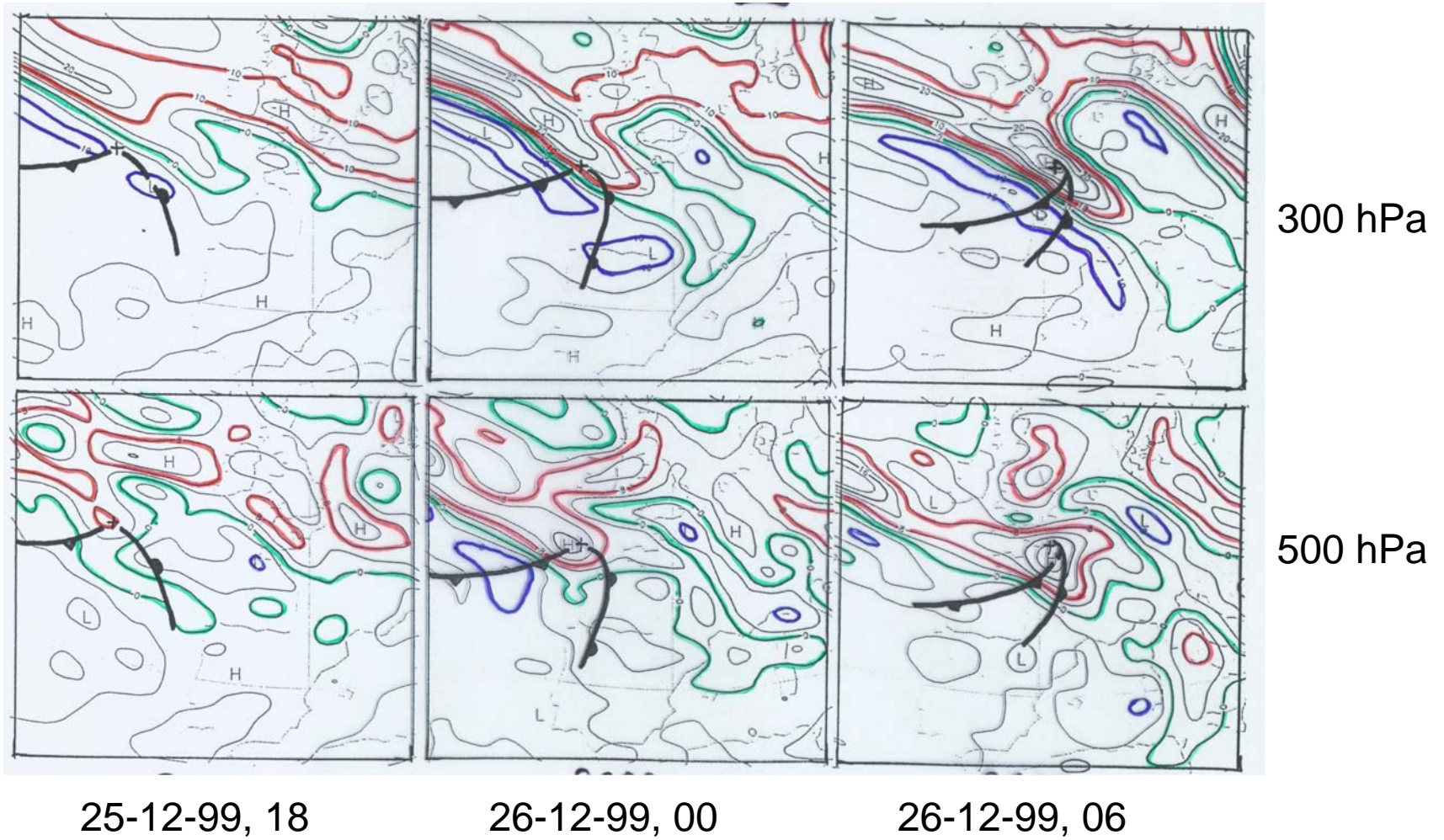


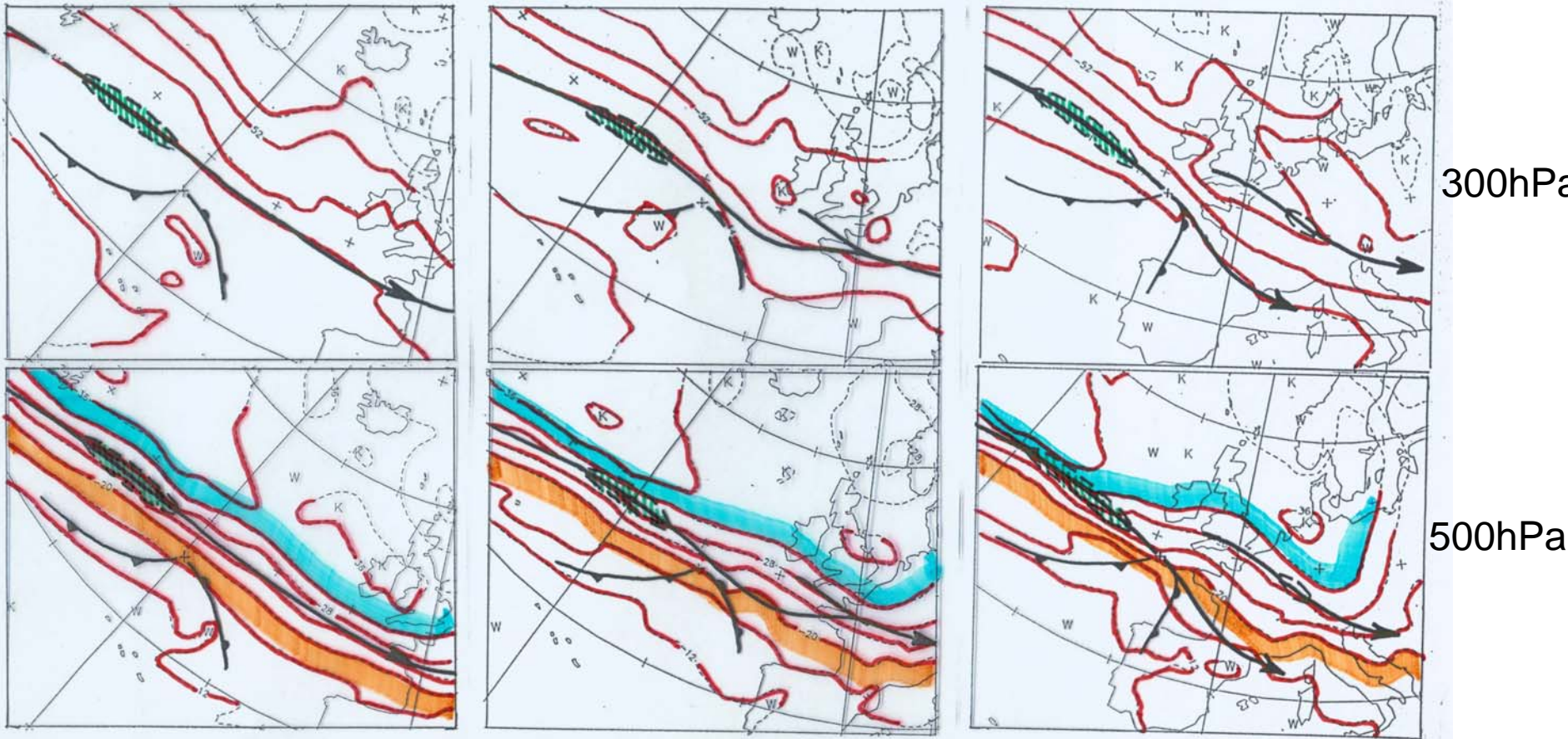
Position of surface low and fronts and vorticity maximum at 300 hPa



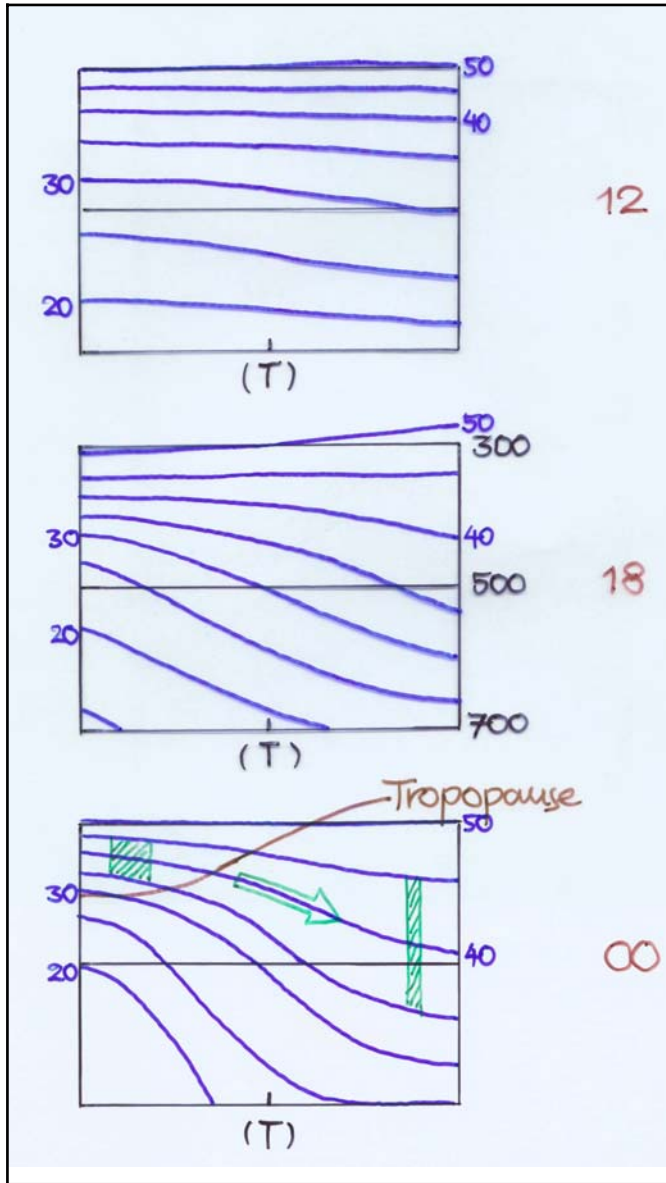
Movement of surface low and vorticity maximum at 300 hPa

Relative vorticity

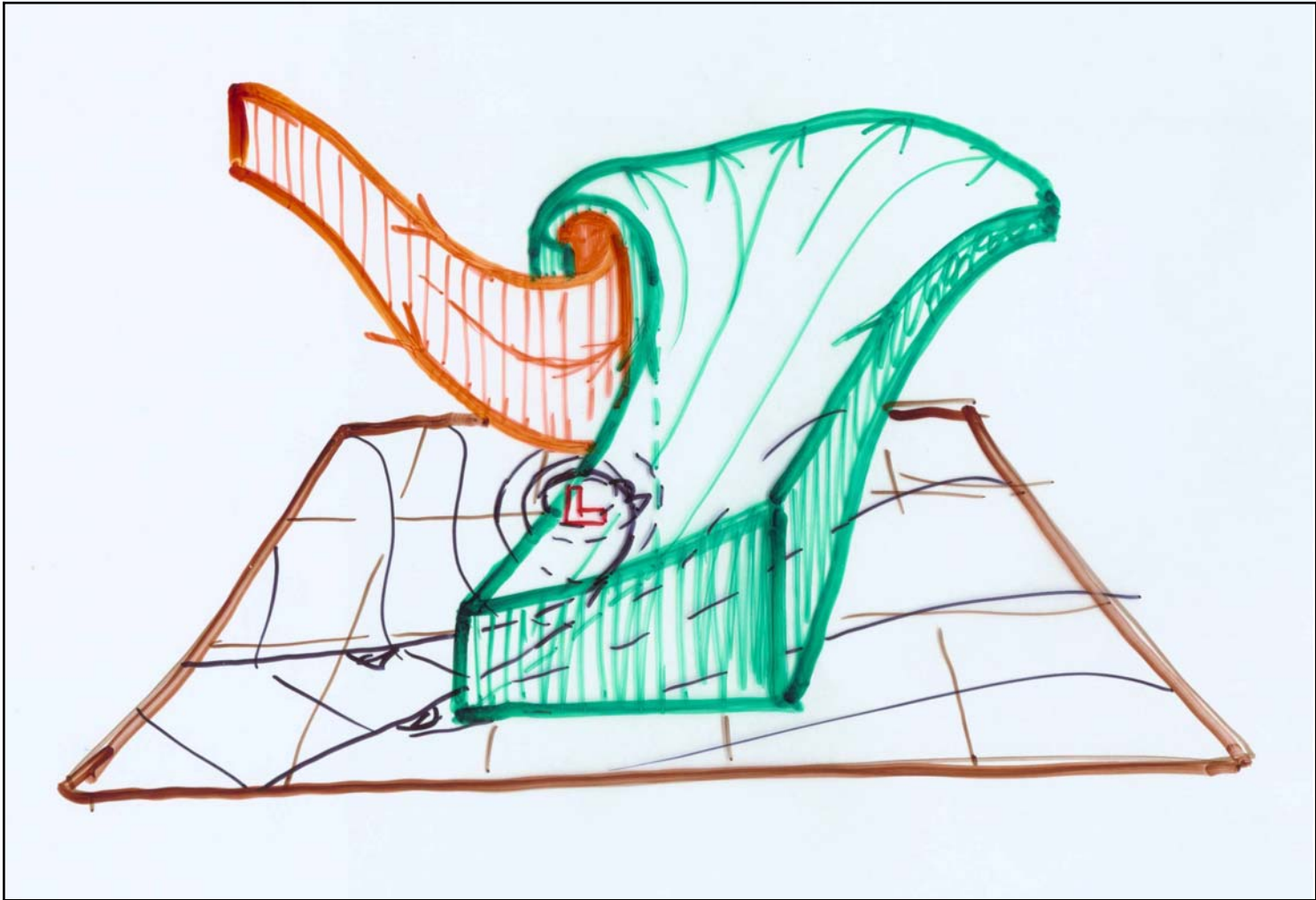




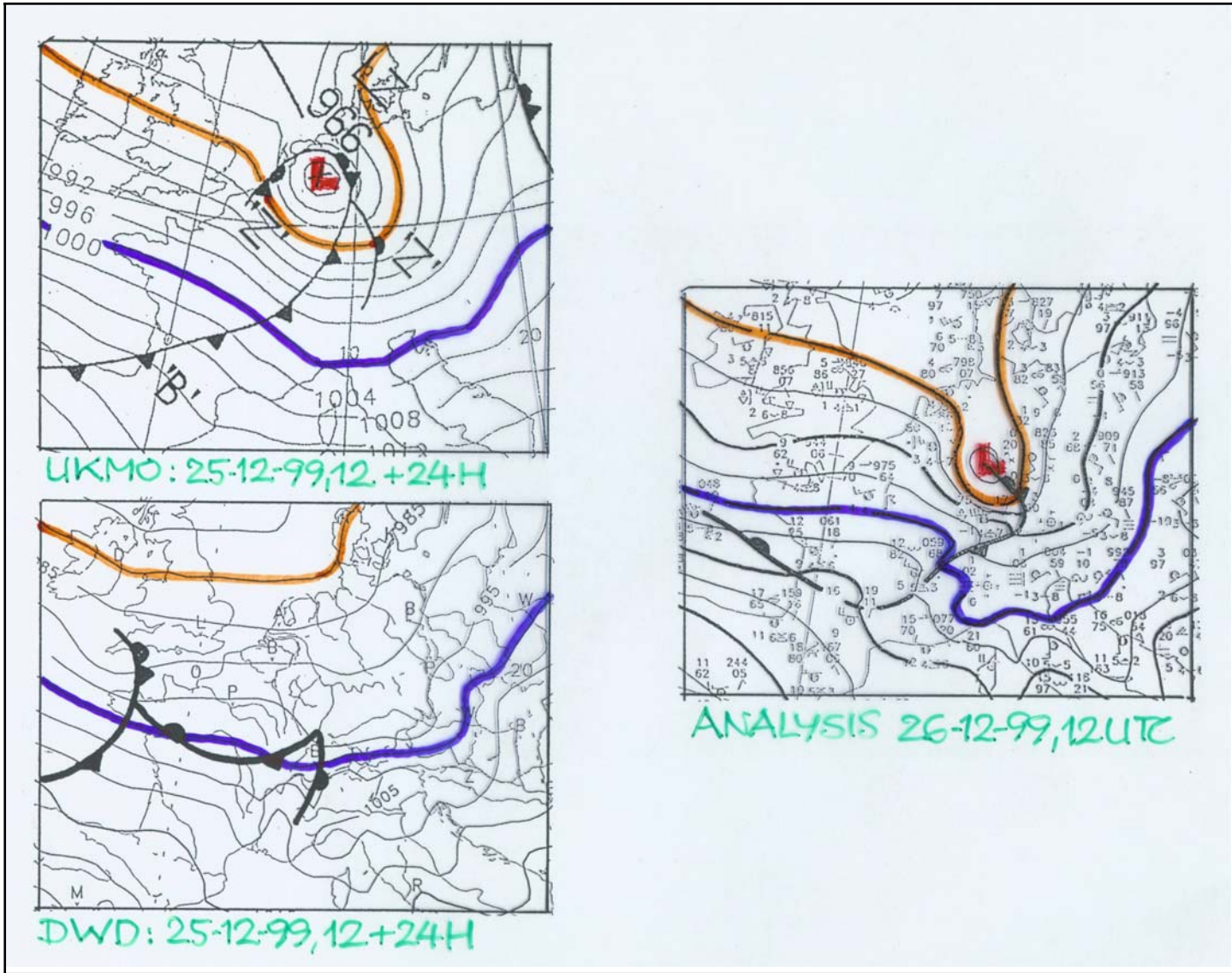
Distribution of temperature at 300 hPa (top) and 500 hPa (bottom) in relation to the jet axis and jet maximum at 300 hPa and to surface low and fronts



Cross-section of potential temperature along cyclonic flank of the jet axis



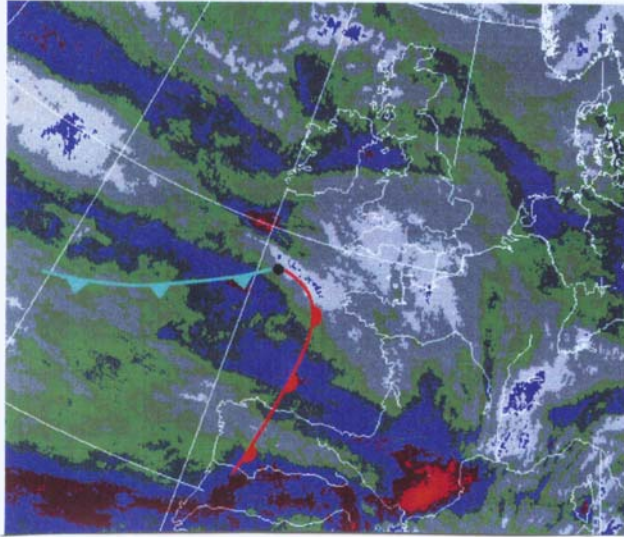
Conceptual model of the mature stage of „Lothar“



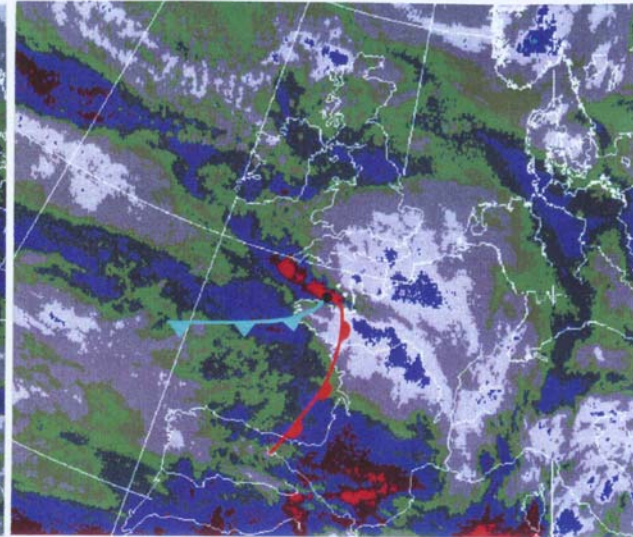
Forecasts of UKMO and DWD and verifying analysis

26-12-1999

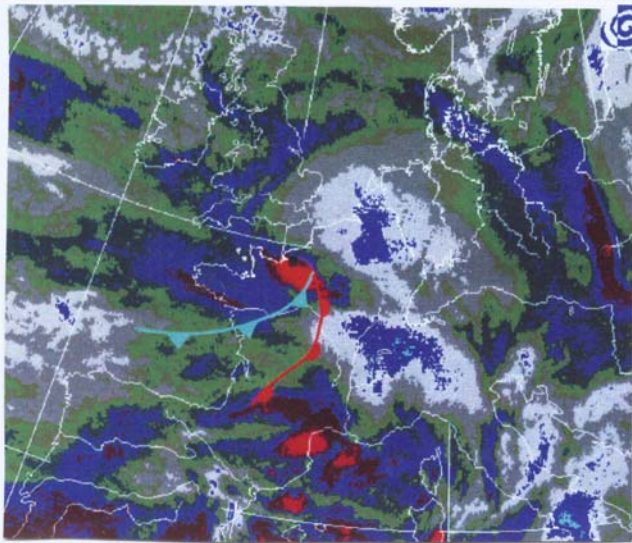
00



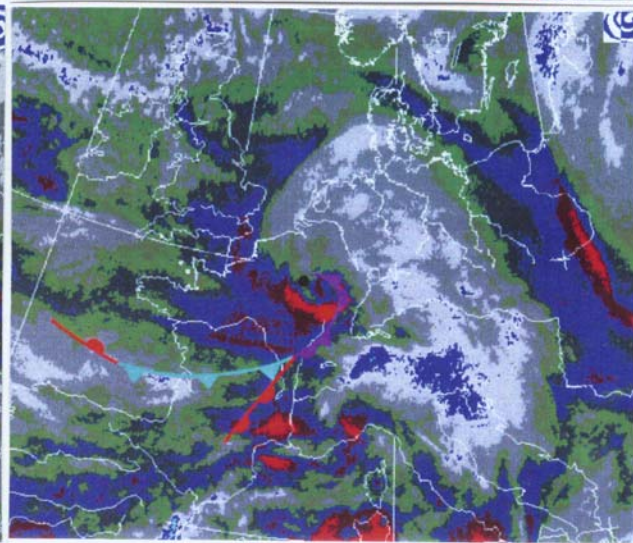
03



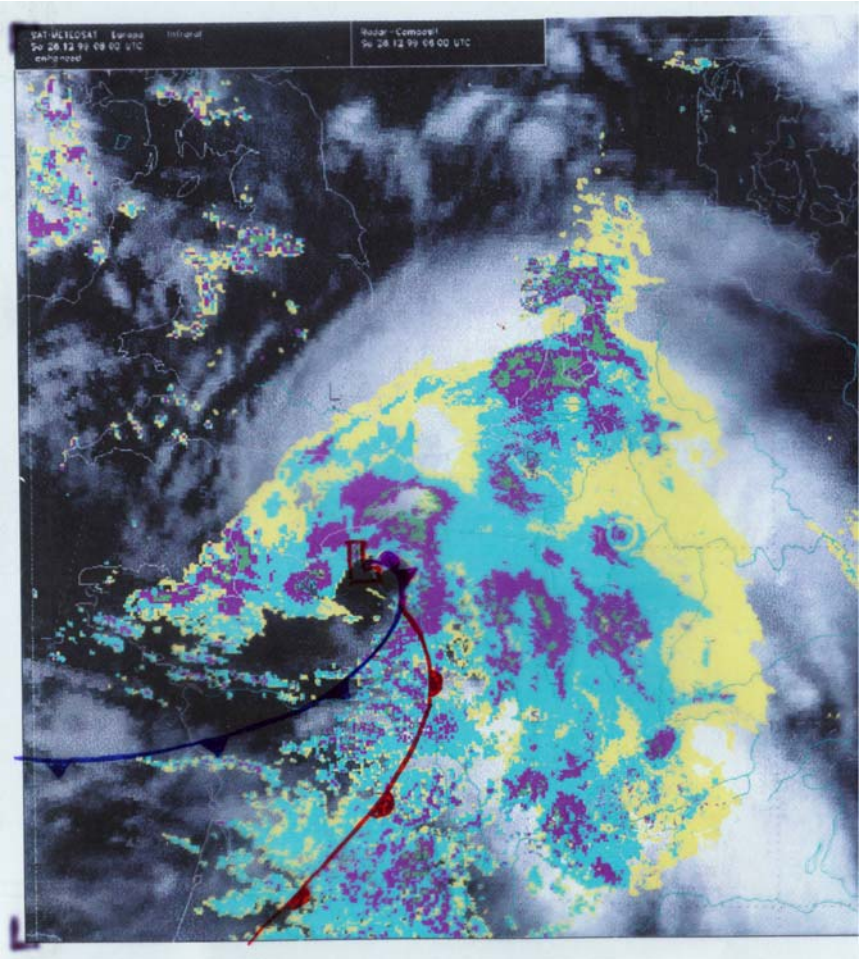
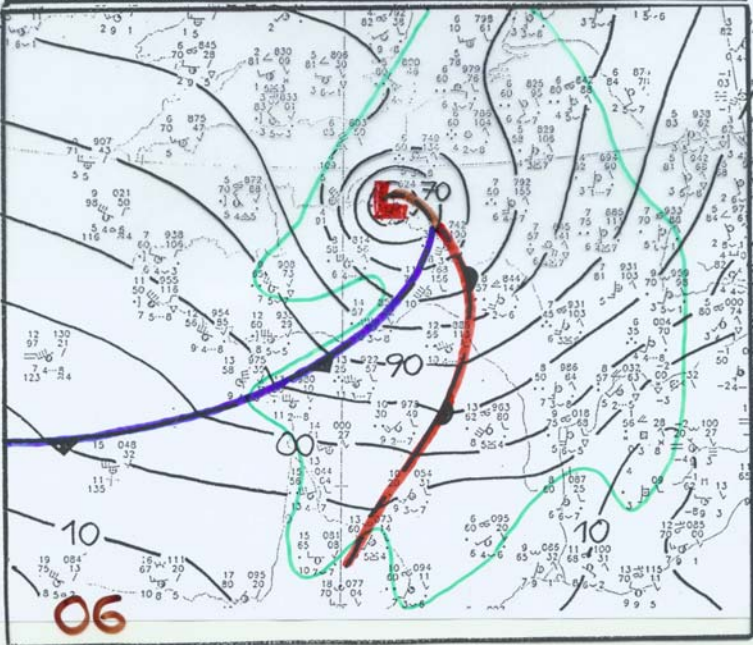
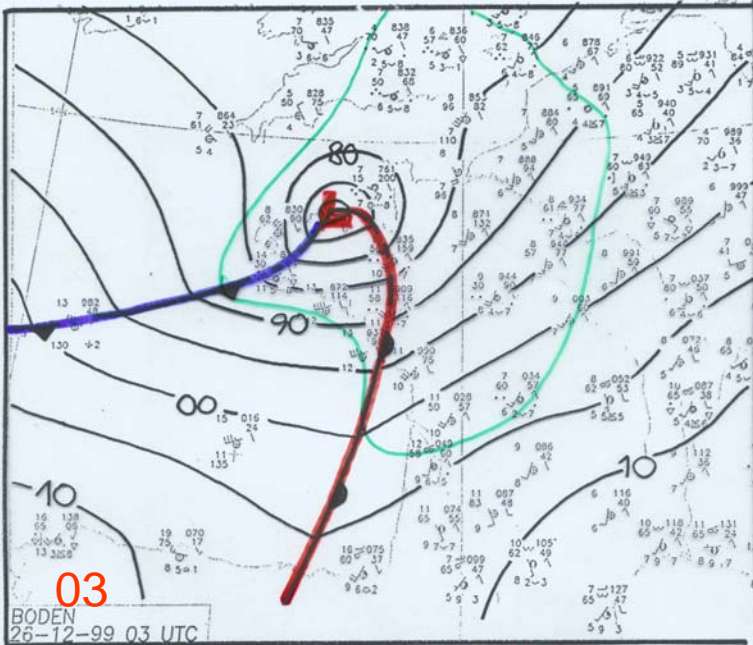
06



09

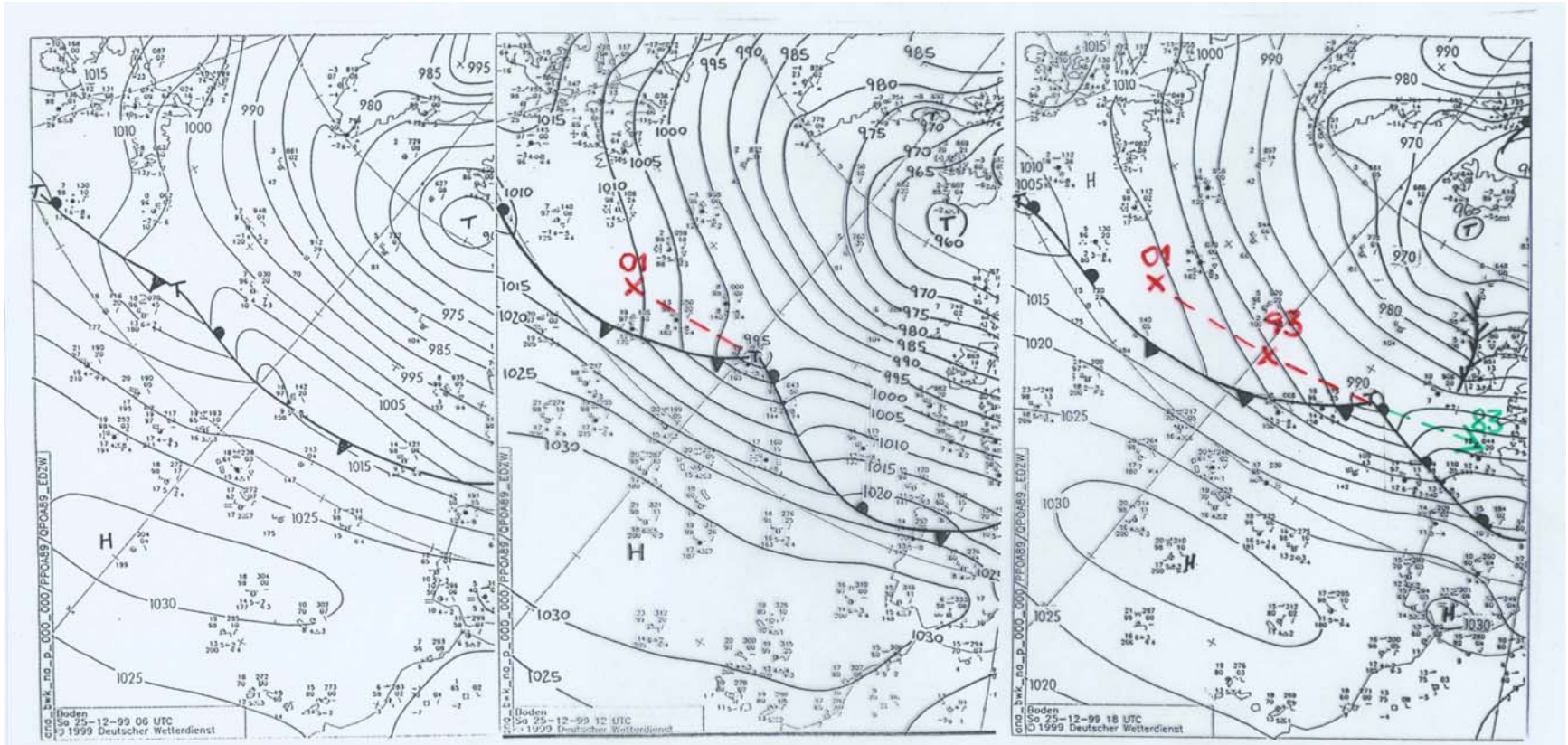


WV-images of METEOSAT with surface fronts and position of the surface low



26-12-1999, 06 UTC: Surface low and fronts with IR-image of METEOSAT and radar measurements

25-12-1999

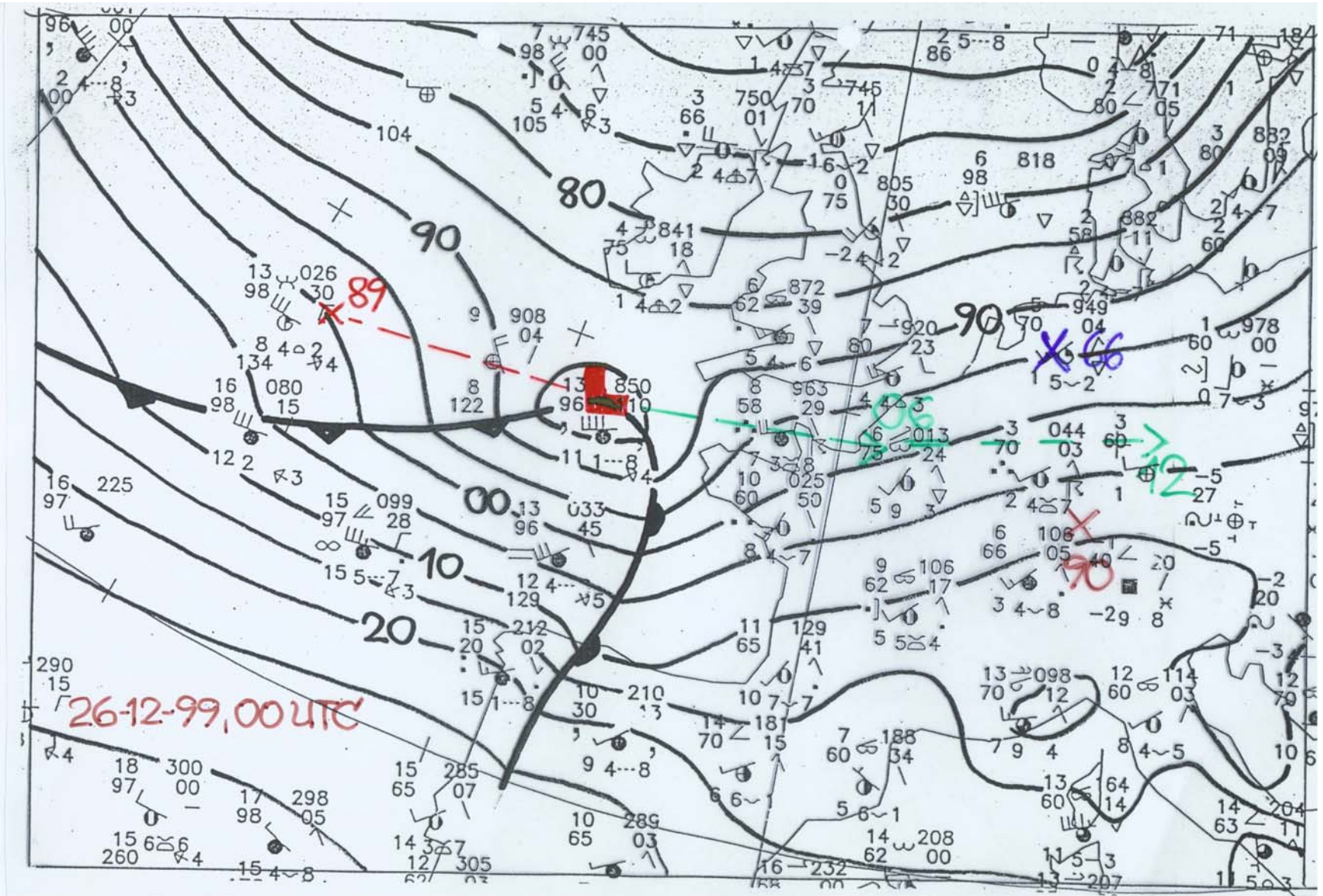


06 UTC

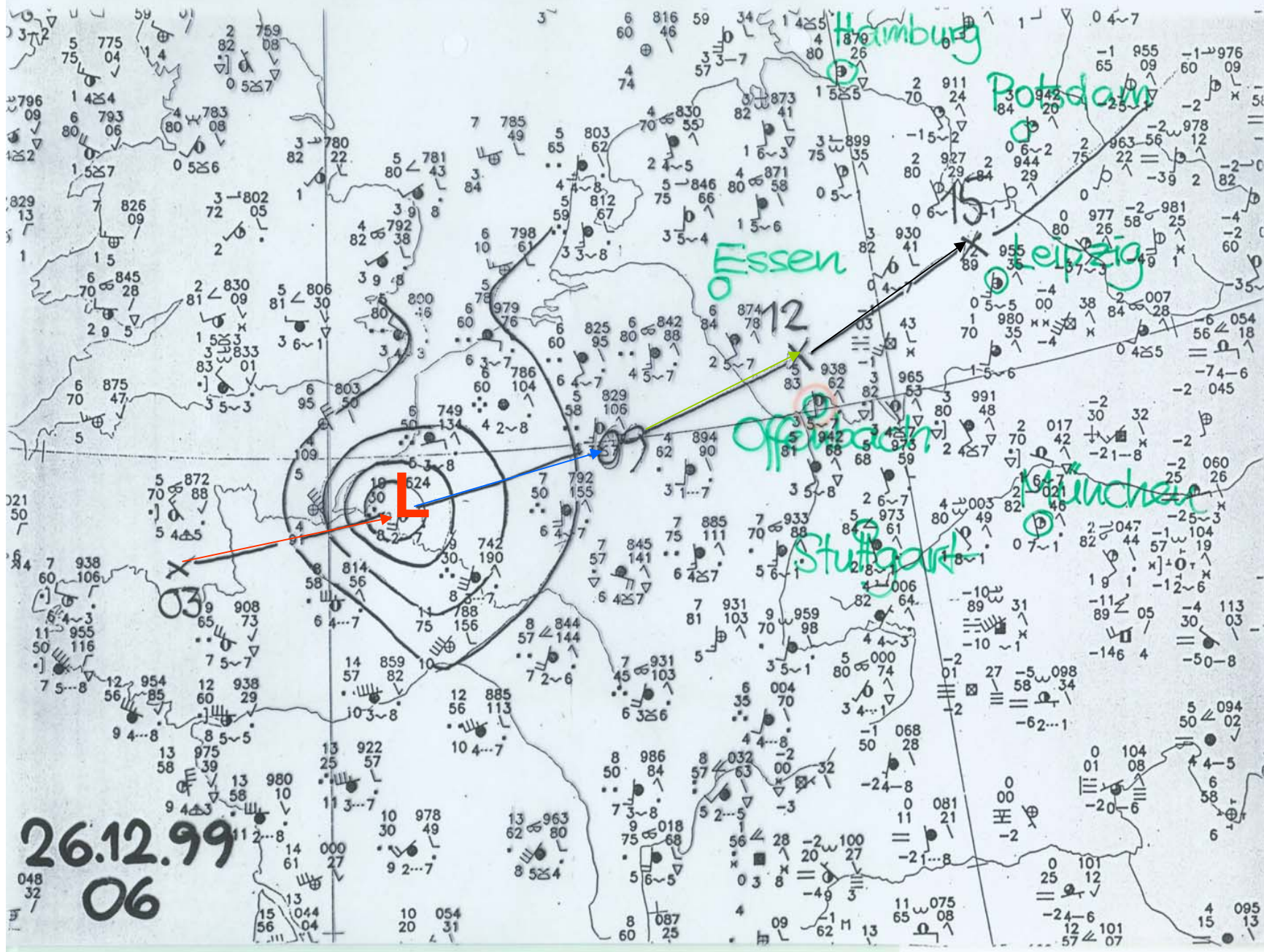
12 UTC

18 UTC

Operational surface analyses and extrapolation of the surface low



26-12-1999, 00 UTC: Manual surface analysis and extrapolation



Operational extrapolation of the movement of „Lothar“

„LOTHAR“ was here

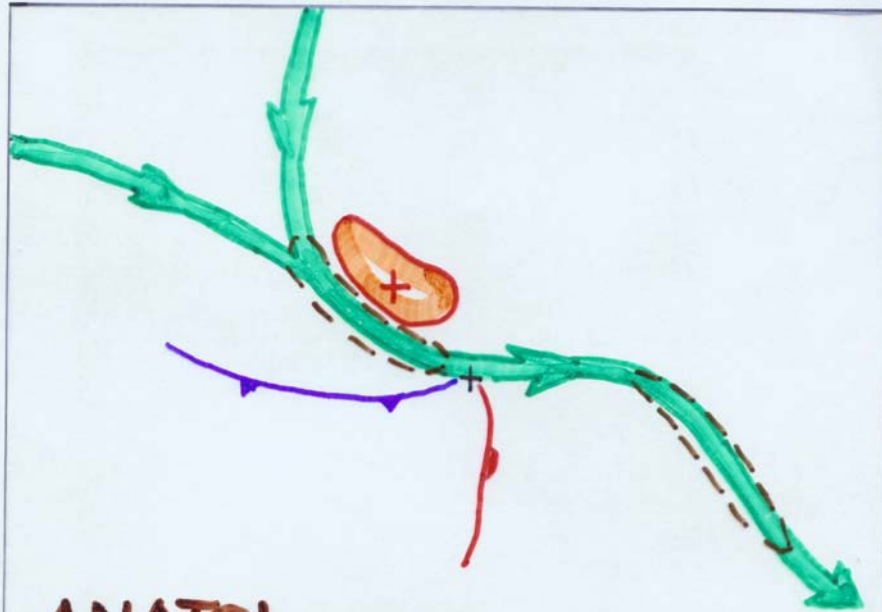


Orkan wütete am Sonntag in Stuttgart und in der Region

Ein Orkan hat am Sonntag eine Spur der Verwüstung durch Stuttgart gezogen. Auf dem Flughafen wurden Kleinflugzeuge durch die Luft gewirbelt und beschädigt (oben li.). An der Alten Weinsteiße stürzte ein Kran auf ein Wohnhaus und mehrere Autos (li.). Wie in der Rotenwaldstraße (oben re.) sah es in vielen Straßen Stuttgarts aus: Umgestürzte Bäume blockierten die Fahrbahn. Viele Straßen mussten von der Polizei über Nacht gesperrt werden. Fotos: Uli Kraufmann

Conclusions (I)

- The development of „Lothar“ proceeded exceptionally: There was no upper trough approaching the surface low, but the explosive deepening occurred as „Lothar“ crossed the upper jet axis and got under the cyclonic part of the exit of a jet streak upstream of it.



ANATOL



LOTHAR

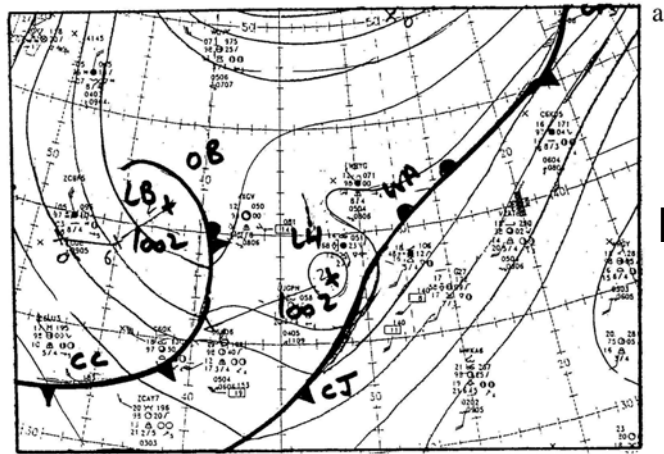
Conclusions (II)

- The models showed a very different performance: Some simulated the described process reasonably well, whereas other totally failed.
- According to the special mechanism, the signals from the satellite imagery pointing to the rapid deepening, became visible only late and provided not much help for the nowcasting of the storm. With the aid of a consequent extrapolation, however, the issue of warnings was possible at least some hours in advance.

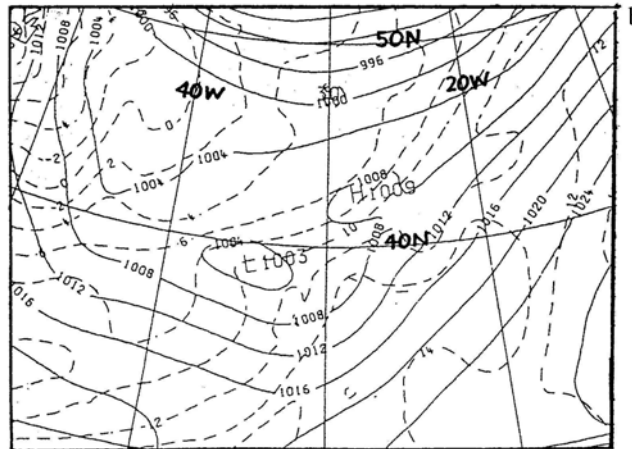
Examples (IV)

- **The Christmas Eve storm 1997**

**Model analysis
problems around
the incipient
depression**



Manual analysis



NWP analysis

Fig 1 Sea-level pressure for 1200UTC 23 December 1997 (a) NMC manual analysis and (b) UK Met Office NWP analysis

METEOSAT IR 23 DEC 1997 14:00 UTC

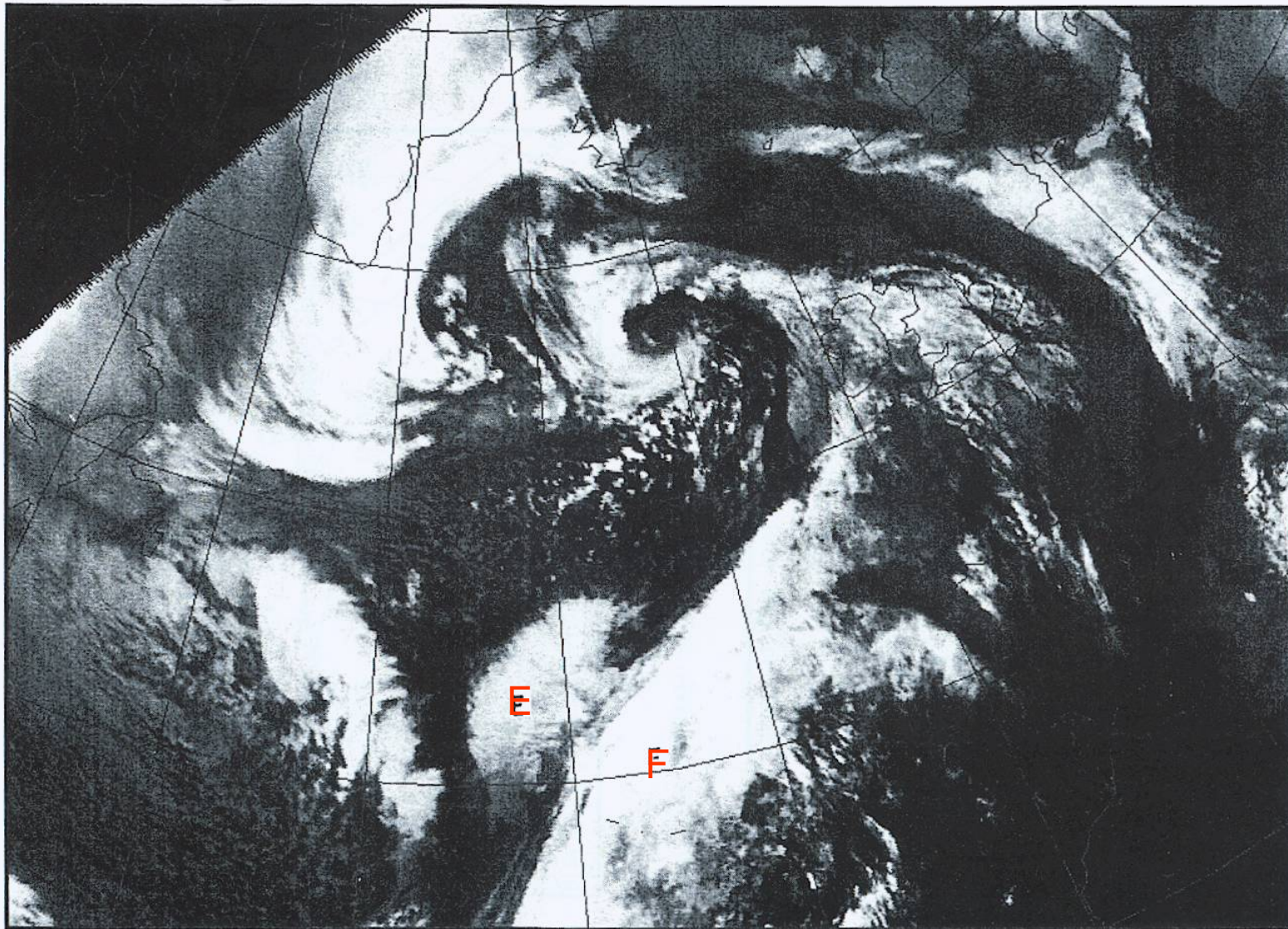
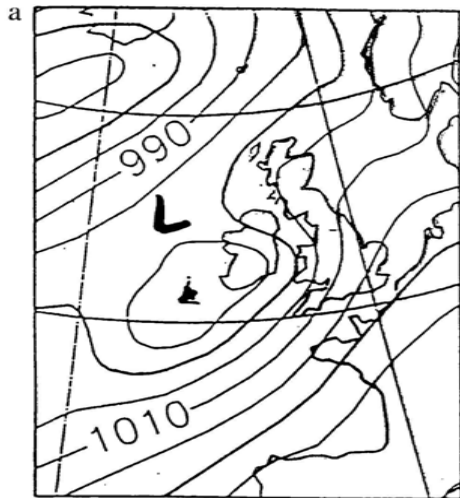
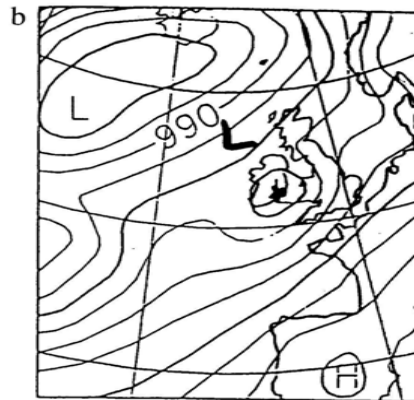


Fig. 2 Infra-red satellite image for 1400UTC 23 December 1997. E and F are referred to in the text

UKMO 23/12/97 12h fc t+24

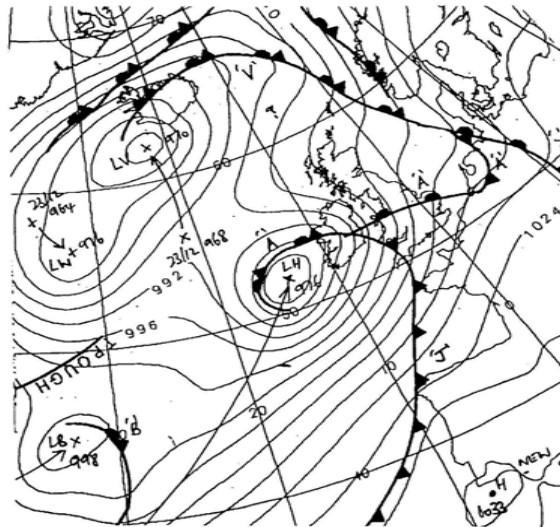


DWD 23/12/97 12h fc t+24



**NWP 24-hour forecasts
of sea-level pressure**

Fig 3 NWP 24-hour forecasts of sea-level pressure valid 1200UTC 24 December 1997
(a) UK Met Office (b) Deutscher Wetterdienst (isobars at 5hpa intervals)



Man-machine mix 24-hour forecast

Fig 4. Man-machine mix 24-hour forecast for 1200UTC 24 December 1997

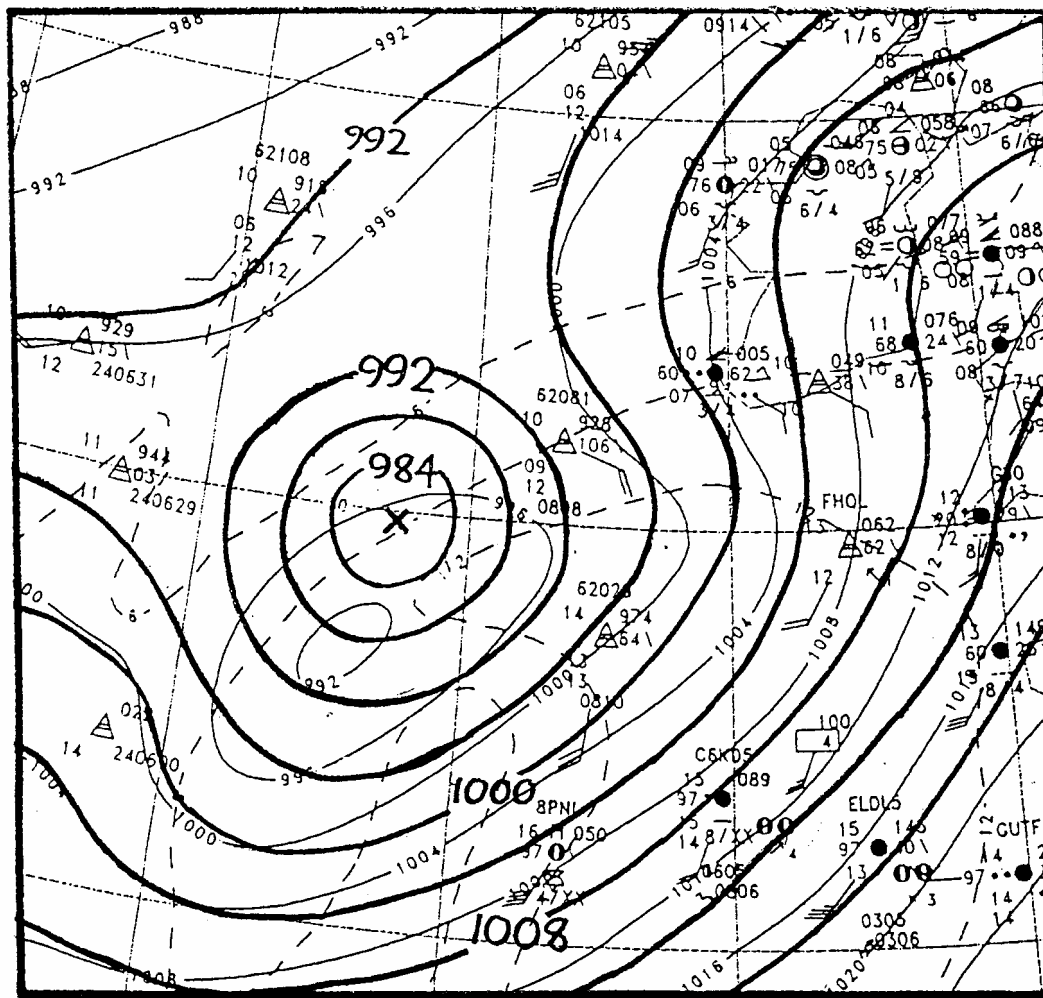
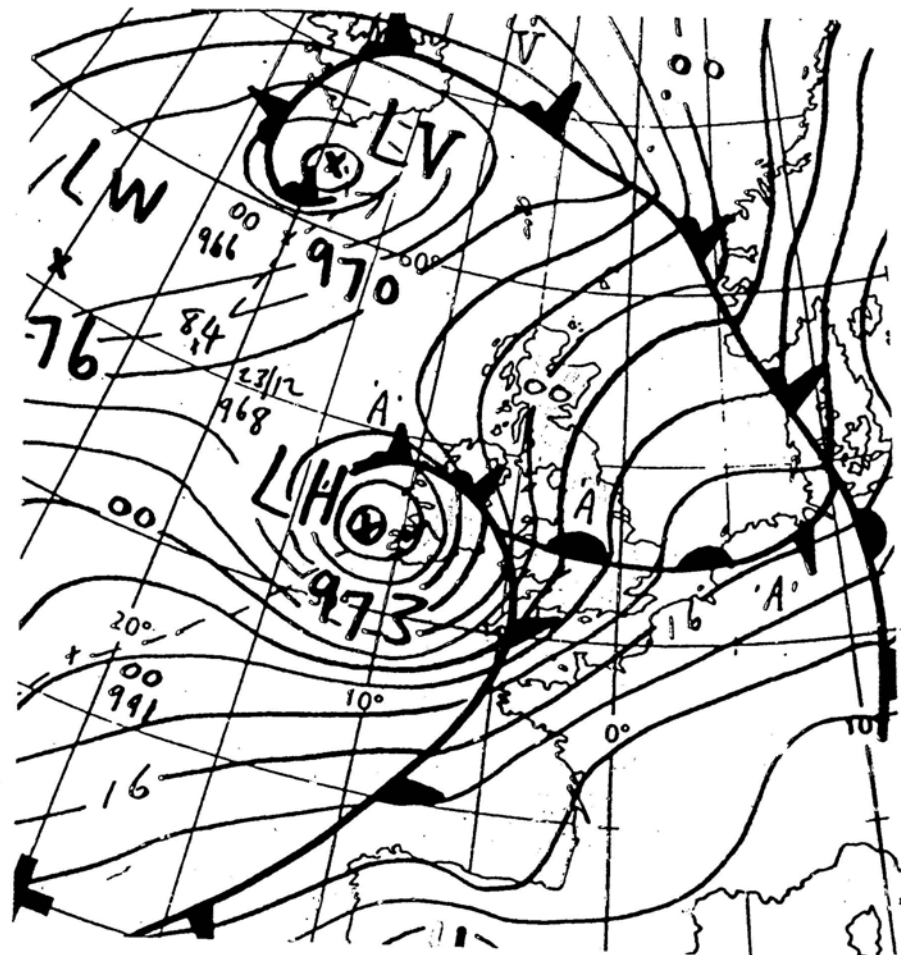


Fig 6. Sea-level pressure at 0600UTC 24 December 1997 showing UK limited area model 6-hour forecast (thin line) and manual analysis (dark line).



ANALYSIS
12Z 24/12/97

Fig 7. NMC manual surface analysis for 1200 UTC 24 December 1997.

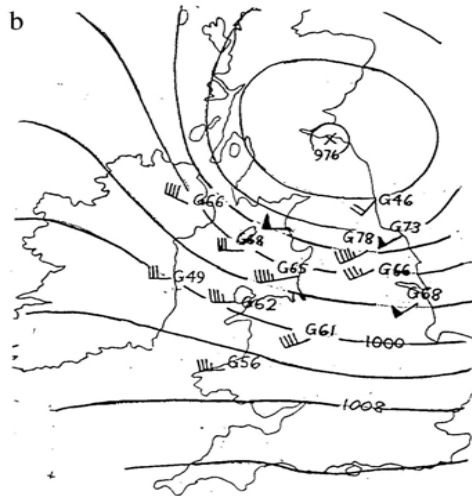
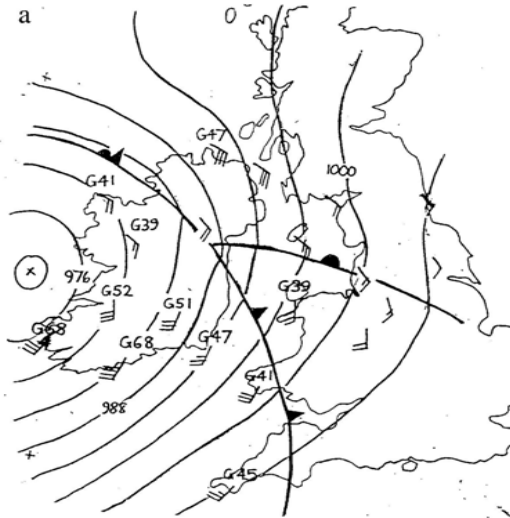


Fig 8. Selected observations of surface wind and hourly gusts (knots) for (a) 1300UTC and (b) 2200UTC 24 December 1997. Sea level pressure also shown in hpa. (Note 1knot = 1.85km/hr)

Selected observations of surface wind and gusts for (a) 13 UTC and (b) 22 UTC 24-12-1997

Forecasting the Christmas Eve Storm 1997

- In this event, the role of the forecaster was crucial in
- Realizing the potential for development – by interpretation of the satellite imagery and recognising the „cloud head“ conceptual model
- Identifying NWP model analysis problems around the incipient depression, including the mismatch between the „dry slot“ on water vapour imagery and model potential vorticity and humidity fields
- Continually monitoring and interpretation of latest asynoptic data – essential for nowcasting in a rapidly developing or changing situation
- Action – timely issue of warnings to public and customers – recognised as the final and most crucial stage in the nowcasting process

Conclusions (I)

- Since NWP models still show deficits in simulating hazardous weather situations, **the experience of well educated and trained forecasters is needed for the issue of warnings as quickly and reliably as possible.**
- **Decisive for a successful intervention in the forecasting process is an own SYNOPTIC DIAGNOSIS.** Since the use of the parameters derived from numerical analyses or forecasts for this purpose might appear questionable in cases with significant errors in the model output, **diagnostic means have to be used which are mainly based on observations.**

Conclusions (II)

- **Very important in this respect are remote sensing data like the imagery of meteorological satellites. They not only allow a continuous monitoring of the weather development, but also show typical signatures from which the potential for the further development can be derived.**